Revista Română de Inginerie Civilă

Indexată în bazele de date internationale (BDI)

ProQuest, IET INSPEC, EBSCO, GOOGLE SCHOLAR, CROSSREF, TDNET, DIMENSIONS, DRJI, J-GATE, INDEX COPERNICUS, ULRICH'S, JOURNALSEEK, RESEARCH GATE, SEMANTIC SCHOLAR, ERIHPLUS, WORLDCAT

Volumul 17 (2026), Numărul 1

MATRIX ROM
3 Politehnicii Street, Bucharest, Romania
Tel. +4021.4113617, +40733882137
e-mail: office@matrixrom.ro
www.matrixrom.ro

EDITORIAL BOARD

Romanian Journal of Civil Engineering is founded, published and funded by publishing house MATRIX ROM
Executive Director: mat. Iancu ILIE

Online edition ISSN 2559-7485

Print edition ISSN 2068-3987; ISSN-L 2068-3987

Study on the parameters influencing the bending and shear behavior of steel fiber reinforced concrete elements

Studiu privind parametrii care influențează comportarea la solicitarea de încovoiere cu forță tăietoare a elementelor din beton armate dispers

Muheeb Altaleb[1], Andrei Gîrboveanu[1], Dan Georgescu[1], Amine Rahaoui[2]

[1]Technical University of Civil Engineering of Bucharest.
121-126 Bvd Lacul Tei, Bucharest, Sector 2, Romania
E-mail: andrei-sorin.girboveanu@phd.utcb.ro

[2]Construcții Erbașu SA.
72 Str Nicolae G. Caramfil, Bucharest, Sector 1, Romania

DOI: 10.37789/rjce.2026.17.1.1

Abstract. *Different types of fibers can be used to improve the mechanical behavior of steel fiber reinforced concrete. However, the degree to which this occurs also depends on certain characteristics of the structural element section. This paper studies the effects of adding fibers on the bending moment and shear force resistance depending on the geometry of the transversely unreinforced section, but also on the amount of longitudinal reinforcement. The results show a significant increase of the resisting moments for a high fiber content and reduced longitudinal reinforcement, but also a significant increase of the resisting shear force for a high fiber content, regardless of the amount of longitudinal reinforcement.*

Key words: *fiber reinfored concrete, bending moment, shear force, strength,*

Rezumat. *Diferite tipuri de fibre pot fi folosite pentru a genera o îmbunătățire a comportării mecanice a betonului armat dispers. Însă gradul în care aceasta se produce, depinde si de anumite caracteristici ale secțiunii elementului structural. În această lucrare sunt studiate efectele adăugării fibrelor în funcție de geometria secțiunii nearmate transversal, dar și de cantitatea de armătură longitudinală asupra rezistenței la moment încovoietor și forță tăietoare. Rezultatele arată o creștere semnificativă a momentelor capabile pentru un dozaj mare de fibre si armări longitudinale limitate, dar si o creștere semnificativă a forței tăietoare capabile pentru un dozaj mare, independent de cantitatea de armătură longitudinală.*

Cuvinte cheie: beton armat dispers, moment încovoietor, forță tăietoare, rezistență

1. Introduction

The beginning of fiber-reinforced concrete (FRC) as a genuine construction material can be traced back to the early 1960s. Fiber-reinforced concrete is a composite material combining a matrix (concrete) and reinforcement (fibers). The main role of the

The article was received on 20.10.2025, accepted on 02.02.2026 and published on 24.02.2026

fibers is to control cracking and absorb stress at any cracks that may develop. They give the concrete performance and properties related to their nature, shape, and mechanical characteristics. The range of uses for FRC has become extremely wide. FRC enriches the range of concrete construction solutions, thanks to the continuous development of a range of fibers with multiple properties.

Depending on their nature, fibers have specific geometric and mechanical characteristics and very different stress-strain behavior. The reinforcing capacity of a fiber depends in particular on its anchorage, tensile strength, and Young's modulus. Each has a particular influence on the mechanical behavior of concrete, which translates into specific, tailored applications. The choice of fiber type therefore depends on the field of application and the desired performance. Fibers are only useful if the concrete is subjected to tensile forces greater than its own strength. If cracks appear in the concrete, they allow the forces to be transmitted through the cracks.

Specific dimensioning methods (for structural applications: slabs, piles, etc.) and implementation techniques are now fully mastered for designing perfectly durable FRC structures.

Methods for optimizing their formulation have been specially developed. Fibers are highly compatible with the various components of concrete, including admixtures.

The structure of FRC and its mechanical characteristics also depend on how it is implemented (effects related to flow; preferential orientation of the fibers parallel to the direction of concrete flow and depending on the geometry of the structure). It is therefore necessary to know the implementation technique in order to develop the formulation and design of structures.

The expertise acquired through numerous research projects, FRC behavior tests, and multiple projects now makes it possible to characterize and specify FRC adapted to the performance requirements for each use. FRC can be formulated to be self-compacting and pumpable. Below, we will detail the behavior of this type of concrete and compare it to reinforced concrete. Finally, we will present a calculation example to illustrate the difference between this new type of concrete and traditional concrete.

2. Metal fibers and the composition of fiber-reinforced concrete

2.1. Metal fiber

This material is obtained by wire drawing and cutting rolled steel.

Whether glued, rounded, or with hooked ends, steel fiber comes in the form of steel wires with a diameter of one millimeter and a length of between 35 and 60 mm.

Micro-metal fibers, which are latest-generation materials, are also available on the market. This type of concrete offers optimal mechanical strength.

Metal fibers come in a variety of types and shapes and are highly compatible with concrete. Fig. 1 shows different metal fiber geometries.

- Straight metal fibers (a)
- Hooked metal fibers (b)
- Corrugated metal fibers (c)

- Milled metal fibers (d)

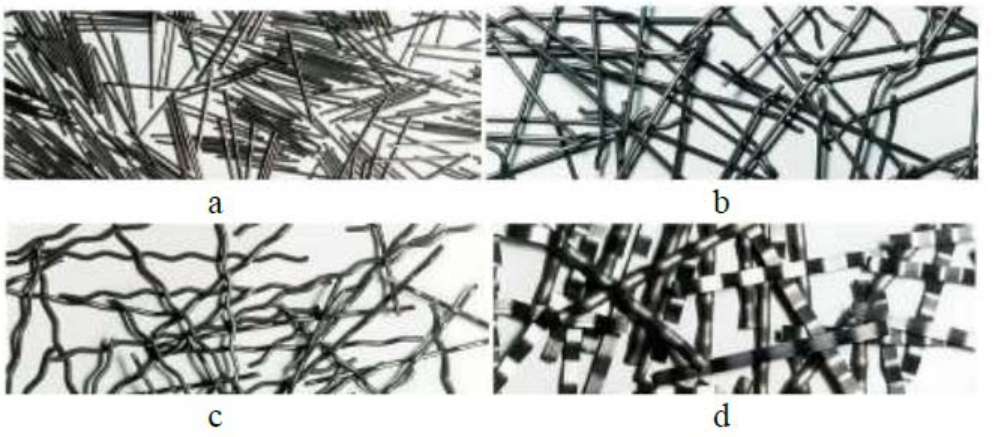

Fig. 1 Different types of fibers [1]

To use fibers, all the ingredients must be mixed for 2 minutes before adding water.
To improve concrete performance, fibers must:

- be flexible without being fragile;
- be relatively long and thin;
- have a large specific surface area;
- offer good deformation capacity;
- ensure good anchoring in the concrete;
- have good adhesion to the cement paste.

Thanks to their mechanical properties, fibers make it possible to better mobilize the intrinsic strength of concrete, produce large thin sections, and offer designers greater architectural freedom.

They give concrete many advantages:

- crack control;
- ease and speed of implementation;
- multidirectional and homogeneous reinforcement;
- partial or total replacement of traditional reinforcement

2.2. The composition of fiber-reinforced concrete

The composition of FRC is very similar to that of ordinary concrete. When designing the mix of fiber-reinforced concrete, the amount of fiber varies depending on the application and type of fiber. In addition, before adding fibers, it must be ensured that they are compatible with the other materials in the mix.

In order to obtain a fluid mix, which is not always easy in the presence of fibers, we must add an admixture. To achieve the correct workability, FRC often requires admixtures such as superplasticizers. These allow to obtain workable concrete, even in the presence of fibers.

The fracture pattern of FRC under tension shows the effect of the fibers: the fibers protrude from the crack surface, indicating that before fracture they connected the

opposite sides of the crack (Fig. 2). This is in fact the main way in which fibers can improve the mechanical behavior of concrete: the bridging effect across the crack, limiting its propagation and opening.

Fig. 2 Fracture pattern of FRC under tension [2]

3. Classification of FRC based on strength and ductility

The classification of FRC according to strength and ductility is carried out, in accordance with the new version of Eurocode 2[3], based on two characteristic values of residual strength obtained from the standard 3-point bending test on notched prisms [4,5]. These are $f_{R3,k}$, the residual strength value for a crack width $w = 2.5mm$, and $f_{R1,k}$, the residual strength value for a crack width $w = 0.5mm$. The value $f_{R3,k}$, rounded down to certain thresholds specified by the standard, gives the strength class, while the value of the ratio $f_{R3,k}/f_{R1,k}$, also rounded down to other thresholds, gives the ductility class. The strength class is expressed by the afore mentioned strength threshold in MPa, a number (1, 1.5, 2, 2.5, 3, 3.5, 4, 4.5, 5, 6, 7, 8), while the ductility class is expressed by a letter (a-e) associated with the ductility threshold (a for $f_{R3,k}/f_{R1,k} > 0.5$; b for $f_{R3,k}/f_{R1,k} > 0.7$; c for $f_{R3,k}/f_{R1,k} > 0.9$; d for $f_{R3,k}/f_{R1,k} > 1.1$ and e for $f_{R3,k}/f_{R1,k} > 0.5$).

4. Calculation of high-strength FRC at ultimate limit state

4.1. Bending calculation

In order to study the influence of certain parameters on the flexural strength and shear strength of a reinforced concrete element, it is first necessary to know the properties of the materials. However, in the specific case of FRC, it is not sufficient to consider only one compressive strength class. This is because the tensile strength class in a cracked state is related not only to the concrete, but also to the quality and quantity of the fibers. Consequently, interdependent concrete strength parameters occur. In this situation, we are led to consider properties corresponding to a real study of the literature (Table 1).

Table 1

Strength and ductility of fiber reinforced concrete [6]

Fiber amount	f_{ck}	Strength and ductility class
$20\ kg\ /\ m^3$	$75\ MPa$	1b
$60\ kg\ /\ m^3$	$75\ MPa$	5a

From this study, not only the strengths for two fiber contents will be used, but also the method for calculation of the resisting bending moment, the ultimate moment, noted $M_{u,d}$. This ultimate moment will be calculated not only for FRC, but also for non-fiber-reinforced concrete, in order to allow a comparison.

The calculation is based on the behavior laws of materials expressed by stress/strain relationships. Depending on the case, the stresses are tensile or compressive. The particularity of FRC consists in the fact that tensile strength is not negligible. Even if the fibers do not prevent the formation of cracks, they oppose their propagation and are subjected to tensile stress at the crack. Their contribution to the strength and stiffness of compressed concrete can be neglected, as it is not significant. Therefore, the behavior laws that need to be taken into account are those of compressed concrete, tension steel reinforcement (and compressed reinforcement, if any), and cracked fiber-reinforced concrete.

Those for compressed concrete and reinforcing steel are known from the strength classes. Behavior laws similar to those in Eurocode 2 [7] are used: parabolic/rectangular for compressed concrete and elastoplastic for steel. For FRC cracked under tension, a stress/crack opening relationship is used [3].

However, in order to determine the ultimate moment for an element at a given section, we do not a relationship between stress and crack opening, but a stress/strain relationship. The solution is to first calculate the relationship between stress and crack opening, and then convert it according to the characteristics of the element into a relationship between stress and strain, which is then taken into account. The tipe of constitutive relationship between stress and crack opening is that illustrated in the article by Buttignol et al (Fig. 3). It is therefore a constant stress f_{Ftu} for crack openings $w < w_u$. The value of the ultimate crack opening, w_u, is determined knowing that only values $w \leq 2.5\ mm$ are acceptable.

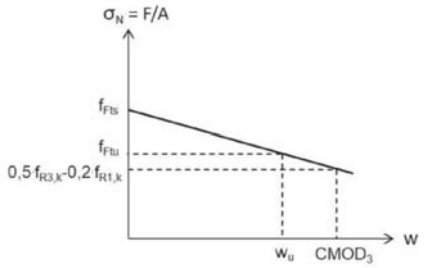

Fig. 3 Stress (σ_N) / crack opening (w) curve for the analysis [6]

In this regard, the values of residual strength in service state, $f_{Fts,k}$, and ultimate limit state, $f_{Ftu3,k}$, are determined from the values $f_{R1,k}$ and $f_{R3,k}$ derived from the strength and ductility class (relations (1) and (2)).

$$f_{Fts,k} = 0{,}45 \cdot f_{r1,k} \quad (1)$$

$$f_{Ftu3,k} = 0{,}5 \cdot f_{r3,k} - 0{,}2 \cdot f_{r1,k} \quad (2)$$

After establishing the constitutive relationship of FRC in tension, the constitutive relationship of compressed concrete is determined. In this regard, the ultimate limit state uses the rectangular block of constant stress, defined based on the factors λ and η, in accordance with Eurocode 2 ((3) and (4)).

$$\lambda := 0{,}8 - \frac{(f_{ck} - 50)}{400} \quad (3)$$

$$\eta := 1 - \frac{(f_{ck} - 50)}{200} \quad (4)$$

For steel, a bilinear behavior law is used, with a horizontal yield point and no stress limit, in accordance with Eurocode 2.

As concerns the section geometry, a rectangular section is used, without compression reinforcement, with a width $b = 12.5\ cm$ and height $h = 25\ cm$, with two longitudinal bars with a diameter $\phi = 16\ mm$, strength class S500, and a cover $c = 20\ mm$.

At this point, it is possible to focus on the constitutive relationship of FRC, and more specifically on the conversion between the stress/crack opening relationship and the one used for calculation, expressed in stress/strain. The essential quantity for this method is the characteristic length, l_{cs}, which is essentially the distance between cracks. In this regard, it is necessary to know the effective height of the tension zone that acts as a tension tie, denoted $h_{c,ef}$. The calculation is performed according to the rules of Eurocode 2 [7], but with a change for the height of compressed concrete, x. For safety reasons, in order to consider the presence of steel fibers, the value corresponding to the ultimate limit state is considered, but neglecting the presence of fibers. The relationships for calculating x and $h_{c,ef}$ are (5) and (6). Consequently, the values of the area of the tie zone working in pure tension, $A_{c,ef}$, and the effective reinforcement ratio, $\rho_{s,f}$, are calculated from the relations (7) and (8).

$$x = \frac{A_s \cdot f_{yd}}{\lambda \cdot \eta \cdot f_{cd} \cdot b} \quad (5)$$

$$h_{c,ef} = \min\left(\left[2{,}5 \cdot (h - d)\frac{h - x}{3}\frac{h}{2}\right]\right) \quad (6)$$

$$A_{c,ef} = b \cdot h_{c,ef} \quad (7)$$

$$\rho_{s,f} = \frac{A_s}{A_{c,ef}} \quad (8)$$

Subsequently, the characteristic length l_{cs} is calculated according to the relationships in the article by Buttignol et al [6]. In order to do this, the average stress in the service state, $f_{Fts,m}$ and the average adhesion stress, τ_{bm} (relations (9) and (10)), are determined using the characteristic service stress, $f_{Fts,k}$ and the average tensile strength of the concrete, f_{ctm}. In this way, we determine the maximum transmission length between cracks, for average stresses, noted $l_{s,max}$ (11), and from this, the maximum distance between cracks, $s_{r,max}$ (12). The characteristic length, l_{cs}, becomes the maximum between the latter and y (the height of the tensioned zone) (13).

$$f_{Fts,m} = \frac{f_{Fts,k}}{0,7} \quad (9)$$

$$\tau_{bm} = 1,8 \cdot f_{ctm} \quad (10)$$

$$l_{s,\max} = k \cdot c + \frac{1}{4} \cdot \frac{\Phi}{\rho_{s,ef}} \cdot \frac{f_{ctm} - f_{Fts,m}}{\tau_{bm}} \quad (11)$$

$$s_{r,\max} = 1,5 \cdot l_{s,\max} \quad (12)$$

$$l_{cs} = \min\left(s_{r,\max} \;\; y\right) \quad (13)$$

Thus, it is possible to determine the ultimate crack opening, w_u, as that corresponding to a strain $\varepsilon_{Fu} = 0.2\%$ (14). Subsequently, the ultimate characteristic stress, $f_{Ftu,k}$ (15), and the ultimate design stress, $f_{Ftu,d}$ (16), are determined using the partial safety coefficient, $\gamma_F = 1.5$.

$$w_u = \min([l_{Cs} \cdot \varepsilon_{Fu} 2,5 \text{ mm}]) \quad (14)$$

$$f_{Ftu,k} = f_{Fts,k} - \frac{w_u}{2,5 \text{ mm}} \cdot f_{Ftu3,k} \quad (15)$$

$$f_{Ftu,d} = \frac{f_{Ftu,k}}{\gamma_F} \quad (16)$$

Then, from the stress-strain relationships of the three components of the section in the ultimate limit state (compressed concrete, steel and cracked concrete), it is possible to determine the resisting (ultimate) moment of the section. First, the height of the compressed concrete, x, is determined from the projection equation onto the section (17). Once this has been determined, it is possible to determine the compressive force in the concrete, R_{cd} (18), and its lever arm relative to the tensioned steel, z_c (19), as well as the tensile force in the cracked concrete, R_{fd} (20) and its lever arm relative to the tension steel, z_f (21). The value of the ultimate moment, M_{ud}, is determined from the moment equation with respect to the center of the tension reinforcement (22).

$$x = \frac{A_s \cdot \sigma_s + f_{Ftu,d} \cdot b \cdot h}{\eta \cdot 0,85 \cdot f_{cd} \cdot b + f_{Ftu,d} \cdot b} \quad (17)$$

$$R_{cd} = n \cdot 0,85 \cdot \frac{f_{ck}}{\gamma_c} \cdot b \cdot x \quad (18)$$

$$z_c = d - \frac{x}{2} \quad (19)$$

$$R_{fd} = f_{Ftu,d} \cdot b \cdot (h - x) \quad (20)$$

$$z_f = \frac{(h - x)}{2} - a_s \quad (21)$$

$$M_{ud} = R_{cd} \cdot z_c - R_{fd} \cdot z_f \quad (22)$$

For concrete without fibers, firstly, the height of the compressed concrete, x (23), is determined and then the value of the ultimate moment from the moment equation written with respect to the center of the tension reinforcement (24).

$$\mathrm{x} = \frac{A_s \cdot f_{yd}}{b \cdot \eta \cdot f_{cd} \cdot 0,85} \quad (23)$$

$$M_{ud} = (b \cdot \eta \cdot x) \cdot f_{cd} \cdot 0,85 \cdot \left(d - \frac{x}{2}\right) \quad (24)$$

4.2. Shear force

The ultimate shear force of FRC reinforced longitudinally, but not transversely, was calculated according to relationship (25):

$$V_{Rd,f} = \left(C_{Rd,c} \cdot k \cdot \left(100 \cdot \rho_l \cdot \left(1 + 7.5 \cdot \frac{f_{Ftu.k}}{f_{ctk}} \right) \cdot f_{ck} \right)^{\frac{1}{3}} \right) \cdot b \cdot d \quad (25)$$

Where f_{ctk} is the tensile strength of concrete without fibers, while $f_{Ftu.k}$ is that of fiber concrete, obtained for a crack opening $w_u = 1.5\,mm$, and f_{ck} is the characteristic compressive strength of concrete.

The resisting shear force of reinforced concrete without fibers, not transversely reinforced, denoted $V_{Rd,c}$ is obtained using relationship (26):

$$V_{Rd,c} = \left(C_{Rd,c} \cdot k \cdot (100 \cdot \rho_l \cdot f_{ck})^{\frac{1}{3}} \right) \cdot b \cdot d \quad (26)$$

5. Parametric study

In order to verify the effectiveness of adding fibers, a parametric study was carried out, focusing on two characteristics: the geometry of the section and the amount of longitudinal reinforcement. To this end, resisting (ultimate) moments and resisting shear forces were calculated for 3 section height/width ratios (noted h/b) and three reinforcement ratios (noted ρ_l). For these cases, the ratios between the resisting moments of FRC and non-FRC ($M_{ud,f}/M_{ud}$) and between the resisting shear forces of FRC and non-FRC ($V_{Rd,f}\ /\ V_{Rd,c}$) were calculated for the two fiber contents ($20kg/m^3$ and $60\ kg\ /\ m^3$). These ratios were represented graphically by means of balls related to the unit reference (Fig. 4).

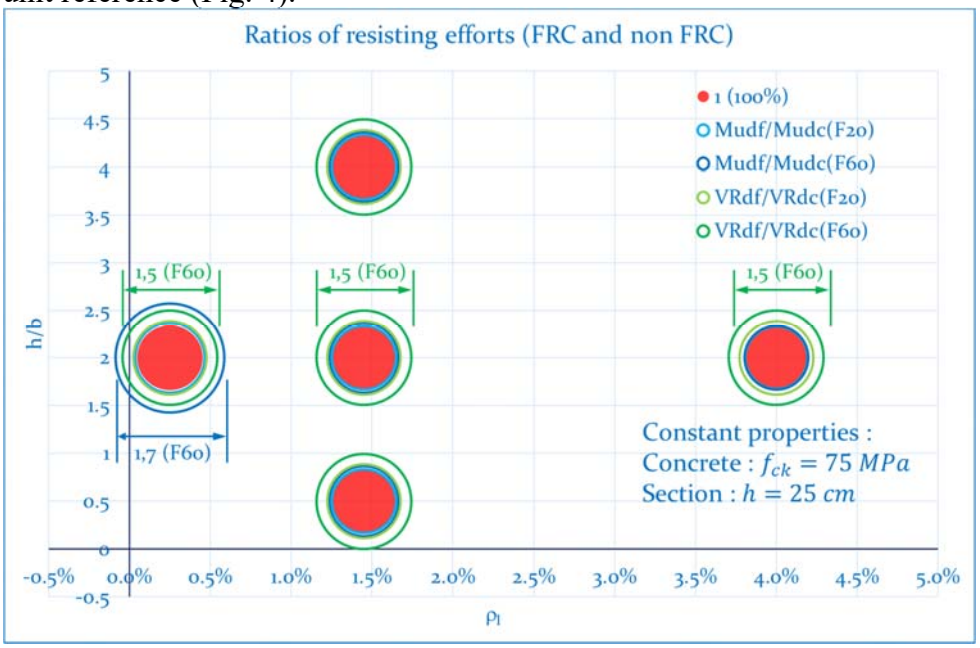

Fig. 4 Ratios between forces with and without fibers for different h/b ratios and longitudinal reinforcement ratios ρ_l

In this figure, we can see that the $M_{ud,f}/M_{ud}$ ratios vary between 1 and 1.11 for FRC with low fiber content ($20kg\ /\ m^3$ shown in light blue) and between 1.02 and 1.7 for concrete with high fiber content ($60\ kg/m^3$ shown in dark blue). The maximum ratios 1.11 and 1.7 were obtained for the lowest reinforcement ratio ($\rho_l = 0.25\%$) and are not influenced by the $h\ /\ b$ ratio on the section (1.02 and 1.11 for the two contents respectively in the presence of $\rho_l = 1.45\%$). For the maximum reinforcement ratio, $\rho_l = 4\%$, the ratios $M_{ud,f}/M_{ud}$ are almost equal to 1 for both fiber contents, the strength increase brought about by the fibers being insignificant. These aspects demonstrate the high effectiveness of fiber addition, particularly in the region of low longitudinal reinforcement ratios and for higher fiber contents. The addition of fibers leads to an increase in ultimate moments, but this is significant particularly for low rates of longitudinal reinforcement, in the range of minimum reinforcement accepted by the standard. At low fiber contents, strength increases are fairly small, even for low longitudinal reinforcement ratios.

In terms of shear forces, the ratios $V_{Rd,f}\ /\ V_{Rd,c}$ range from 1.17 for FRC with low fiber content ($20kg/m^3$ shown in light green) to 1.5 for FRC with high fiber content ($60kg/m^3$ shown in dark green). These ratios are unaffected by either the section slenderness ratio, h/b, or the reinforcement ratio ρ_l. It can therefore be seen that the addition of fibers has a significant effect on shear strength, particularly for higher fiber contents. This observation is valid in the context where the reinforced concrete section considered is transversely unreinforced. Therefore, it would be possible to replace a certain amount of transverse reinforcement with a quantity of fibers that brings about the same increase of resistant shear force. Depending on the case, if the increase needed of resistant shear force is low, even a low fiber content could be sufficient, as its effect is not negligible.

6. Conclusion

In this study, the effect of fiber addition on bending moment and shear strength was investigated for a reinforced concrete element without transverse reinforcement, by varying the cross-section geometry and longitudinal reinforcement ratio.

Bending moment and shear force resistances were obtained in accordance with current standards and with certain adaptations for fiber-reinforced concrete, following procedures used in the literature.

The effect of adding fibers was found to be most significant in terms of increased bending moment, for low longitudinal reinforcement ratios but high fiber content. For low fiber content, the increase in bending moment resistance is quite small, even for low longitudinal reinforcement rates.

As far as shear strength is concerned, the effect is significant for high fiber content, and also not negligible for low contents either.

The practical utility of this study is to verify the possibility of replacing conventional reinforcement by means of steel rebar by adding fibers to the concrete to ensure a certain resisting effort, whether flexural or shear. The results show that this is

possible, particularly for high fiber contents. However, in terms of bending moment, fibers are only effective in the presence of low levels of longitudinal reinforcement.

7. References

[1] L.N. Thrane, Guideline for execution of steel fibre reinforced SCC, Danisk Technological Institute, 2013.
[2] LafargeHolcim, https://app.materlibrary.ro/ro/materiale/LFHCM-3401.
[3] CEN, EN 1992-1-1:2023 Eurocode 2: Design of concrete structures – general rules and rules for buildings, bridges and civil engineering structures, 2023.
[4] European Standards, Test method for metallic fibered concrete - Measuring the flexural tensile strength (limit of proportionality (LOP), residual), Eur. Stand. CEN. (2005) 1–17.
[5] RILEM TC 162-TDF, RILEM TC 162-TDF : Test and design methods for steel fibre reinforced concrete: Bending test, Mater. Struct. 33 (2000) 3–5. http://www.springerlink.com/index/10.1007/BF02481689.
[6] T.E.T. Buttignol, J.F. Fernandes, T.N. Bittencourt, J.L.A.O. Sousa, Design of reinforced concrete beams with steel fibers in the ultimate limit state, Rev. IBRACON Estruturas e Mater. 11 (2018) 997–1024. https://doi.org/10.1590/s1983-41952018000500006.
[7] CEN, EN 1992-1-1:2004. Eurocode 2: Design of concrete structures-Part 1: General rules and rules for buildings, 2004.

Effects of Bitumen Content on the Quality of Asphalt Used for the Construction of Flexible Pavements

Efectele conţinutului de bitum asupra calităţii asfaltului utilizat pentru construcţia pavejelor flexibile

Olufikayo Aderinlewo[1], Israel Olabode[1], Funso Orogbangba[1], Sunday Akinte[1], Matthias Abraham[1]

[1]Civil Engineering Department
Federal University of Technology Akure, Nigeria
Email: *oluade2010@gmail.com, israel.oluwatosin.olabode@gmail.com, abrahammathias66@gmail.com, funsoorogbangba96@gmail.com, akinteoluwabunmisunday@gmail.com*

DOI: 10.37789/rjce.2026.17.1.2

Abstract: Road pavements in Nigeria and other developing regions are often faced with premature failures due to suboptimal asphalt mix designs, particularly related to bitumen content (5%, 6%, 7% and 8%) as this affects the mechanical and durability properties of asphalt used for flexible pavement construction. Laboratory tests, including penetration, ductility, viscosity, flash and fire points, Marshall Stability, flow, bulk density, air voids and drying shrinkage tests were conducted. The results indicate that an optimum bitumen content of approximately 6.67% provides the best balance of stability, density and durability. Higher contents lead to excessive deformation and rutting, while lower contents result in inadequate cohesion and strength. These findings highlight the importance of adequate mix design to enhance pavement performance and longevity in similar conditions

Keywords: bitumen content, asphalt, flexible pavement, Marshall Stability, optimum

1. Introduction

The transportation industry is an important aspect of the economic growth of any given country, since road systems contribute to commerce, trade and social interaction [1]. Flexible pavements are the most common types of pavements because of their low cost of construction, maintenance and their ability to accommodate different traffic demands [2]. Hot mix asphalt, comprising aggregates and bitumen as a binding agent, is the main material used in flexible pavement construction. The composition of asphalt pavements and bitumen content are the key factors that determine the performance of these materials and durability of asphalt pavements [3].

The surface layer of the pavement structure is the most important layer as it is

The article was received on 26.01.2026, accepted on 02.02.2026 and published on 24.02.2026

expected to provide the ultimate function of an economic, safe and comfortable riding surface to users thereby protecting the sub- structure layers from infiltration of water and foreign materials and distributing stresses from axle loads satisfactorily to layers beneath without comprising durability [4].

Bitumen is a viscoelastic material that provides cohesion within asphalt mixtures, ensuring structural stability and resistance to external loads [5]. However, variations in bitumen content can significantly affect pavement performance. A low bitumen content results in weak bonding between aggregates, leading to high air voids, premature cracking and raveling. Conversely, excessive bitumen content can cause bleeding, rutting and reduced resistance. Thus, determining the optimal bitumen content is essential for achieving a balance between durability and flexibility in asphalt pavements.

In Nigeria, road infrastructure continues to face challenges such as premature failure, potholes and frequent maintenance due to poor asphalt mix design. Several roads deteriorate within a few years of construction,
quality of asphalt used in flexible pavements construction, with a focus to improving mix design for better road performance.

2. Methodology

This study adopts an experimental research design, which is appropriate for evaluating the effects of varying bitumen content on the quality of asphalt used in the construction of flexible pavements. The experimental design involves the laboratory preparation and testing of asphalt samples with different bitumen contents to assess their mechanical and durability properties. The results obtained from these tests will provide empirical evidence on the optimal bitumen content required to achieve high-quality asphalt pavement [7].

2.1 Sample Collection and Preparation

The materials used for this study include bitumen and aggregates (coarse and fine) and filler material. The bitumen was sourced from a bitumen supplier in Omuo-Ekiti, Ekiti State, Nigeria. The grade of the bitumen used was 60/70 grade. The aggregates (granite and stone dust) were sourced from a sales point along Akure- Ijare road. The filler material is a modified material made from combining crushed ceramic tiles sourced locally and very fine stone dust.

Asphalt samples were prepared with varying bitumen contents to determine its impact on asphalt performance. The bitumen content variations were set at 5%, 6%, 7% and 8% by weight of the total mix. These percentages were chosen based on Federal Ministry of Works (FMW 2007) standards [8]. The aggregates and bitumen were thoroughly mixed under controlled conditions to ensure even distribution and proper coating of the aggregates, creating consistent and reliable samples for testing.

The asphalt mixtures were shaped into cylindrical specimens using a Marshall compactor, ensuring they were ready for testing. Compaction was carried out following standard protocols to guarantee consistent density and structural integrity across all samples. Once compacted, the specimens were left to cure properly before being subjected to laboratory tests. This step ensures the samples are stable and representative of real-world conditions for accurate evaluation.

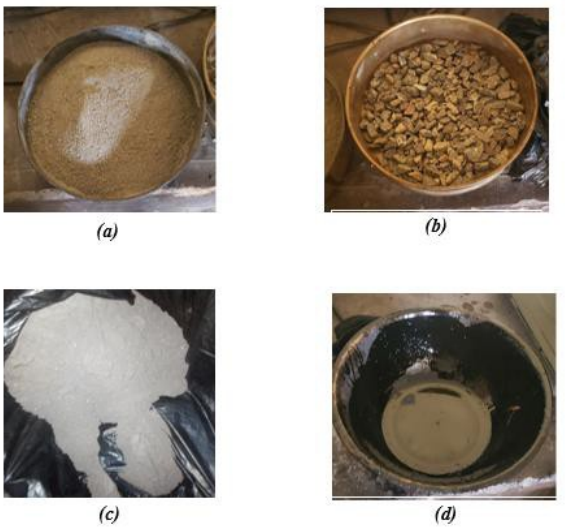

Figure 1 (a) to (d): Materials used in preparing the asphalt samples.
(a) stone dust, (b) granite, (c) filler material, (d) bitumen

Figure 2: Cast Asphalt Samples

2.2 Laboratory Tests

All laboratory tests were carried out at the Transport and Materials Laboratory in the Department of Civil and Environmental Engineering, Federal University of Technology Akure (FUTA), Akure, Nigeria. To evaluate the effects of bitumen content on asphalt quality, the following laboratory tests were conducted:

2.2.1 Bitumen Tests

- Penetration Test: The penetration test evaluates the hardness or softness of bitumen by measuring how far a standard needle can penetrate into it under controlled

conditions. The test is conducted at 25°C with a penetrometer having a 100-gram weight applied for 5 seconds. The depth of penetration is measured in tenths of a millimeter [9].

- Viscosity Test: The viscosity test checks how easily bitumen flows at different temperatures. It is usually carried out at 60°C (representing road temperature) and 135°C (representing mixing and compaction temperature). The test is conducted using a viscometer, which measures how much time it takes for bitumen to flow through a standard orifice [10].
- Flash and Fire Point Test: The flash and fire point test determines the temperatures at which bitumen controlled manner. In the Pensky-Martens closed-cup apparatus method, a sample of binder is placed in a sealed cup that is gradually heated (typically at 5-6°C/min) while a standardized ignition source is introduced at regular temperature intervals [11].
- Ductility Test: The ductility test measures how far bitumen can be stretched before breaking, indicating its ability to form a continuous film and resist cracking. It involves heating bitumen to a fluid state and pouring it into a briquette mould. The filled mould is cooled in air for 30-40 minutes, then placed in water bath at a standard temperature for a specified time [12].
- Specific Gravity Test: The specific gravity test determines the density of binder relative to water by using a calibrated pycnometer at 25°C: after heating the bitumen, the empty pycnometer is weighed (M_1), then filled with water (M_2), partly filled with bitumen and submerged (M_3) and finally filled with bitumen topped to the mark with water (M_4). The specific gravity is then calculated as shown in equation 1 [13].

2.2.2 Asphalt Mechanical Tests

- Marshall Stability Test: Marshall Stability refers to the maximum load an asphalt sample can withstand before failure, while flow measures the extent of deformation under loading. The Marshall Stability Test is essential in determining the strength and stability of asphalt mixtures. It involves loading a compacted asphalt specimen until failure to measure its maximum load-bearing capacity [14].
- Durability Tests: Durability tests assess how well asphalt can withstand long-term exposure to environmental conditions such as temperature changes, moisture and oxidation. Durability tests were conducted to assess the resistance of asphalt to weathering and aging. These tests simulate long-term exposure to environmental conditions such as moisture, temperature variations and oxidation [15].

3 Results and Discussions

The fundamental properties of the bitumen were evaluated to establish a baseline for mix design and to assess its conformity with typical specification requirements.

3.1 Analysis of the Bitumen Properties

3.1.1 Penetration Test

The penetration test measures the hardness of bitumen by measuring the depth (in tenths of a millimeter) a standard needle penetrates under specified conditions. The average penetration value of 69.3 as shown in table 1 places the bitumen in the 60/70 grade. The results indicate that the bitumen has a balanced consistency and can resist deformation under loading while maintaining flexibility [9].

Table 1

Penetration test values

S/N	First trial (d-mm)	Second trial (d-mm)
1	75.80	66.90
2	76.20	67.40
3	69.20	60.30
AVG		**69.3**

3.1.2 Ductility Test

Ductility measures the distance a standard briquette of bitumen can be elongated before breaking, indicating its tensile properties and internal cohesion. The average ductility value recorded as shown in table 2 suggests that the bitumen is relatively highly flexible and capable of withstanding significant elongation before failure. According to standard specifications, ductility value should be ≥100cm, which indicates good quality for most paving applications [12].

Table 2

Ductility Test Results

S/N	Ductility Tests (cm)
1	88.00
2	84.10
3	137.20
AVG	**103.10**

3.1.3 Flash and Fire Point Tests

The flash point is the lowest temperature at which the binder produces ignitable vapors, while the fire point is the lowest temperature at which sustained combustion occurs. These are critical safety parameters for handling and mixing. The flash point, as shown table 3, is relatively low for bitumen, particularly for grade 60/70 bitumen. According to standard specifications, a minimum flash point of 220°C is required for safety during storage, transportation and hot-mix asphalt production. The flash point suggests that the bitumen may release volatile vapors at a lower temperature, increasing the risk of ignition during heating process [11].

Table 3

Flash and fire point Test Results

S/N	Flash point (^{0}C)	Fire point (^{0}C)
First trial	172.3	221.2
Second trial	167.5	240.0
AVG	**169.9**	**230.6**

3.1.4 Viscosity Tests

Viscosity measures the bitumen's resistance to flow. The average viscosity value, as shown in table 4 suggests that the bitumen is relatively resistant to flow within a 60/70 grade, which can enhance resistance to rutting, especially in hot climates [10].

Table 4

Viscosity Test Results

S/N	Viscosity Reading (mPa.s)
1	3442.00
2	3360.00
3	3259.00
AVG	**3353.67**

3.1.5 Specific Gravity Test

The specific gravity of the bitumen was determined using a pycnometer and the following weights:
Weight of empty bottle M_1 = 63.12g
Weight of bottle + Sample M_2 = 87.13g
Weight of bottle + sample + water M_3 = 122.71g
Weight of bottle + water = M_4 = 122.35g

$$\text{Specific gravity (SG)} = \frac{M_2 - M_1}{(M_4 - M_1) - (M_3 - M_2)}$$

$$\text{SG} = \frac{87.30\text{-}63.12}{(122.35\text{-}63.12)\text{-}(122.71\text{-}87.30)}$$

SG=1.02

3.2 Marshall Mix Design Analysis for Optimum Bitumen Content

The Marshall mix design method was employed to determine the optimum content by evaluating key performance parameters across a range of bitumen contents (5% to 8%). The relationship between bitumen content and these properties (shown in table 5) is fundamental in understanding mix behaviors [14].

Table 5

Relationship between bitumen percentages and stability and flow values

% bitumen	Dry weight (g)	Wet weight (g)	Submerged weight	Stability in kg	Flow in mm
5%	984.58	992.77	562.25	22.91	3.79
6%	1007.70	1013.73	581.45	18.65	3.91
7%	1035.32	1040.10	586.17	23.19	6.06
8%	1058.30	1063.25	601.23	20.06	5.94

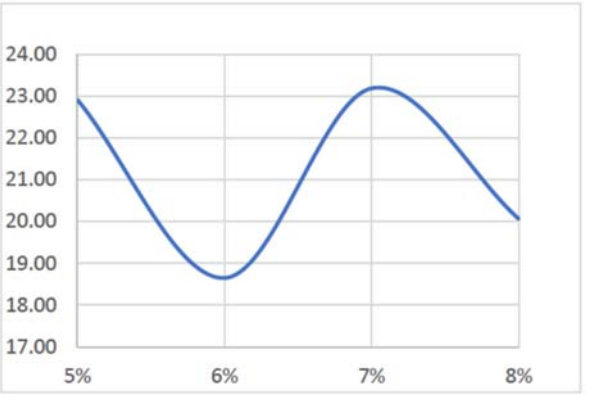

Figure 2: Graph of stability against bitumen percentages

The stability values, as in figure 1, demonstrate a non-linear relationship, initially decreasing from 5% to 6% before peaking at 23.19 kg for the 7% mix and then decreasing at 8%. This occurs because at low bitumen contents (i.e. 5%), the mix is lean and incomplete coating of aggregates leads to lower cohesion and stability. As bitumen increases to 7%, it provides optimal coating and lubrication during compaction, resulting in a strong, cohesive matrix that maximizes internal friction and stability. At high bitumen contents (i.e. 8%), excess binder acts as a lubricant, pushing aggregates particles apart and reducing inter-particle friction and stability [14].

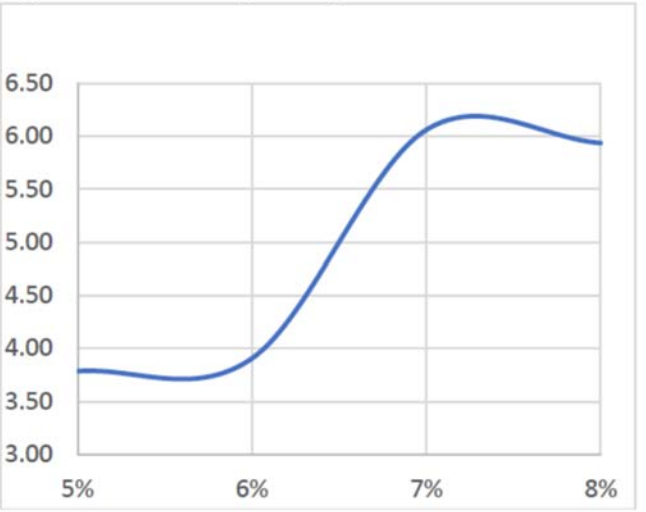

Figure 3: Graph of flow against bitumen percentages

The flow values, as shown in figure 2, indicate a significant increase after 6% bitumen content. The rise from 3.91 mm at 6% bitumen content to 6.06 mm at 7% bitumen content indicates a transition from a stiff and elastic mix to a more plastic and deformable one. According to standard specification, the typical acceptable flow range is 2-4 mm. The 7% and 8% mixes exceed this limit, indicating a potential for excessive plastic deformation and rutting under traffic [14].

Calculation of Bulk density

$$\text{Specific Gravity } (G_{mb}) = \frac{\text{dry mass}}{\text{saturated surface dry mass} - \text{mass of sample submerged in water}} \quad (2)$$

For 5%, $G_{mb} = \frac{984.58}{992.77-562.25} = 2.29$

For 6%, $G_{mb} = \frac{1007.70}{1013.73-581.45} = 2.33$

For 7%, $G_{mb} = \frac{1035.32}{1040.10-586.17} = 2.28$

For 8%, $G_{mb} = \frac{1058.30}{1063.25-601.23} = 2.29$

Table 6

Relationship between Bulk density and varying bitumen contents

% bitumen	Bulk Specific Gravity
5%	2.29
6%	2.33
7%	2.28
8%	2.29
AVG	**3353.67**

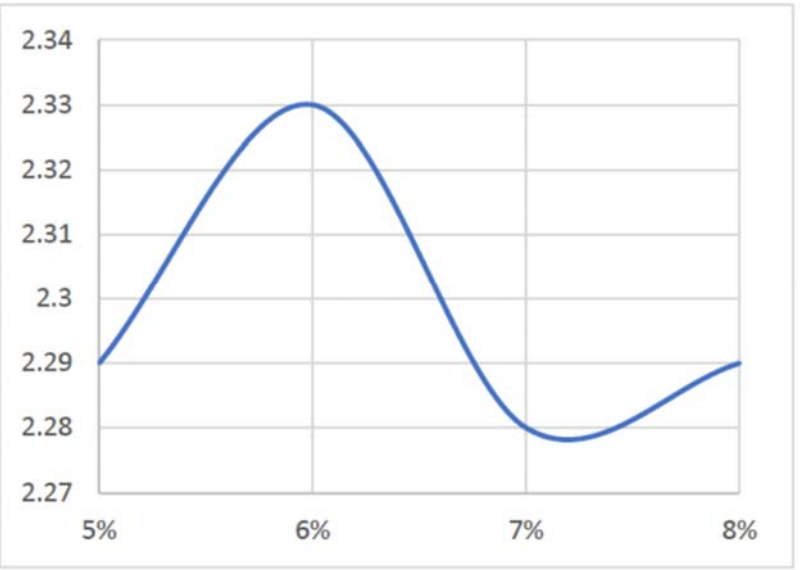

Figure 4: Graph of bulk density against bitumen percentages

The bulk specific gravity (G_{mb}), representing the bulk density (as in figure 3) of the compacted mix shows a clear peak at 6% bitumen content. This occurs because up to 6%, the additional bitumen provides better lubrication, allowing aggregate particles to be arranged into a denser configuration during compaction. Beyond 6%, the volume of bitumen exceeds the void space available in the mineral aggregates' matrix. Since bitumen is less dense than aggregate, the overall mix density begins to decrease.

Calculation of Percentage Air Voids

$$P_a = \frac{Gmm - Gmb}{Gmm} x100 \quad (3)$$

P_a - percentage air voids in in the asphalt samples
G_{mm} - maximum specific gravity of the asphalt samples
G_{mb} - bulk specific gravity of the asphalt samples

But maximum specific gravity (G_{mm}) is given as

$$G_{mm} = \frac{100}{\left(\frac{Ps}{Gse}\right)+\left(\frac{Pb}{Gb}\right)} \quad (4)$$

G_{mm} - maximum specific gravity of the asphalt samples
P_s - Percentage by weight if aggregates
P_b - Percentage by weight of bitumen
G_{se} - Effective specific gravity of the aggregates (assumed to be constant for different asphalt contents
G_b - Specific gravity of asphalt
$P_s = 95\%$
$G_{se} = 2.7$ [13]
$P_b = 5\%$ to 8%
$G_b = 1.02$ (from laboratory tests)

$$\therefore \text{For } 5\%,\ G_{mm} = \frac{100}{\left(\frac{95}{2.7}\right)+\left(\frac{5}{1.02}\right)} = 2.495$$

$$\text{For } 6\%,\ G_{mm} = \frac{100}{\left(\frac{95}{2.7}\right)+\left(\frac{6}{1.02}\right)} = 2.435$$

$$\text{For } 7\%,\ G_{mm} = \frac{100}{\left(\frac{95}{2.7}\right)+\left(\frac{7}{1.02}\right)} = 2.378$$

$$\text{For } 8\%,\ G_{mm} = \frac{100}{\left(\frac{95}{2.7}\right)+\left(\frac{8}{1.02}\right)} = 2.324$$

$$\therefore P_a = \frac{Gmm - Gmb}{Gmm} \times 100$$

$$\text{At } 5\%,\ P_a = \frac{2.495 - 2.29}{2.495} \times 100 = 8.032\%$$

$$\text{At } 6\%,\ P_a = \frac{2.435 - 2.33}{2.435} \times 100 = 4.312\%$$

$$\text{At } 7\%,\ P_a = \frac{2.378 - 2.28}{2.28} \times 100 = 4.121\%$$

$$\text{At } 8\%,\ P_a = \frac{2.324 - 2.29}{2.324} \times 100 = 1.463\% \quad (5)$$

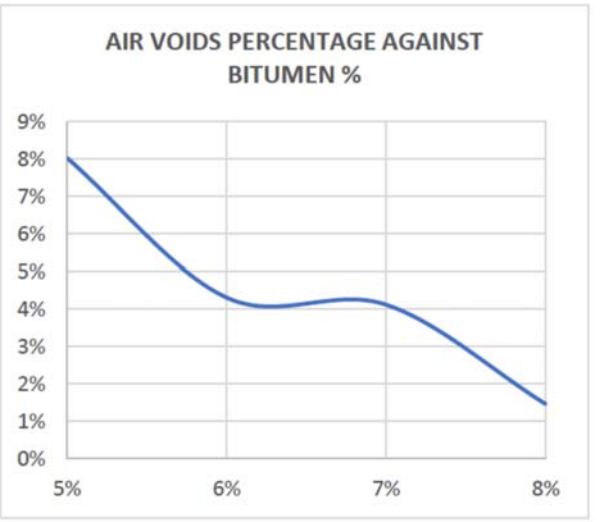

Figure 5: Graph of percentage air voids against bitumen percentages

The percentage of air voids (VTM), as shown in figure 3, exhibits a steady, inverse relationship with bitumen content. This is a result of the additional binder progressively filling the voids between the compacted aggregates particles. According to standard specification, the target air void percentage is 4%, which is achieved at approximately 7% bitumen content. Air void below 3% can lead to bleeding and rutting, as seen in the 8% mix [15].

Calculation of Optimum Bitumen Content

Optimum Bitumen Content

$$= \frac{Optimum\ Marshall\ stability + Optimum\ bulk\ density + 4\%\ air\ voids}{3}$$

$$= \frac{7 + 6 + 7}{3}$$

$$= \frac{20}{3}$$

$$= 6.67\% \quad (6)$$

3.3 Analysis of Drying Shrinkage Test

Table 7

Drying shrinkage values of the varying bitumen content

% bitumen	after casting			after 7 days				after 28 days			
	diameter (cm)	height (cm)	Volume (cm^3)	diameter (cm)	height (cm)	Volume (cm^3)	% volume change	diameter (cm)	height (cm)	Volume (cm^3)	% volume change
5%	10.20	5.92	483.80	10.13	5.90	475.57	-1.70%	10.12	5.82	468.20	-3.23%
6%	10.23	5.92	486.65	10.21	5.90	483.11	-0.73%	10.20	5.62	459.29	-5.62%
7%	10.18	6.27	510.40	10.05	6.21	492.69	-3.47%	10.00	6.03	473.66	-7.20%
8%	10.27	6.30	521.95	10.12	6.09	489.92	-6.14%	10.05	6.00	476.02	-8.80%

All samples shrank over the 28-day period. This is because as the bitumen cures, volatile materials evaporate and the materials consolidate under their own weight. The highest total volume loss occurs at 6% bitumen content. Its significant height loss is a major red flag for stability. At 8% bitumen content, the volume loss was highest overall, indicating poor initial stability. At 7% bitumen content, the mix shrank more uniformly and in a stable manner; its deformation was mostly complete after the first 7 days, showing good curing stabilization. At 5% bitumen content, the mix showed gradual but consistent shrinkage, which may be as a result of insufficient binder content.

In summary, it can be deduced that the optimal bitumen content for achieving the best balance of initial workability and long-term dimensional stability of the mix was at 7%.

4. Conclusions

This study investigated the effects of bitumen content (5%, 6%, 7% and 8%) on the properties of asphalt for flexible pavement construction using the Mashall mix design method. Based on the laboratory experiments and subsequent analysis, the following conclusions are drawn [7]:

i. Determination of Optimum Bitumen Content (OBC): The study established the optimum bitumen content (OBC) for the specific materials and conditions tested. The OBC was calculated to be 6.67%, derived from the optimum values for Marshall Stability, Bulk Density and 4% Air Voids. This value falls within the range specified by the Federal Ministry of Works (FMW) Nigeria standards (i.e. 5.0% -8.0%) and represents the binder proportion that provides the best balance of strength, density and durability [8].

ii. Effects on Mechanical Properties: The bitumen content significantly influenced the mechanical properties of the asphalt mix. Marshall Stability, which indicates load-

bearing capacity, peaked at 7% bitumen content. However, the flow value at this percentage bitumen content exceeded the acceptable standard range (i.e. 2-4mm), indicating excessive deformation. At 6% bitumen content, the mix showed a better balance of adequate stability and acceptable flow, highlighting the trade-off between strength and flexibility [14].

iii. Effects on Volumetric Properties: The bulk specific gravity, which is related to density and compactness, was highest at 6% bitumen content. The percentage of air voids (Pa) decreased progressively with increasing bitumen content. The 4% air void criterion was met at approximately 7% bitumen content. This demonstrates that volumetric properties are highly sensitive to binder content and are critical for determining the OBC [13].

iv. Dimensional Stability: The drying shrinkage test revealed that all samples experienced volume reduction over 28 days. The mix with 7% bitumen content demonstrated the most uniform and stable curing behavior. This suggests that the OBC provides not only good mechanical and volumetric properties but also superior long-term dimensional stability, reducing the potential for cracking.

v. Bitumen Binder Quality: The tests on the bitumen with 60/70 penetration grade showed a high ductility value (103.10cm), indicating good flexibility and cohesion. However, the flash point (169.9°C) was below the standard safety threshold (i.e. 220°C according to ASTM standards), necessitating strict temperature control during handling and production to prevent fire hazards [11].

References

[1] Garber, N.J. and Hoel, L.A. (2009). Traffic and Highway Engineering. Fourth Edition. Canada: Cengage Learning.
[2] Fadhi, T. H., & Ahmed, T. M. (n.d.). Flexible pavement layers. University of Anbar, College of Engineering – Department of Civil Engineering.
[3] Pipintakos, G., Sreeram, A., Mirwald, J., & Bhasin, A. (2024). Engineering bitumen for future asphalt pavements: A review of chemistry, structure and rheology. Materials & Design, 244, Article 113157.
[4] Raja, E. W. (2021). Basic components of road structure and method of construction. The Civil Engineering.
[5] Indian Institute of Technology Bombay. (n.d.). Pavement materials: Bitumen.
[6] Juta, E. (2021). Assessment of factors affecting road pavement design and remedial actions. Journal of University of Shanghai for Science and Technology, 23, 962–973.
[7] Asphalt Institute. (2020). MS-2 asphalt mix design methods (8th ed.). Asphalt Institute.
[8] Federal Ministry of Works. (2007). General specifications for roads and bridges. Federal Ministry of Works.
[9] American Association of State Highway and Transportation Officials. (2021). Standard specification for penetration-graded asphalt cement for use in pavement construction (AASHTO M 20-21/M 20M-21).
[10] Federal Highway Administration. (2019). Performance-based asphalt binder specification

guidelines. U.S. Department of Transportation.
[11] American Association of State Highway and Transportation Officials. (2018). Standard specifications for transportation materials and methods of sampling and testing. American Association of State Highway and Transportation Officials.
[12] American Association of State Highway and Transportation Officials. (2020). Guide for design of pavement structures. American Association of State Highway and Transportation Officials.
[13] Florida Department of Transportation. (2021). Flexible pavement design manual.
[14] Gilson Co. (2020). Marshall test method: Everything you need to know.
[15] National Asphalt Pavement Association. (2021). Effect of asphalt binder content on pavement life cycle performance.

Proposals to energy efficiency cooling processes and hot water preparation in buildings located near surface water sources

Propuneri de eficientizare energetică a proceselor de răcire și prepararea apei calde în clădiri situate în apropierea surselor de apă de suprafață

Adriana Tokar[1], Marius Adam[1], Daniel Bisorca[1], Cristian Păcurar[1], Alexandru Dorca[1], Dănuț Tokar[1], Daniel Muntean[1]

[1] University Politehnica Timișoara.
Piața Victoriei 2, Timișoara 300006, Romania
E-mail: adriana.tokar@upt.ro, marius.adam@upt.ro, daniel.bisorca@upt.ro, cristian.pacurar@upt.ro, alexandru.dorca@upt.ro, danut.tokar@upt.ro, daniel-beniamin.muntean@upt.ro

DOI: 10.37789/rjce.2026.17.1.3

Abstract. *The article aims to present in general terms a concept that can be applied to streamline the cooling and hot water preparation processes in buildings located near surface water sources. The proposed solutions use logical principles, available equipment and are economically accessible from the point of view of cost-benefit analysis.*

Key words: energy efficiency, free cooling, hot water, water-water heat pump

1. Introduction

In recent years, reducing energy consumption in buildings has become a priority, especially in developed countries around the world, and has led to significant efforts in terms of improving energy efficiency and implementing it in all building categories [1]. In practice, the concept of energy efficiency in buildings is related to the energy supply necessary to ensure environmental comfort conditions while minimizing energy consumption [2], [3]. In most building categories (residential, public, industrial, etc.) most of this energy is used in heating, cooling and mechanical ventilation systems and it is expected that by 2050, energy consumption for cooling buildings will triple [4], especially in urban areas. A distribution of energy consumption for residential and commercial buildings is shown in Fig. 1.

The article was received on 28.04.2025, accepted on 02.02.2026 and published on 24.02.2026

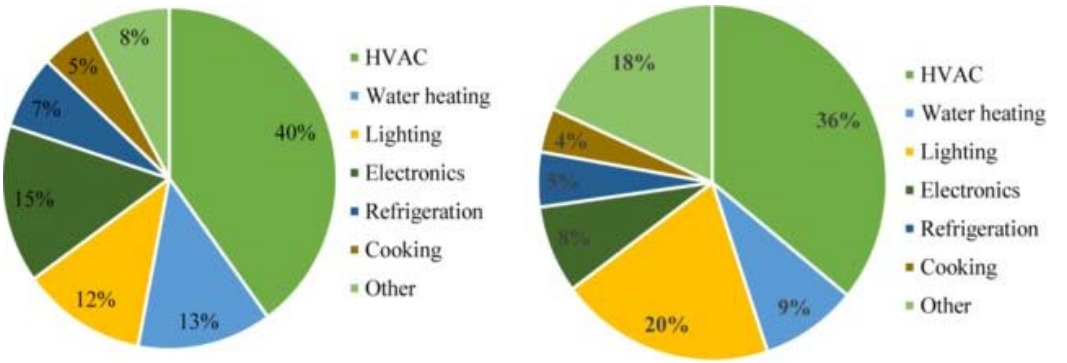

Fig. 1. Energy consumption distribution [4-7]
a) commercial buildings, b) residential buildings

F. J. Zarco-Soto et all. say that it is expected that by 2030, in the world, the population living in cities will reach 60% and by 2050 it will exceed two thirds. Moreover, currently, in Europe these percentages exceed 75%, and it is estimated that in 2050 they will reach 85% [8]. Therefore, the highest energy consumption is and will be recorded in urban areas. In 2023, in a report by the United Nations Environment Programme, it is stated that the built environment sector is responsible for 37% of CO2 emissions and over 34% of global energy demand [9].

On the other hand, F. J. Zarco-Soto et all. and Shahrokni et al. also say that, usually, natural gas is used for heating buildings, and electricity for cooling [8], [10]. Practically, for a correct approach to energy efficiency solutions, it is necessary that design criteria that can reduce energy demand are addressed in the design phase. Regarding the heating and cooling of buildings, the criteria are based on the adoption of appropriate parameters, the parameters that are synthesized by Ekici and Aksoy, as follows [11]:

- *physical parameters of the environment:*
  - daily outdoor temperature, in °C;
  - solar radiation, in W/m^2;
  - wind direction and speed, in m/s.
- *design parameters:*
  - building form factor and orientation;
  - thermophysical properties of building materials;
  - building spacing;
  - type of roof;
  - glazed surfaces;
  - shading systems;
  - passive heating and cooling mechanisms.

Thus, to design an energy-efficient building, the design variables and parameters of the building must be optimized [12], and the integration of sustainable strategies should be done in the conceptual design phase. W. Wang et al. demonstrated that if these mechanisms are put into action right at the beginning of the construction phase, the implementation costs will be reduced compared to the situation in which

they are implemented in the later stages of construction [13]. Obviously, these concepts based on energy-saving criteria will reduce costs and CO_2 emissions throughout the life of the building, due to lower energy consumption, and this is worth more than a large initial investment.

Typically, building cooling can be achieved using passive or active methods, such as:

- passive cooling: natural ventilation (indoor air refreshening by creating a volumetric flow to dissipate heat) [14], [15], thermal mass (the material's property to absorb, store, and release heat - thermal lag is the time rate at which a thermal material releases the stored heat) [16], evaporative cooling (the process where water evaporates, absorbing latent heat and cooling the surroundings-used for dry climates) [17], [18], etc;
- active cooling: earth-to-air heat exchanger-ground coupling (an earth-to-air heat exchanger draws ventilation supply air through buried ducts or tubes in the ground) [1], [19], open or closed loop water-to-air heat exchanger (exploits the relatively stable temperature) [20], mechanical (or forced) ventilation (is driven by fans or other mechanical plant and can be of several types, for example: wall fan extract ventilation system, the roof fan extract ventilation system, the spot cooling system, etc) [21] , chilled water (Chilled water is typically provided by chiller units using absorption refrigeration or compression refrigeration) [22], [23], refrigerants (is based on the flow of refrigerant between an external condensing unit and multiple internal evaporators - typically fan coil units) [24], [25], etc.

Taking into account all the aspects presented above, the article proposes a conceptual approach to energy efficiency of cooling processes and hot water preparation in buildings located near surface water sources. For cooling buildings, it is proposed to reduce energy consumption by approaching the free cooling concept. The proposed free cooling system involves using the thermal potential of surface waters to cool buildings. That is, when surface water is cold enough, it can be used as a cooling medium or as a direct source of cold for buildings. Recent studies by the authors have shown that the external temperature of surface water (Bega Chanel) in the city of Timișoara in Romania is lower than the temperature inside buildings for the summer period, making free cooling of the analyzed space possible [26]. Studies by Hainan Zhang et al. show this is true for a long period of the year [27]. Recently, a new type of free cooling system has been developed and put into operation, namely the heat pipe cooling system, which can achieve considerable reductions in building energy consumption [28], but raises problems regarding the transmission of bacteria inside buildings.

2. Description of the concept

The concept is based on the use of the most favorable thermal potential for the preparation and supply of chilled water necessary for cooling indoor spaces. Such a cooling system is mainly composed of a water-water heat pump that uses, according to a logical prioritization system, a low-potential coolant from various sources, namely: water from the surface source, atmospheric air, cold water used for the preparation of hot water for consumption or for the consumption of sanitary objects.

Figure 2 presents the concept of a system that proposes energy efficiency the cooling processes and the preparation of hot water in buildings located near surface water sources using a heat pump and a local electricity production system using photovoltaic panels.

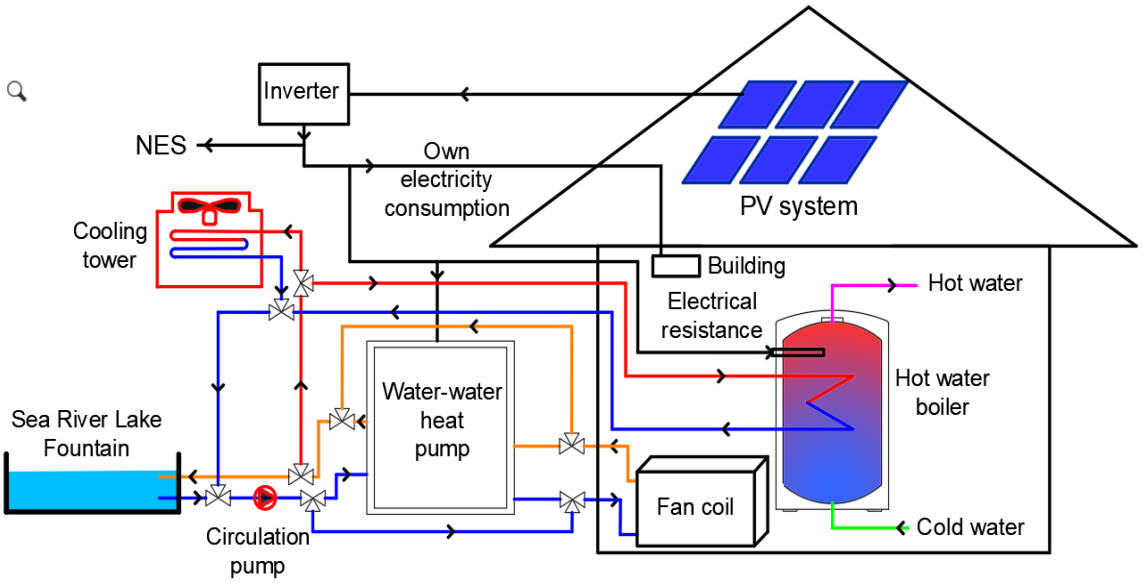

Fig. 2. Schematic diagram for energy efficiency of the cooling and hot water preparation system

The proposed concept can be applied, in the general situation proposed, for the energy efficiency of existing buildings. An improved version, with an electrical energy storage system and a diurnal storage system for chilled and hot water, is generally suitable as a solution for the design and construction of new buildings because they may require additional spaces to accommodate this equipment. In the case of the latter, the implementation of a cooling/heating system that allows the accumulation of thermal energy in the building's construction elements must also be considered.

The entire system is based on the logical correlation of input data that the automation system processes and interprets in order to make the best decision for prioritizing the energy sources that will be used so that the overall efficiency of the installation is optimal for the respective conditions.

Among the input data required by the system, we list: indoor temperature, outdoor air temperature, surface water source temperature, cold water temperature, hot water temperature, photovoltaic system electricity production, building operating

schedule, cooling demand, heating demand, hot water demand, weather forecast, thermal inertia of the envelope system, annual history of surface water temperatures, etc.

All this data will be integrated into the building and HVAC control system so that the control system operates automatically and requires minimal operator intervention.

The physical implementation of the logical signals and decisions will be made simply by starting up equipment and operating three-way valves that will open/close various circuits as needed. The main elements of the system are temperature sensors, pressure gauges, and the PLC or ECL control system.

The conditioning method will be done by transmitting the given signals depending on the state of some logical operators of the type (and, or, etc.)

For even greater energy independence, the proposed concept also allows for other subsequent developments such as:

- using a system for storing electrical energy in accumulators to be used by HVAC systems when their efficiency is maximum;
- extracting the energy necessary to prepare hot water for consumption from surface water using a heat pump;
- the inclusion of solar panels for direct preparation of hot water and for providing a contribution to cover the thermal energy requirement during the cold season;
- use of tanks for accumulation in the daytime of cooled water and heated water in order to increase the energy efficiency of the system;
- analyzing the possibility of using the public district heating network to supply the adjacent buildings with surplus chilled water and hot water in case of availability (for example during the holidays);
- the system is designed to allow periods of the year when the surface water temperature allows, the use of the free/direct cooling mode of the interior spaces, reducing in this situation the consumption of electricity to a minimum.

3. Conclusions

Given the European Union's assumed objective of reducing the energy consumption of all public buildings by 2050, it is imperative to identify and exploit to the maximum and in a realistic manner all locally available renewable natural resources and all forms of residual energy resulting from technological, commercial or residential processes.

In this context, the article analyses a possibility of capitalizing on the energy potential of surface water courses. Thus, the thermal potential in the form of thermal energy contained in the surface water source was considered to be a resource that is found in abundance, and which is currently not sufficiently well capitalized, although in some cases these water sources are found even in the near of buildings. Therefore, the article proposes a concept that is based on the use of the most favorable thermal

potential for the preparation and supply of chilled water necessary for cooling indoor spaces. Such a cooling system is mainly composed of a water-water heat pump that uses, following a logical prioritization system, a low-potential coolant from various sources, namely: water from the surface source, atmospheric air, cold water used for the preparation of hot water for consumption or for the consumption of sanitary objects.

The authors of the article intend to implement this concept on a pilot scale and compare the results obtained with the estimates obtained by using mathematical models that calculate the energy efficiency of the system for various configurations and loading and operating regimes.

References

[1] C. Zhang, J. Wang, L. Li, F. Wang, W. Gang, „Utilization of Earth-to-Air Heat Exchanger to Pre-Cool/Heat Ventilation Air and Its Annual Energy Performance Evaluation: A Case Study", in Sustainability, vol. 12, no. 20, October 2020, ID Article 8330.

[2] A. M. Omer, „ Energy, environment and sustainable development", in Renewable and Sustainable Energy Reviews, vol. 12, no. 9, December 2008, pp. 2265-2300.

[3] R. Pacheco, J. Ordóñez, G. Martínez, „ Energy efficient design of building: A review", in Renewable and Sustainable Energy Reviews, vol. 16, no. 6, August 2012, pp. 3559-3573.

[4] M.A. Jamil, B. B. Xu, L. Dala, M. Sultan, L. Jie, M.W. Shahzad, „ Experimental and normalized sensitivity based numerical analyses of a novel humidifier-assisted highly efficient indirect evaporative cooler", in International Communications in Heat and Mass Transfer, vol. 125, 2021, ID Article: 105327.

[5] K.J. Chua, M.R. Islam, N. Kim Choon, M.W. Shahzad, Advances in Air Conditioning Technologies, Springer Singapore, Singapore, 2021.

[6] National Academy of Sciences, National Academy of Engineering and National Research Council, „Real Prospects for Energy Efficiency in the United States", The National Academies Press, Washington, DC, 2010.

[7] International Energy Agency (IEA), „ Air Conditioning Use Emerges as One of the Key Drivers of Global Electricity-demand Growth", in News - IEA, 15 May 2018, available at: https://www.iea.org/news/air-conditioning-us e-emerges-as-one-of-the-key-drivers-of-global-electricity-demand-growth, accessed 25 April, 2025

[8] F. J. Zarco-Soto, I. M. Zarco-Soto, S. S. S. Ali, P. J. Zarco-Periñán, „ Energy consumption in buildings: A compilation of current studies", in Energy Reports, vol. 13, June 2025, pp. 1293-1307.

[9] A. Dyson, N. Keena, M. Lokko, B. K. Reck, C. Ciardullo, „Building materials and the climate. constructing a new future", in United Nations Environment Programme , 2023.

[10] H. Shahrokni, F. Levihn, N. Brandt, „ Big meter data analysis of the energy efficiency potential in Stockholm's building stock", in Energy and Buildings, vol. 78, August 2014, pp. 153-164.

[11] B.B. Ekici, U. T. Aksoy, „ Prediction of building energy needs in early stage of design by using ANFIS", in Expert Systems with Applications, vol. 38, no. 5, May 2011, pp. 5352-5358.

[12] Y. Feng, „ Thermal design standards for energy efficiency of residential buildings in hot summer/cold winter zones", in Energy and Buildings, vol. 36, no. 12, December 2004, pp. 1309-1312.

[13] W. Wang, H. Rivard, R. Zmeureanu, „ Floor shape optimization for green building design", in Advanced Engineering Informatics, vol. 20, no. 4, October 2006, pp. 363-378.

[14] M. Krarti, „ Optimal Design and Retrofit of Energy Efficient Buildings, Communities, and Urban Centers, Chapter 6 - Integrated Design and Retrofit of Buildings", pp. 313-384, Elsevier Inc. All, 2018.

[15] M. Zhang, W. Han, Y. He, J. Xiong, Y. Zhang, „Natural Ventilation for Cooling Energy Saving: Typical Case of Public Building Design Optimization in Guangzhou, China", in Applied Sciences, vol. 14, 2024, ID Article 610.

[16] F. Sharaf, „The impact of thermal mass on building energy consumption. A case study in Al Mafraq city in Jordan", in Civil and Environmental Engineering, vol. 7, no. 1, October 2020, pp. 1-18.

[17] X. Zhao, „Materials for Energy Efficiency and Thermal Comfort in Buildings, Chapter 17 - Porous materials for direct and indirect evaporative cooling in buildings, Woodhead Publishing Series in Energy", pp. 399-426, Woodhead Publishing Limited, 2010.

[18] Ł. Stefaniak, S. Szczęśniak, J. Walaszczyk, K. Rajski, K. Piekarska, J. Danielewicz, „Challenges and future directions in evaporative cooling: Balancing sustainable cooling with microbial safety", in Building and Environment, vol. 267, Part A, January 2025, ID Article 112292.

[19] B. Happold, „Earth to air heat exchanger", in Designing Buildings, available at https://www.designingbuildings.co.uk/wiki/Earth_to_air_heat_exchangers, accessed: april 24, 2025.

[20] U. Berardi, P. La Roche, J. M. Almodovar, „Water-to-air-heat exchanger and indirect evaporative cooling in buildings with green roofs", in Energy and Buildings, vol. 151, no. 20, September 2017, pp. 406-417.

[21] M. Elhadary, A. Alzahrani, R. Aly, B. Elboshy, „A Comparative Study for Forced Ventilation Systems in Industrial Buildings to Improve the Workers' Thermal Comfort", in Sustainability, vol. 13, no. 18, September 2021, ID Article: 10267.

[22] J. Deng, S.He, Q. Wei, M. Liang, Z. Hao, H. Zhang, „Research on systematic optimization methods for chilled water systems in a high-rise office building", in Energy and Buildings, vol. 209, February 2020, ID Article: 109695.

[23] E.B. Kyere, T.C. Jen, L. Tartibu, „Analysis of the Influence of Chilled Water Temperature Setpoint on Thermal Comfort and Energy Consumption", in Arabian Journal for Science and Engineering, vol. 49, 2024, pp. 10409–10429.

[24] R. Dreepaul, „A study of alternative refrigerants for the refrigeration and air conditioning sector in Mauritius", in IOP Conference Series Earth and Environmental Science, vol. 93, no.1, November 2017, ID Article: 012054.

[25] K. Uddin, B. B. Saha, „An Overview of Environment-Friendly Refrigerants for Domestic Air Conditioning Applications", in Energies, vol. 15, no.21, October 2022, ID Article: 8082.

[26] A. Tokar, D. Muntean, D. Tokar, D. Bisorca, „Decarbonization of Heating and Cooling Systems of Buildings Located Nearby Surface Water Sources: Case Study", in Energies, July 24, 2024, vol. 1, no. 15, ID Article: 3673.

[27] H. Zhang, S. Shao, H. Xu, H. Zou, C. Tian, „Free cooling of data centers: A review", in Renewable and Sustainable Energy Reviews, vol. 35, July 2014, pp. 171-182.

[28] W. Yao, C. Liu, X. Kong, Z. Zhang, Y. Wang, W. Gao, „A systematic review of heat pipe applications in buildings", in Journal of Building Engineering, vol. 76, October 2023, ID Article: 107287.

Engineered Cementitious Composites (ECC): A Review of the Most Common Laboratory Testing Methods

Materiale Compozite Cementoase (ECC): O analiză a celor mai utilizate metode de testare în laborator

Ioan Ștefan Zavaschi[1], Călin Grigore Radu Mircea[2], Tudor Panfil Toader[3]

[1]Technical University of Cluj-Napoca, Faculty of Civil Engineering
15 Constantin Daicoviciu (400020), Cluj-Napoca, Romania
E-mail: zavaschistefan@gmail.com

[2]Technical University of Cluj-Napoca, Faculty of Civil Engineering
15 Constantin Daicoviciu (400020), Cluj-Napoca, Romania
E-mail: Calin.Mircea@dst.utcluj.ro

[3]NIRD URBAN-INCERC, Cluj-Napoca Branch
117 Calea Floresti (400524), Cluj-Napoca, Romania
E-mail: toader.tudor@yahoo.com

DOI: 10.37789/rjce.2026.17.1.4

Abstract. *Recent advancements in material research and technological innovations in the processing of raw materials for concrete production, combined with global shifts and the pursuit of sustainability, have prompted increased interest in the development of novel concrete mixtures. Despite several decades of intensive research in concrete technology, the practical implementation of these advancements remains relatively limited. This paper reviews existing testing methods and synthesizes the most relevant findings, while emphasizing the specific contributions and limitations of each study.*

Key words: *engineered cementitious composites, mechanical properties, sustainability*

1. Introduction

Concrete has been used since antiquity, most prominently during the Roman Empire and in other early civilizations, and continues to serve as an indispensable construction material in the modern era. Its inherent lack of tensile strength led to the development of reinforced concrete (RC), followed by fiber-reinforced concrete (FRC) and, more recently, engineered cementitious composites (ECC) [1].

Incorporating randomly oriented short fibers into concrete leads to notable enhancements in its mechanical performance, particularly in tensile and flexural strength, ductility, fatigue performance and resistance to impact loading [2].

The article was received on 30.10.2025, accepted on 02.02.2026 and published on 24.02.2026

Despite their superior properties, these advanced materials face limited adoption due to high production costs, absence of standardized design guidelines, and insufficient practical knowledge. Establishing a solid research foundation and translating findings into design standards and reference materials are essential steps towards enabling the widespread implementation of ECC in construction practice [3].

The distinctive response of ECC mixtures under impact loading and tensile strain has prompted extensive research aimed at developing design guidelines for their use in protective and other structural applications. Numerous experimental and numerical studies have investigated the impact resistance of ECC elements. Recent research has primarily focused on the impact behaviour of cement-based composites reinforced with either mono-fibers or hybrid-fibers incorporating two or more fiber types. Due to the technical challenges and high costs associated with large-scale impact tests, researchers have often employed small-scale drop-weight tests, projectile impact tests, or weighted pendulum tests, despite the intrinsic limitations of these methods.

This paper reviews the predominant laboratory testing methods used to assess the mechanical properties of fiber-reinforced concrete, highlighting their key contributions and inherent limitations.

2. Classification and ECC behaviour

Engineered Cementitious Composites, along with related mixtures, are classified within the broader category of high-performance fiber-reinforced cementitious composites (HPFRCCs). The defining attributes of ECC are their enhanced tensile ductility, typically reported in the range of 3-5% strain, and their tensile strength, generally between 4-6 MPa, achieved with a fiber volume fraction of approximately 1.5-2%. Under uniaxial tensile loading, ECCs exhibit a characteristic tensile-strain-hardening response, initiated by the formation of multiple fine cracks and sustained by effective stress redistribution through fiber bridging mechanisms. The progressive development of cracks ultimately results in localized deformation and failure along a preferential plane where the tensile stress surpasses the material's capacity.

Under certain conditions, however, the formation of a single dominant crack may govern the material response during testing, resulting in tensile-strain-softening. The principal parameters governing this behaviour include the following:

- Fiber type, such as polyethylene (PE), polypropylene (PP), polyvinyl alcohol (PVA), or steel.
- Relative proportions of the primary mix constituents.
- Mixing sequence and associated processing parameters.
- Type of mechanical test employed and corresponding testing parameters.
- Fiber dispersion within the matrix.

Figure 1 presents the stress-strain and deformation responses up to failure, as obtained from uniaxial tensile tests reported by Fakharifar et al. [4].

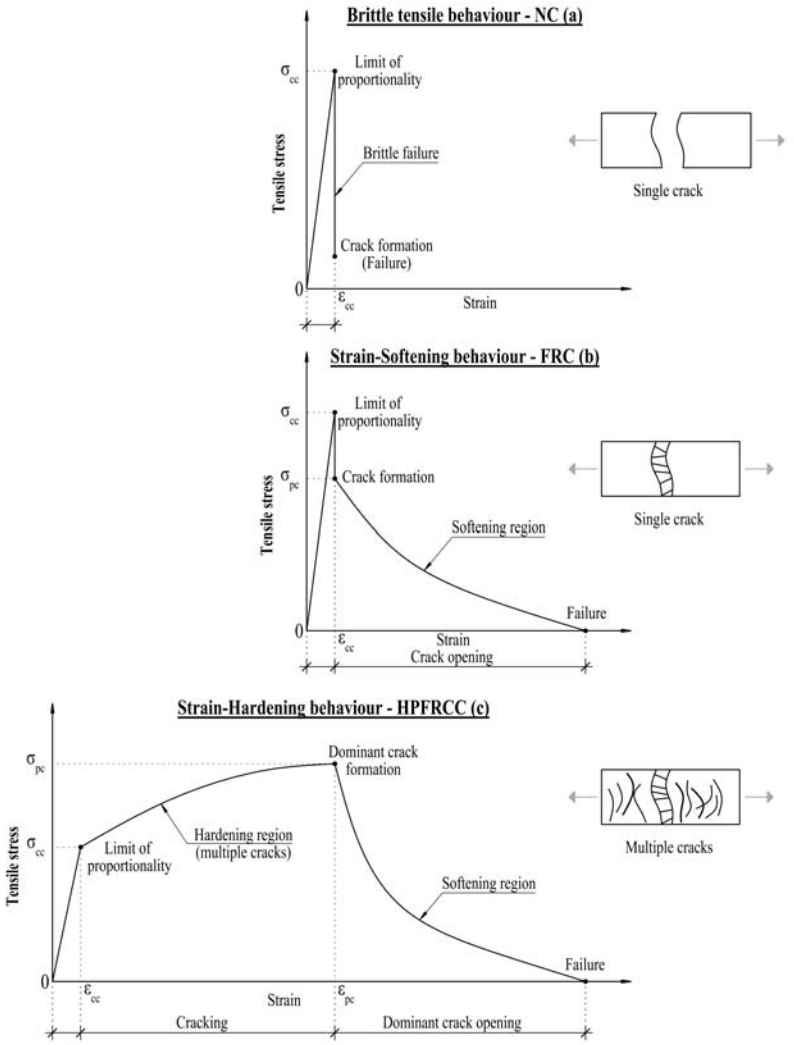

Fig. 1. Typical tensile stress-strain or deformation relation up to failure of: (a) Normal Concrete (NC); (b) Fiber Reinforced Concrete (FRC); and (c) High Performance Fiber Reinforced Cementitious Composites (HPFRCC); σ_{cc}, First cracking stress; σ_{pc}, Post cracking stress; ε_{cc}, First cracking strain; ε_{pc}, Post cracking strain.

3. Common laboratory testing methods used for the evaluation of mechanical properties

While RC is a widely adopted material and has been extensively employed in conventional construction projects in conjunction with steel, fiber-reinforced concrete has experienced relatively limited adoption and remains uncommon in standard practice. The widespread use of RC in recent decades can be attributed, in part, to the accumulation of a substantial body of knowledge and the accessibility of this information to practitioners, combined with its low production cost and broad range of applications. Moreover, governing bodies have established comprehensive standards

that regulate the application, design, and conditions of use for RC, thereby facilitating its integration into mainstream construction practices.

Due to the high level of academic interest in ECC, numerous studies have been published on the mechanical behaviour and properties of these mixtures. Typically, these properties are assessed using the standard methods applied to plain concrete, namely the uniaxial compression test, the uniaxial tension test and the beam flexural (bending) test. However, because ECC exhibit significantly enhanced tensile strain capacity and superior performance under dynamic loading, these conventional tests alone are insufficient to fully capture its mechanical response. Consequently, additional testing methods are frequently employed, including the drop-weight test (instrumented or non-instrumented), the instrumented gas gun test and the instrumented pendulum test, which provide further insight into the behaviour of ECC under impact and high-strain-rate conditions. Table 1 summarizes the testing methods and outlines the distinguishing characteristics of each study.

Table 1

Summary of tests conducted in literature

Reference	Mixture type	Fiber type	Fiber content	Testing method(s)	Particularities
6	FRC	Steel and PP	0.2–1%	C, ST, DWT	Dual fiber reinforcement
7	N/A	N/A	N/A	C, DWT (I)	Crumb rubber substitute for aggregates
10	ECC	PVA and SMA	2% PVA 0-1.5% SMA	T, DWT	Dual fiber reinforcement
11	ECC	Steel and PE	0.5% and 1.5%	T, P	Dual fiber reinforcement
12	FRC	CF and HF	0.5-1.5%	F, DWT	Dual fiber reinforcement
13	ECC	PP	2%	C, F, DWT	Exposure to 500 °C
14	ECC	PVA	2%	C, T, F, DWT	Varying FA proportions
15	Concrete	Micro-steel	0.5-1%	DWT	Self-compacting concrete
16	ECC/EGC	PVA	2%	C,T, DWT (I)	Different drop heights
17	ECC	SMA and PVA	2% PVA 0-1.5% SMA	C,T, DWT (I)	Dual fiber reinforcement
18	Concrete	N/A	N/A	P	Model comparison
19	ECC	PVA and Steel	1.75% PVA 0.58% Steel	P	Dual fiber reinforcement
20	ECC	N/A	N/A	Ch	Review and commentary

FRC, Fiber Reinforced Concrete; ECC, Engineered Cementitious Composite; EGC, Engineered Geopolymer Composite; PP, Polypropylene; PVA, Polyvinyl Alcohol; SMA, Shape Memory Alloy; PE, Polyethylene; CF, Crimped Fiber; HF, Hooked end Fiber; C, Compression; ST, Splitting Tensile, T, Tension; DWT, Drop-Weight Test; DWT (I), Drop-Weight Test Instrumented; P, Penetration; F, Flexural; Ch, Charpy Test; FA, Fly Ash; N/A, Not Applicable.

3.1. Uniaxial compression test

The uniaxial compression test is one of the most widely employed material tests for concrete, primarily due to its relevance in characterizing the material's resistance under compressive stresses, which may range from 20 MPa to 95 MPa in the case of ECC [5]. In accordance with established standards (ASTM C39, EN 12390-3), the procedure involves subjecting standardized specimens – commonly cylinders or cubes to a gradually increasing load applied along a single axis, while permitting lateral deformation. The specimen is positioned between two rigid plates to ensure uniform load transfer, and the compressive force is increased at a controlled rate until failure occurs.

The principal parameter obtained from this test is the compressive strength (f_c) which is widely recognized as a fundamental indicator of concrete quality and performance. Furthermore, additional mechanical properties, such as the elastic modulus (E), may also be determined in accordance with relevant standards (ASTM C469, EN 12390-13), thereby providing a more comprehensive understanding of the material's behaviour.

One study reported a 14.4% increase in compressive strength when fibers were incorporated into the mixture to produce FRC, compared with plain concrete [6]. In contrast, another investigation examining the replacement of the aggregate with crumb rubber observed substantial reductions in both compressive strength (94%) and elastic modulus (96%) when comparing specimens with 100% crumb rubber to control specimens containing no rubber [7].

3.2. Uniaxial tension test

When considering ECC as a primary building material, its superior tensile strength (ranging from 4 MPa to 12 MPa) represents a key advantage over conventional concrete, as this mechanical property enhances crack resistance, ductility and long-term structural durability [5].

Given its importance, tensile strength is frequently employed to characterize ECC specimens and to evaluate the overall performance of the material. This property is typically measured using standardized coupon or cylindrical specimens, in accordance with the Japan Society of Civil Engineers (JSCE) [8], which are clamped at both ends and subjected to a controlled displacement rate of 0.5 mm/min in opposing directions, thereby generating a uniaxial tensile stress response. Although numerous experimental tensile test have been reported in the literature, ACI 544 [9] acknowledges that no standardized tensile testing procedure has been established specifically for FRC or ECC to accurately characterize the tensile response, particularly in the cases where strain-hardening behaviour and multiple cracking under tension are observed.

In a 2017 study published by Ali et al., the ultimate tensile strength of the ECC mixture containing 2% PVA fibers was 301.7% higher than that of the control mixture without fibers [10]. Similar results were obtained by Maalej et al. in a study that

investigated the dynamic properties of ECC specimens, observing an increase in ultimate tensile strength of 190% with higher strain rates applied to the samples [11].

As an alternative to the direct uniaxial tensile test, indirect methods are recommended, in particular the splitting tensile test conducted in accordance with ASTM C496 or EN 12390-6. In this procedure, compressive load is applied to a cylindrical specimen along two diametrically opposed generating line, inducing a uniform tensile stress perpendicular to the line of loading which leads to failure of the specimen once the ultimate tensile strength is reached.

3.3. Beam flexural (bending) test

To address the inherent difficulties associated with performing direct tensile tests, several standards recommend flexural testing methods [9], specifically three-point or four-point bending. These are conducted in accordance with ASTM C293 or EN 12390-5 in the case of three-point bending. The testing method involves applying point loads to beam-sized specimens at prescribed locations, with the specimen typically supported in a simply supported configuration. During the test, both the first peak load and the residual load at specified deflections can be recorded, while simultaneously determining the modulus of rupture (MOR).

Several studies have reported that the incorporation of fibers leads to a significant enhancement in flexural strength, with FRC or ECC exhibiting improvements of 13% to 55% over plain concrete, depending on the fiber type, fiber volume fraction and mixture proportions [12]. One study reported that exposure to 500 °C resulted in a reduction of approximately 43% in the flexural strength of both ECC and PC specimens, a decrease more pronounced than that observed in compressive strength. This behaviour was attributed to the melting of PP fibers in the ECC matrix at approximately 180 °C and their subsequent evaporation at around 350 °C, which generated continuous voids within the microstructure and consequently weakened the material [13].

In a 2023 study, Guo et al. investigated the dynamic mechanical behaviour of ECC and found that increasing the fly ash (FA) content reduced the flexural peak load while increasing the flexural peak displacement. This behaviour was attributed to the ability of FA to lower the bonding force between the PVA fibers that were used and the matrix, thereby enhancing deformability [14].

3.4. Impact performance tests

In recent years, considerable research has been devoted to enhancing the understanding of the behaviour of ECC and FRC mixtures under various loading conditions. Particular attention has been directed toward impact loading, driven by recent global events (such as explosions, terrorist attacks, bombings and wars) and the consequent demand for construction materials with superior performance characteristics. It should be noted that, in the case of impact testing, the most

commonly used standards are the ACI 544 [9] and the JSCE Concrete Engineering Series 82 [8], both of which provide guidelines for various types of testing procedures.

The multiple drop-weight test, either non-instrumented or instrumented, is the most widely employed method for evaluating impact performance. In the conventional non-instrumented drop-weight test, a weight is released from a predetermined height, and the number of impacts required to induce a defined level of distress is recorded. Although limited to qualitative assessment, the non-instrumented method enables comparative evaluation of different ECC specimens and provides a general indication of their impact resistance. In a study on the impact performance of self-compacting concrete reinforced with micro-steel fibers, it was observed that the specimen with 1% fiber volume required 672 blows from a 4.5 kg mass dropped at a height of 450 mm to initiate first cracking, while 789 blows were required to reach failure [15]. A similar high number of impacts was documented in another study on impact resistance that utilized two different types of fibers with varying volume fractions [12]. In instrumented impact testing, a specialized drop tower is typically employed, allowing sensors to capture parameters such as impact forces, displacements, and total energy absorption, thereby enabling a quantitative analysis of the results. A 2022 study on the low-energy impact behaviour of ECC and engineered geopolymer composite (EGC) reported dissipated energy values ranging from 2.1 J to 12.2 J, depending on drop height and mass [16]. Comparable results were documented in another study which reported a range of 10.3 J to 11 J on first impact and noted a nearly elastic response with no physical damage at lower energy levels [17].

During projectile testing, a projectile is launched toward a panel or comparable ECC specimens, and the dimensions of the resulting impact crater or scab are recorded. In the evaluation of concrete-based specimens, several challenges may arise, including the generation of dust that can hinder data acquisition of the impact event, as well as the ejection of debris from both the impact face and the rear face of the specimens. In a paper by Li et al., which addressed some of the shortcomings of projectile testing, it was concluded that coarse aggregate size has a greater influence on the impact resistance of the target than its hardness, thereby leading to the proposal of a new model for predicting the depth of penetration [18]. In another study on the impact resistance of ECC panels, Soe et al. reported that ECC panels absorbed nearly all of the impact energy compared to plain concrete, while exhibiting different failure modes depending on the number of impacts and the impact velocity [19]. These findings confirmed the results of an earlier study by Maalej et al. [11].

In certain studies, weighted pendulum tests are conducted using a conventional Charpy pendulum machine. The procedure consists of raising the pendulum to a predetermined height and subsequently releasing it to strike the test specimen. Upon impact, the specimen fractures and absorbs part of the pendulum's energy. The residual energy enables the pendulum to ascend to a final height, from which the absorbed energy can be quantified. It should be emphasized that, a considerable portion of energy is dissipated during the test through friction and vibration. In a review study on the Charpy impact test applied to ECC, the authors concluded that several issues require further attention in the literature. These include specimen size

and inconsistencies related to specimen dimensions, the advantages of using notched versus unnotched samples, and the detailed reporting of testing procedures, constituent materials and specimen characteristics [20]. The conventional testing machine may be instrumented with load cells, accelerometers and photocells to enable more precise measurements during the testing procedure.

Alternative impact tests may be performed using hydraulic universal testing machines, which are capable of inducing failure within short time intervals (on the order of 20 milliseconds), or by applying variable loading rates so as to generate distinct strain-rate conditions in the specimen.

4. Conclusions

Recent advancements in concrete research have led to the publication of numerous studies investigating fiber-reinforced mixtures and their potential integration into mainstream construction practices. To establish a robust understanding of the material's behaviour, various testing methodologies are employed to evaluate its mechanical properties and performance under diverse conditions. Nevertheless, notable discrepancies exist among testing procedures, standards used and other important criteria that may significantly influence the resulting data and interpretations. To facilitate further advancements in this field and promote the widespread adoption of fiber-reinforced concrete in practical applications, it is essential to develop and implement unified testing standards. Such standardization would provide the foundation for experimental evaluation and contribute to the subsequent formulation of comprehensive design guidelines.

References

[1] *J. Li, Y.X. Zhang*, „Evaluation of constitutive models of hybrid-fiber engineered cementitious composites under dynamic loadings", in Construction Building Materials, vol. **30**, May 2012, pp. 149-160.

[2] *R. F. Zollo*, „Fiber-reinforced concrete: An overview after 30 years of development", in Cement and Concrete Composites, vol. **19**, 1997, pp. 107-122.

[3] *M. A. Kewalramani, O. A. Mohamed, Z. I. Syed*, „Engineered cementitious composites for modern civil engineering structures in hot arid coastal climatic conditions", Procedia Engineering, vol. **180**, May 2017, pp. 767-774.

[4] *M. Fakharifar, A. Dalvand, A. Arezoumandi, M. K. Sharbatdar, G. Chen, A. Kheyroddin*, „Mechanical properties of high performance fiber reinforced cementitious composites", in Construct. Build. Materials, vol. **71**, Nov. 2014, pp. 510-520.

[5] *V. C. Li*, „Engineered Cementitious Composites (ECC) – Material, Structural, and Durability Performance", University of Michigan, Aug. 2007.

[6] *A. Alavi Nia, M. Hedayatian, M. Nili, V. Afrough Sabet*, „An experimental and numerical study on how steel and polypropylene fibers affect the impact resistance in fiber-reinforced concrete", in International Journal of Impact Engineering, vol. **46**, Jan. 2012, pp. 62-73.

[7] *A. O. Atahan, A. Ö. Yücel*, „Crumb rubber in concrete: Static and dynamic evaluation", in Construction Building Materials, vol. **36**, Apr. 2012, pp. 617-622.

[8] JSCE-Concrete Engineering Series 82, „Recommendations for Design and Construction of High Performance Fiber Reinforced Cement Composites with Multiple Fine Cracks (HPFRCC)", Japan Society of Civil Engineers, 2008.

[9] ACI 544.9R-17, „Report on Measuring Mechanical Properties of Hardened Fiber-Reinforced Concrete", American Concrete Institute, 2017.

[10] *M. A. E. M. Ali, A. M. Soliman, M. L. Nehdi*, „Hybrid-fiber reinforced engineered cementitious composite under tensile and impact loading", in Materials and Design, vol. **117**, Dec. 2016, pp. 139-149.

[11] *M. Maalej, S. T. Quek, J. Zhang*, „Behavior of Hybrid-Fiber Engineered Cementitious Composites Subjected to Dynamic Tensile Loading and Projectile Impact", in Journal of Materials in Civil Engineering, vol. **17**, Apr. 2005, pp. 143-152.

[12] *M. Ganesh, A. S. Santhi, G. Murali*, „Impact Resistance And Strength Reliability Of Fiber-Reinforced Concrete In Bending Under Drop Weight Impact Load", in International Journal of Technology, vol. **5**, July 2005, pp. 111-120.

[13] *R. A. Al-Ameri, M. Özakça, E. E. Karataş, M. T. Göğüş, A. H. Tanrıkulu*, „Drop-Weight Impact Tests on Engineered Cementitious Composites heated to 500 °C", in Wasit Journal of Engineering Sciences, vol. **10**, Aug. 2022, pp. 240-251.

[14] *W. Guo, Y. Tian, W. Wang, B. Wang, P. Zhang, J. Bao,* „Dynamic mechanical behavior of strain-hardening cementitious composites under drop weight impact loading", in Journal of Materials Research and Technology, vol. **23**, Feb. 2023, pp. 5573-5586.

[15] *S. R. Abid, M. L. Abdul-Hussein, N. S. Ayoob, S. H. Ali, A. L. Kadhum,* „Repeated drop-weight impact test on self-compacting concrete reinforced with micro-steel fiber", in Heliyon, vol. **6**, Jan. 2020.

[16] *J. Cai, J. Pan, J. Han, Y. Lin, Z. Sheng,* „Low-energy impact behavior of ambient cured engineered geopolymer composites", in Ceramics International, vol. **48**, Dec. 2021, pp. 9378-9389.

[17] *M. L. Nehdi, M. A. E. M. Ali*, „Experimental and Numerical Study of Engineered Cementitious Composite with Strain Recovery under Impact Loading", in Applied Sciences, vol. **9**, Mar. 2019.

[18] *Y. Li, H. Wu, Q. Fang, Y. Peng,* „A note on the impact resistance of concrete target against rigid projectile", in International Journal of Protective Structures, vol. **9**, Apr. 2018, pp. 397-411.

[19] *K. T. Soe, Y. X. Zhang, L. C. Zhang,* „Impact resistance of hybrid-fiber engineered cementitious composite panel", in Composite Structures, vol. **104**, Feb. 2013, pp. 320-330.

[20] *R. J. Thomas, A. D. Sorensen,* „Charpy Impact Test Methods for Cementitious Composites: Review and Commentary", in Journal of Testing and Evaluation, vol. **46**, Nov. 2018, pp. 2422-2430.

Evaluation of algae drying process using a solar air dryer built from recycled materials

Evaluarea unui uscător solar cu aer, construit din materiale reciclate, pentru uscarea algelor

Rafaela Pontes[1]*, Răzvan Calotă[1], Charles Berville[1], Paul Dancă[1]

[1]*Technical University of Civil Engineering of Bucharest (UTCB) Building Services Engineering Faculty, Bucharest, Romania*
121-126 Bvd Lacul Tei, Bucharest, Sector 2, Romania
**E-mail: pontesrafac@gmail.com; razvan.calota@gmail.com*

DOI: 10.37789/rjce.2026.17.1.5

Abstract. *This article presents a preliminary evaluation of a low-cost solar drying system, built entirely from recycled materials and tested for marine biomass applications. The experiment was set up using an air solar collector constructed from a reused window frame and a drying chamber housed inside a repurposed refrigerator. Tests were conducted on commercial wakame (Undaria pinnatifida) under forced convection, using a solar simulator with 2.0 kW halogen lamps. After 3.75 hours of system operation, a 47.2% reduction in mass was observed, from 477.7 g to 252.3 g. The recycled collector raised the drying air temperature by about 14...15°C above ambient, with a peak of 33.9°C and an air velocity of 0.5...0.6 m/s. The results show that the system is promising, but insulation and airflow need improvement to increase even further the drying air temperature.*

Key words: *solar drying, TSC, recycled materials, algae, energy efficiency*

1. Introduction

1.1 Background

Interest in algae applications is increasing worldwide due to the fact that they contain high levels of protein, minerals, antioxidants, and other important active compounds. These qualities make seaweed useful for many purposes, such as food, beauty products, medicine, and green energy. New studies show that seaweed is important for the production of sustainable and environmentally friendly products [1], [2]. However, the final product after extracting the substances necessary for cosmetics can be further used as algae pellets. In order to reach this format, the drying process is high energy consumer.

Undaria pinnatifida, which people call wakame, is one of the most eaten brown seaweeds globally. It has good nutritional value, including lipids, essential minerals, and

The article was received on 27.11.2025, accepted on 02.02.2026 and published on 24.02.2026

pigments such as fucoxanthin [3], [4]. Wakame naturally has a high level of humidity, often more than 80%, fact generally common in the case of algae and from the point of view of elemental composition is similar with a vast range of algae species.

Drying, besides being a necessary process before transforming algae into pellets, is the most common way to keep seaweed fresh and prevent spoilage. If dried properly, seaweeds become safer to store, easier to move, and last longer. But the drying method can significantly alter important features, such as color, chemical composition, and antioxidant activity of the seaweed [5-7].

A number of drying methods are currently available for processing seaweeds, such as sun drying, hot-air drying, lyophilization, and microwave drying. While freeze-drying produces an excellent-quality product, the high cost makes it impractical for smaller producers. Hot-air drying is easy to manage but, over time, it can destroy sensitive compounds. Recent research on modern drying techniques has shown that they can alter the levels of pigments and antioxidants in wakame [8], [9].

Solar drying is an energy efficient alternative. By using renewable energy, the operational costs are cut down on. Studies suggest solar dryers can significantly speed up the drying process. Furthermore, they keep the material safe from dust and contamination [10], [11]. Researchers have already tested various types of solar systems, for example mixed-mode or forced-convection, for different seaweeds [12-14]. It is worth noting that the method has even been used successfully to dry microalgae [15].

In Romania, green seaweeds like *Ulva*, *Enteromorpha*, and *Cladophor*a are common along the Black Sea coast [16]. Although these species could be useful for supplements (nutraceutical) or industry, there are still very few studies about using solar dryers for marine algae in this specific region, as well as the possibility to valorize them in efficient burning equipment.

Studies on macroalgae drying show that moderate air velocity (about 0.3 to 2 m/s) works best, as it can efficiently remove moisture without overheating the biomass [17]. Still, there is very little information available on simple, low-cost solar collectors. Specifically, there is a lack of data on those built with recycled materials and tested in colder and temperate climates.

Because of these gaps in the research, the current study aims to investigate a low-cost solar air heater built from recycled materials for drying *Undaria pinnatifida*. The main goal is to understand how this system performs under controlled airflow and assess its potential for use in areas with variable sunlight, such as the Romanian region.

2. Methodology

2.1 Algae from Romania and target species

There are several types of seaweed that grow along the Romanian Black Sea coast, the most common being *Ulva lactuca, Enteromorpha intestinalis*, and

Cladophora vagabunda [16]. These algae contain numerous bioactive compounds such as polysaccharides, pigments, vitamins, and minerals. They are therefore considered promising sources for new nutraceutical products. Researchers are also studying polysaccharides from green algae, such as ulvan, for use in edible films and coatings for food packaging [18].

Due to climatic and seasonal conditions, Romanian green algae were not used in this experiment. Instead, *Undaria pinnatifida*, also known as wakame, was chosen as the model algae, a well-studied brown alga. *The goal of the study was to evaluate the time interval needed to reduce the mass to around 50% from the initial mass through drying*. It has a complex lipid profile, including many glycolipids and phospholipids, which makes it highly nutritious [3], [4]. Recent research has used wakame to compare different drying methods and their effects on pigments and antioxidant compounds [6-8], [19].

Wakame contains more than 80% water (very similar to other types of macroalgae), so it spoils quickly if not processed immediately after harvesting. This makes it a good material for testing new drying systems. In this project, the use of wakame is only the first step. Our main goal is to apply this solar dryer project to local green algae in Romania, after perfecting the system and, of course, during the appropriate season.

2.2 Solar air collectors for drying

Solar drying is tested for processing seaweed and other foods, as it relies on renewable energy and helps reduce costs. Studies show that solar dryers can dry algae faster and offer better protection against contamination than traditional sun drying [12-14]. Many projects use simple or recycled materials, making this technology easy for small producers to adopt [20], [21].

The effectiveness of the drying process depends mainly on temperature and air flow. Some studies on macroalgae suggest using temperatures between 40 ... 60 °C and moderate air flow rates of 0.3...2.0 m/s. These settings help to remove moisture efficiently without overheating the product or causing any type of degradation [17], [22]. Air speeds of 0.5 to 1.0 m/s are presented as a good balance between efficiency and energy use.

3. Experimental Set Up

The experimental drying setup is illustrated in Figure 1, comprising a solar air collector and a drying chamber. The detailed internal configuration of the chamber is shown in Figure 1(a), while the full assembled system can be seen in Figure 1(b). The controlled heat input was provided by a solar simulator, as depicted in Figure 1(c).

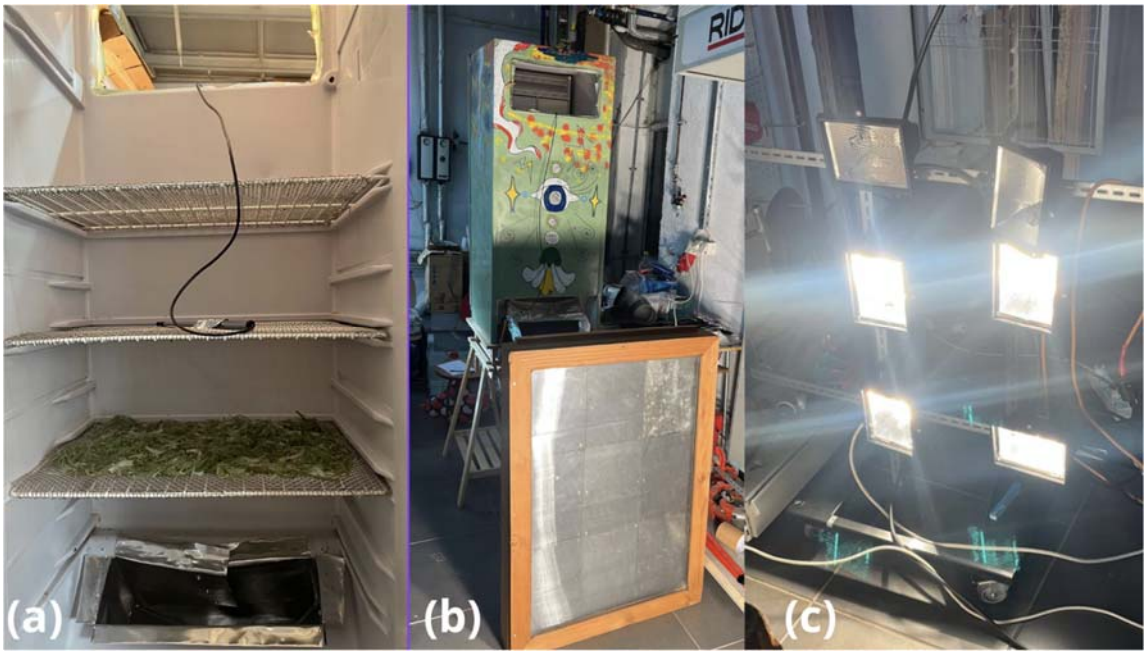

Fig. 1. Drying setup. (a) Interior of the drying chamber with seaweed samples on trays. (b) Overall view of the recycled solar dryer, showing the solar air collector and the drying chamber. (c) Halogen lamps used as a solar simulator to provide a controlled heat source.

3.1 Solar Air Collector (Recycled Window Frame)

The solar air collector was made from an old window frame, using a glass panel as the cover. The inside was painted black to absorb more heat. Air entered through a back lower opening, passed through the heated collector, and exited through an upper outlet into the drying chamber. This design warmed the air efficiently with sunlight or artificial light and kept the structure lightweight and inexpensive.

3.2 Drying Chamber (Repurposed Refrigerator Body)

The drying chamber was constructed from the body of an old refrigerator which is no longer in operation. All internal parts were removed or adapted as drying trays. In addition, insulation was applied to maintain a stable temperature during testing. The algae samples were spread in a single thin layer to ensure that air flowed evenly over the entire material. The fan speed was adjusted to maintain an air velocity in approximately 0.5 m/s inside the chamber (the recommended speed for gently and efficiently drying macroalgae), and the speed was measured with a Testo 410-2 pocket anemometer.

The dryier indoor temperature and velocity were measured using a Testo 425 hot wire anemometer. Moisture loss was determined gravimetrically.

3.3 Light Source (Solar Simulator)

To provide constant heat (in the absence of natural sunlight), four halogen lamps (J500-118 Ecolite, 500 W) were mounted above the collector. These lamps acted as a

solar simulator, providing a constant heat source so that the system could operate under controlled and repeatable conditions, even indoors or when there was insufficient natural light.

3.4 Sample Preparation and Procedure

The experiment used a commercially available frozen algae salad mix comercially available. The product was brought to the room temperature and then rinsed three times with fresh water to remove oils and sugars [6], [23]. After the final wash, the seaweed was drained. The initial mass was measured, and the algae was spread evenly on the drying tray. The samples were weighed before and after drying to monitor moisture loss, which marked the end of the process.

4. Results and discussions

4.1 Drying Conditions

During the test, the air temperature entering the collector was mantained at 20±1°C. The temperature inside the drying chamber gradually increased during the process reaching 33.9 °C by the end of the test. This showed that the recycled system could raise the air temperature by roughly 14...15 °C above ambient air temperature. The air velocity inside the chamber remained stable at 0.5-0.6 m/s.

The total drying time was 3.75 h, achieved using the four 500 W halogen lamps to simulate sunlight.

4.2 Mass Loss of the Seaweed

Table 1 summarizes the main results for the single batch of commercial algae.

Table 1

Drying performance of the recycled solar dryer (single batch)

Parameter	Value
Initial mass, m_0 (g)	477.7
Final mass, m_0 (g)	252.3
Mass Loss, Δ_m (g)	225.4
Relative mass loss (%)	47.2
Drying time (h)	3.75
Air temperature range (C)	28.7...33.9
Air velocity (m/s)	0.5...0.6

The relative mass loss was calculated using a simple gravimetric approach:

$$Mass\ loss\ (\%) = \frac{m_0 - m_f}{m_0} \times 100 \quad (1)$$

The system removed about 47% of the initial mass in 3.75 h. The results clearly show that the small, recycled stand successfully removed a significant amount of water from the biomass under mild drying conditions.

Visual analysis of the samples shown in Figure 2 confirms a mild alteration in the algae green color following the drying process. This change suggests that even the low air temperature range of 28.7...33.9°C employed was sufficient to affect the pigments of the wakame sample. This observation is relevant because the drying method, even at low temperatures, can affect the color and quality of the final product, a finding often discussed in the literature regarding pigment degradation [5], [6].

Figure 2. Comparison of the seaweed sample mass before and after drying. (a) Initial mass of the fresh sample (477.7 g) used for the experiment. (b) Final mass of the dried sample (252.3 g) after 3.75 hours of operation.

To reach the recommended 40...60°C range for algae drying, the optimum period is during summer, when the average temperature in Romania is around 30°C. By increasing the air temperature at the dryer inlet, the temperature around the algae will also rise. Additional improvements include using better insulation around all components of the setup and eliminating unsealed areas.

4.3 Practical Implications and Scalability

Even with these limits, the experiment shows that a low-cost dryer made from recycled materials can raise temperatures and effectively remove water from seaweed. Reusing a window frame as a collector and a refrigerator body as a chamber confirms that simple materials work well for drying applications to promote sustainability and smart recycling.

Although only one batch was tested, the stand's design allows more trays to be added inside the recycled refrigerator body. This means the system can be scaled up to process larger amounts by increasing the drying area. Future work will focus on improving insulation, testing the set up under real outdoor sun, and applying this method to local green macroalgae from the Romanian Black Sea coast or even invasive species present in lakes in Bucharest. After drying these products can be further used as pellets in thermal efficient burning equipment.

References

[1] C. Alves and M. Diederich, "Marine Natural Products as Anticancer Agents," *Mar. Drugs*, vol. 19, no. 8, p. 447, Aug. 2021, doi: 10.3390/md19080447.

[2] M. Farghali, I. M. A. Mohamed, A. I. Osman, and D. W. Rooney, "Seaweed for climate mitigation, wastewater treatment, bioenergy, bioplastic, biochar, food, pharmaceuticals, and cosmetics: a review," *Environ. Chem. Lett.*, vol. 21, no. 1, pp. 97–152, Feb. 2023, doi: 10.1007/s10311-022-01520-y.

[3] D. Coniglio, M. Bianco, G. Ventura, C. D. Calvano, I. Losito, and T. R. I. Cataldi, "Lipidomics of the Edible Brown Alga Wakame (Undaria pinnatifida) by Liquid Chromatography Coupled to Electrospray Ionization and Tandem Mass Spectrometry," *Molecules*, vol. 26, no. 15, p. 4480, July 2021, doi: 10.3390/molecules26154480.

[4] V. N. Salomone and M. Riera, "Proximal Composition of Undaria pinnatifida from San Jorge Gulf (Patagonia, Argentina)," *Biol. Trace Elem. Res.*, vol. 196, no. 1, pp. 252–261, July 2020, doi: 10.1007/s12011-019-01905-1.

[5] U. O. Badmus, M. A. Taggart, and K. G. Boyd, "The effect of different drying methods on certain nutritionally important chemical constituents in edible brown seaweeds," *J. Appl. Phycol.*, vol. 31, no. 6, pp. 3883–3897, Dec. 2019, doi: 10.1007/s10811-019-01846-1.

[6] S. Cox, S. Gupta, and N. Abu-Ghannam, "Effect of different rehydration temperatures on the moisture, content of phenolic compounds, antioxidant capacity and textural properties of edible Irish brown seaweed," *LWT*, vol. 47, no. 2, pp. 300–307, July 2012, doi: 10.1016/j.lwt.2012.01.023.

[7] S. S. Hamid, M. Wakayama, T. Soga, and M. Tomita, "Drying and extraction effects on three edible brown seaweeds for metabolomics," *J. Appl. Phycol.*, vol. 30, no. 6, pp. 3335–3350, Dec. 2018, doi: 10.1007/s10811-018-1614-z.

[8] R. M. Cuario Templonuevo, K.-H. Lee, and J. Chun, "Influence of various drying conditions on the functional pigments and antioxidant properties of Undaria pinnatifida," *Food Sci. Preserv.*, vol. 32, no. 3, pp. 475–485, June 2025, doi: 10.11002/fsp.2025.32.3.475.

[9] R. M. Templonuevo, K.-H. Lee, S.-M. Oh, Y. Zhao, and J. Chun, "Bioactive Compounds of Sea Mustard (Undaria pinnatifida) Waste Affected by Drying Methods," *Foods*, vol. 13, no. 23, p. 3815, Nov. 2024, doi: 10.3390/foods13233815.

[10] N. Khan, K. Sudhakar, and R. Mamat, "Seaweed processing: efficiency, kinetics, and quality attributes under solar drying," *Food Chem. Adv.*, vol. 6, p. 100859, Mar. 2025, doi: 10.1016/j.focha.2024.100859.

[11] P. Santhoshkumar, K. S. Yoha, and J. A. Moses, "Drying of seaweed: Approaches, challenges and research needs," *Trends Food Sci. Technol.*, vol. 138, pp. 153–163, Aug. 2023, doi: 10.1016/j.tifs.2023.06.008.

[12] K. Khasiya, S. Jasani, B. K. Markam, V. Veeragurunathan, K. Prasad, and S. Maiti, "Feasibility of the Mixed-Mode Solar Dryer for Sustainable Seaweed Drying," *ACS Sustain. Resour. Manag.*, p. acssusresmgt.5c00385, Nov. 2025, doi: 10.1021/acssusresmgt.5c00385.

[13] M. Mulyadi, Marhatang, and R. Nur, "The forced convection biomass and solar collector dryer for drying seaweed using exhaust fan," presented at the HUMAN-DEDICATED SUSTAINABLE PRODUCT AND PROCESS DESIGN: MATERIALS, RESOURCES, AND ENERGY: Proceedings of the 4th International Conference on Engineering, Technology, and Industrial Application (ICETIA) 2017, Surakarta, Indonesia, 2018, p. 060011. doi: 10.1063/1.5043023.

[14] S. Suherman, Moh. Djaeni, A. C. Kumoro, R. A. Prabowo, S. Rahayu, and S. Khasanah, "Comparison Drying Behavior of Seaweed in Solar, Sun and Oven Tray Dryers," *MATEC Web Conf.*, vol. 156, p. 05007, 2018, doi: 10.1051/matecconf/201815605007.

[15] B. Schmid *et al.*, "Drying Microalgae Using an Industrial Solar Dryer: A Biomass Quality Assessment," *Foods*, vol. 11, no. 13, p. 1873, June 2022, doi: 10.3390/foods11131873.

[16] E. Cadar *et al.*, "Biocompounds from Green Algae of Romanian Black Sea Coast as Potential Nutraceuticals," *Processes*, vol. 11, no. 6, p. 1750, June 2023, doi: 10.3390/pr11061750.

[17] C. Walker and M. Sheehan, "Drying Kinetics of Macroalgae as a Function of Drying Gas Velocity and Material Bulk Density, Including Shrinkage," *Clean Technol.*, vol. 4, no. 3, pp. 669–689, July 2022, doi: 10.3390/cleantechnol4030041.

[18] H. Wang, Z. Cao, L. Yao, T. Feng, S. Song, and M. Sun, "Insights into the Edible and Biodegradable Ulvan-Based Films and Coatings for Food Packaging," *Foods*, vol. 12, no. 8, p. 1622, Apr. 2023, doi: 10.3390/foods12081622.

[19] V. Solana, V. Ixtaina, and F. G. Dellatorre, "Postharvest processing of Undaria pinnatifida: Effect of blanching and salting parameters on the quality of yudoshi-enzo wakame," *Algal Res.*, vol. 90, p. 104178, Aug. 2025, doi: 10.1016/j.algal.2025.104178.

[20] R. H. Santos, L. Hayashi, G. J. P. O. Andrade, and A. L. T. Novaes, "Performance of dryer adapted to dry macroalgae," in *XLIII Congresso Brasileiro de Engenharia Agrícola - CONBEA 2014*, 2014.

[21] C. Berville, "Optimization of solar air collectors for multipurpose drying needs," Doctoral Thesis / Dissertation, Technical University of Civil Engineering of Bucharest, Bucharest, 2022.

[22] F. Chenlo, S. Arufe, D. Díaz, M. D. Torres, J. Sineiro, and R. Moreira, "Air-drying and rehydration characteristics of the brown seaweeds, Ascophylum nodosum and Undaria pinnatifida," *J. Appl. Phycol.*, vol. 30, no. 2, pp. 1259–1270, Apr. 2018, doi: 10.1007/s10811-017-1300-6.

[23] X. Lu, T. Suzuki, N. Shimoyama, Z. Wang, and C. Yuan, "Visual identification of material attributes in wakame: exploring thickness, strength, and chlorophyll content," *Front. Sustain. Food Syst.*, vol. 8, p. 1493220, Dec. 2024, doi: 10.3389/fsufs.2024.1493220.

Study of variable refrigerant flow systems: an alternative to traditional air conditioning

Studiul sistemelor cu flux variabil de agent frigorific: o alternativă la climatizarea clasică

Iulian Enaru[1], Marius-Costel Balan[1], Andrei Burlacu[1], Robert Stefan Vizitiu[1], Stefanica Eliza Tansanu[1]

[1] Technical University Gheorghe Asachi Iasi
D. Mangeron 67 str., 700050, Romania
E-mail: iulian.enaru@student.tuiasi.ro, marius-costel.balan@academic.tuiasi.ro, andrei.burlacu@academic.tuiasi.ro, robert-stefan.vizitiu@academic.tuiasi.ro, stefanica-eliza.tansanu@academic.tuiasi.ro

DOI: 10.37789/rjce.2026.17.1.6

Abstract. *Variable refrigerant flow systems offer significant advantages over traditional air conditioning systems. They enable individual temperature control for each indoor unit, providing superior comfort compared to the uniform settings of conventional systems. VRF optimizes energy efficiency by adjusting the refrigerant flow according to overall demand, thus preventing excessive energy consumption. Due to their scalability and easier integration into modern buildings, VRF systems represent a highly efficient and adaptable solution for contemporary climate control.*

Key words: Variable, efficiency, systems, refrigerant

1. Introduction

Sustainability in building design depends on implementing systems that preserve future access to resources. Ensuring efficient maintenance of comfort conditions poses challenges for air conditioning systems, particularly during transitional seasons like autumn and spring. Smooth transitions between heating and cooling operations are often based on preset external temperatures.

2. Theoretical aspects

The VRF systems (Variable Refrigerant Flow) are similar to a normal domestic air conditioning system, but designed on a larger scale. A VRF system consists of one or a group of outdoor units that supply refrigerant through a piping network connected

The article was received on 28.04.2025, accepted on 02.02.2026 and published on 24.02.2026

to multiple indoor units. Each indoor unit, by opening its expansion valve, can access the refrigerant for either cooling or heating purposes. Each individual indoor unit determines the capacity it needs based on the actual indoor temperature and the desired (set) temperature. The total demand from all the indoor units determines how the outdoor unit regulates the volume and temperature of the refrigerant. VRF is a technology that adjusts the refrigerant volume within the system to match the exact needs of the building. To maintain the set temperatures and automatically stop operation when no one is present in the room, only a minimal amount of energy is required. VRF systems are carefully engineered, featuring single or multiple compressors, multiple indoor units, and advanced refrigerant management and control components. They offer flexibility, allowing the use of various types of indoor units (with different capacities and configurations), individual zone control, and the unique ability to simultaneously provide heating and cooling in separate zones on a shared refrigerant circuit. They also allow heat recovery from one zone to another. Typical capacities range from 5.3 to 223 kW for outdoor units and from 1.5 to 35 kW for indoor units. VRF systems are equipped with at least one variable-speed compressor and/or variable-capacity compressor. Figure 1 illustrates the capacity control of a single variable-speed compressor; the compressor varies its speed to operate only at the levels necessary to maintain the indoor environments at the specified requirements.

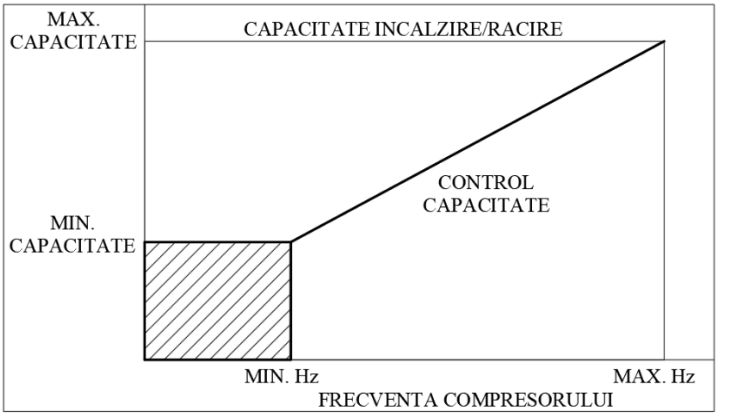

Fig. 1. Capacity control of a single variable-speed compressor

The studied system is a Variable Refrigerant Flow (VRF) configuration utilizing two pipes for both heating and cooling modes, combined with a heat recovery function to maximize energy efficiency.

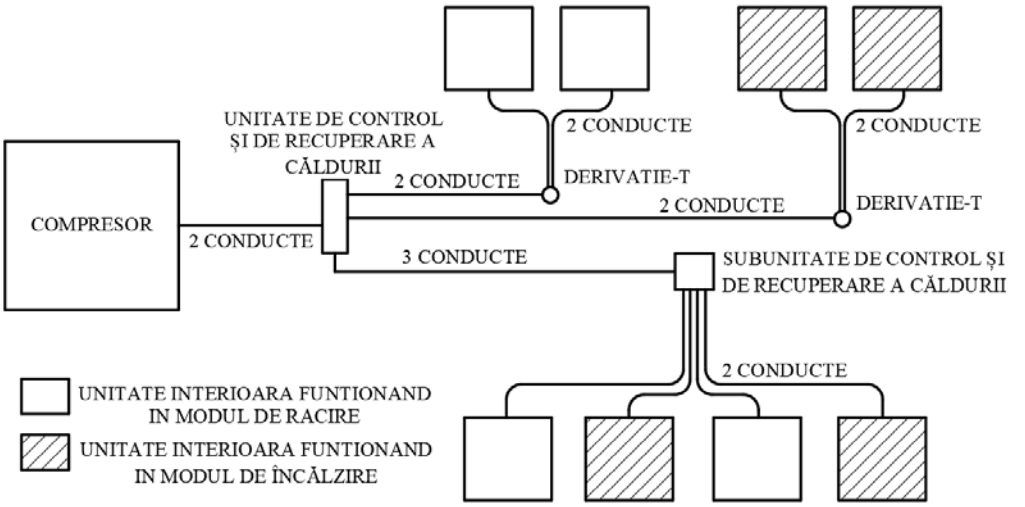

Fig. 2. VRF Systems in two pipes with heat recovery

VRF systems can be used in various applications, such as: office buildings, educational facilities (schools, universities), historic buildings, retail stores, production facilities (factories), cooling-only applications for data centers. VRF systems achieve individual temperature control for each zone, primarily by managing the refrigerant flow. Indoor units constantly react to changes in heating/cooling loads within each zone and maintain set conditions by controlling superheat through the use of an electronic expansion valve or a linear expansion valve. Inverter compressors, or a combination of inverter and constant-speed compressors, commonly found in VRF systems, modulate the refrigerant flow and work in synchronization with the refrigerant volume required by the indoor units. The major advantage of VRF air conditioning systems is energy efficiency. If the system operates at only 20% capacity, it does not consume energy as if it were running at 100% (unlike recirculation pumps that operate at full capacity), and the piping network where no indoor units are active has no energy consumption. In spaces with multiple rooms, a VRF system is much easier to manage because its electronic controls inherently know how to manage all indoor units. This also makes it very easy to implement a centralized control system for the VRF network, which, for example, allows all indoor units to be turned off from a single point.

3. Case study

This study addresses both the comparative analysis between a classic system (boiler – chiller – fan coil units) and a modern system (VRF – Variable refrigerant flow – indoor units) for heating and cooling, as well as the design approach and cost analysis for the construction of a Production hall – Sewing factory.
Building characteristics:
Importance category: “C”
Importance class: III (according to P100-1/2013)

Fire resistance rating: II
Height regime: Ground floor only (P)
External climate parameters:
Winter outdoor temperature: −18°C
Summer outdoor temperature: 35°C
Summer relative humidity: 35%
Winter relative humidity: 80% (seems duplicated; might need checking)
Indoor temperature targets:
25–27°C during the warm season for the production hall (sewing factory)

The cooling of indoor spaces, to maintain the temperature levels specified in standards (SR 6648-1,2), will be achieved through the following systems:
a) Chiller and fan coil units
b) VRF (Variable Refrigerant Flow) system with indoor units
Temperature regulation within the space will be performed using manual room thermostats. All equipment will be supplied through multilayer pipes with high resistance, certified for buried installation. The pipes will be insulated to prevent condensation and energy loss. Distribution will occur vertically through dedicated pipe shafts and horizontally through suspended ceilings. Pipes will be fixed to the building structure (where applicable) using single or double pipe clamps with rubber gaskets.
Number of people = number of workstations: 448 workstations
Specific heat released: 23 W/person (based on I5 standard, light work category)
From lighting: 20 W per m² in the production area
From other sources: 26.88 kW from sewing machines (300 W/sewing machine × 448 machines)
The distribution of the heating medium (hot water) will be made at the upper part, through the false ceiling in the main hallway.
The shortest routes from the distribution system to the fan coil units will be selected.
Supply pipes will use multilayer high-resistance pipes, certified for buried installation.
For straight pipe sections longer than 7 meters, expansion loops will be provided.
Following the calculations to determine the cooling requirement, a total of 96.34 kW was needed.

Description of HVAC Systems
a) Classic system:
Boiler with a power of 60 kW (running on liquid fuel/gas)
Chiller with a power of 100 kW
10 fan coil units (Heating capacity: 3 kW each, Cooling capacity: 10 kW each)

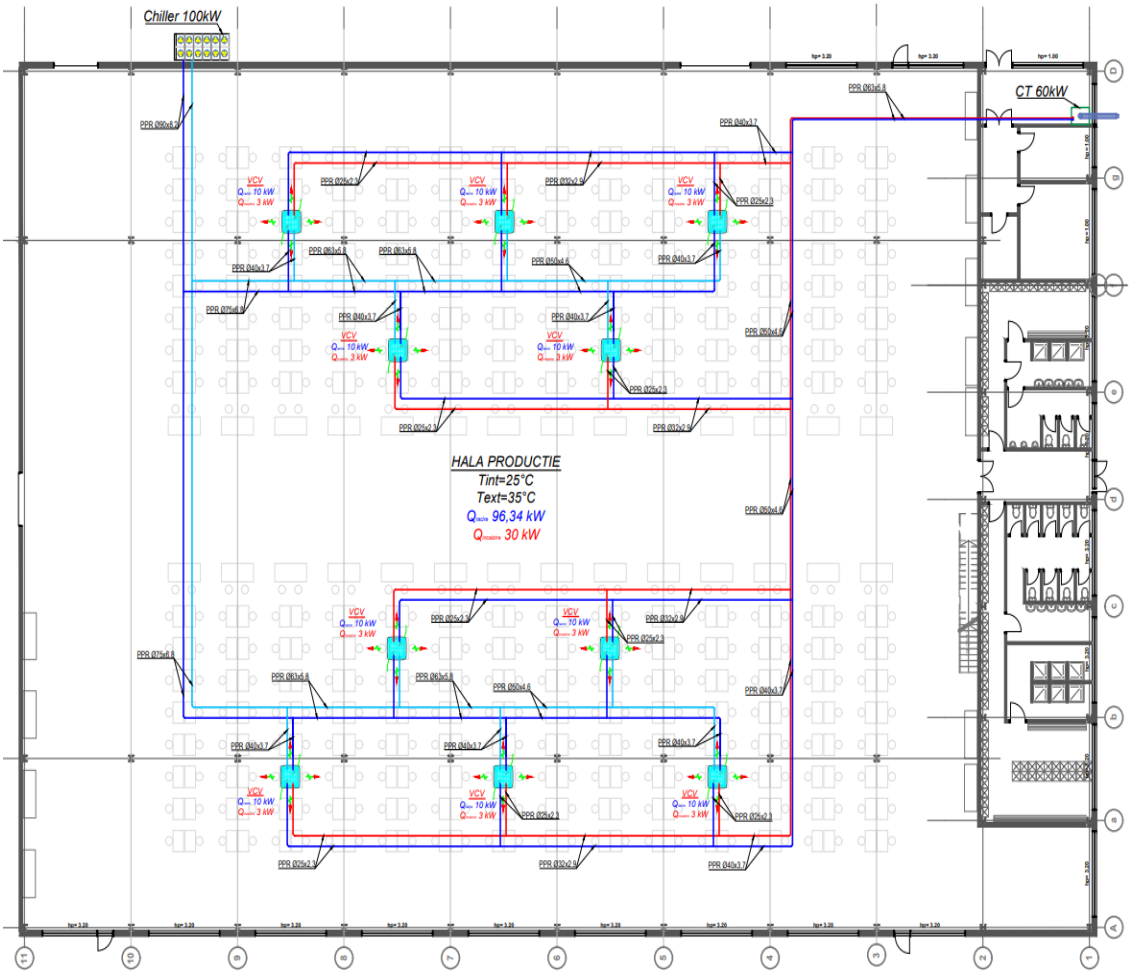

Fig. 3. Classic System

b) Modern system:
VRF (Variable Refrigerant Flow) system with one outdoor module
Cooling capacity: 100 kW
8 indoor units (5 units of 14.2 kW and 3 units of 11.2 kW)

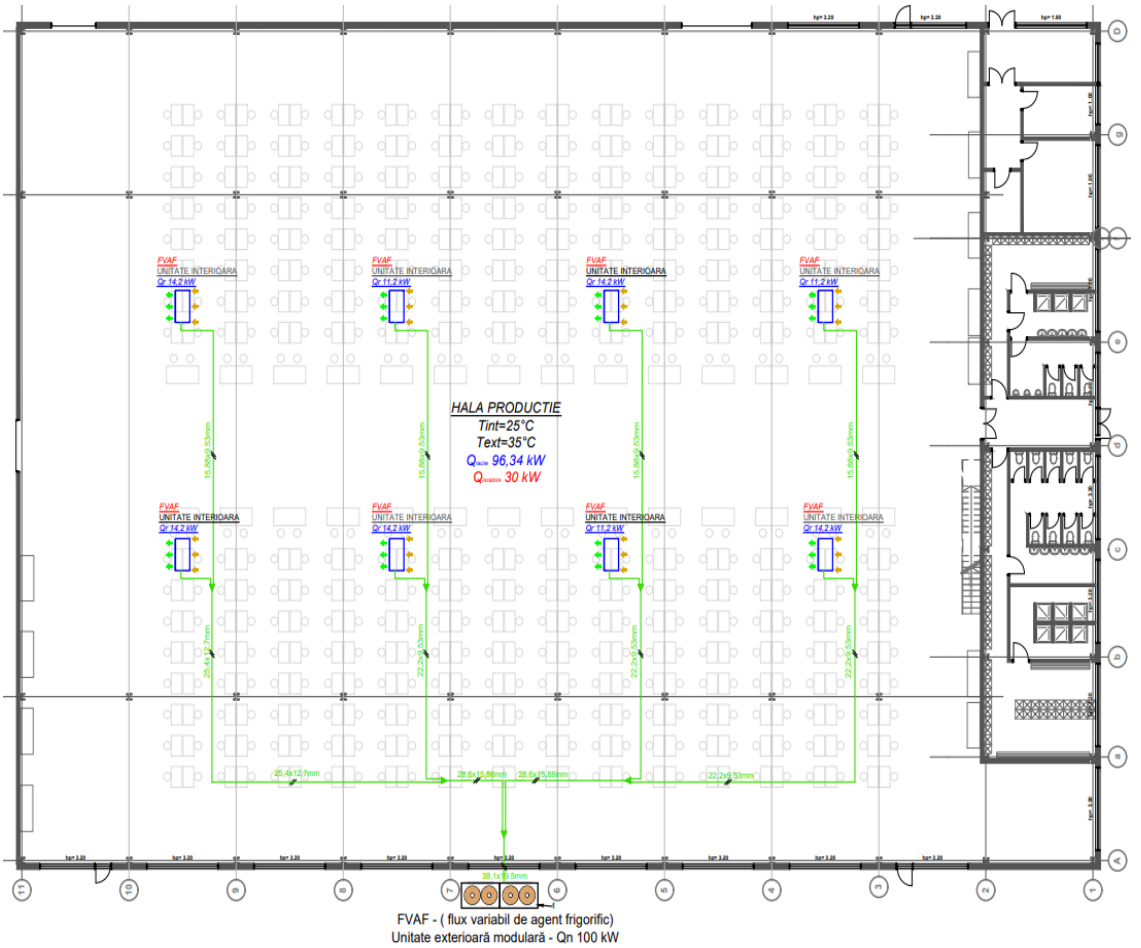

Fig. 4. Modern System

4. Conclusions

Following the study, the following conclusions were drawn:

- The VRF (Variable Refrigerant Flow) system offers greater long-term sustainability, as clients save on energy costs while simultaneously reducing carbon emissions by 35%.
- Higher energy efficiency - VRF systems use inverters and variable-speed compressors, adjusting the refrigerant flow based on actual needs, and are known for their enhanced energy efficiency.

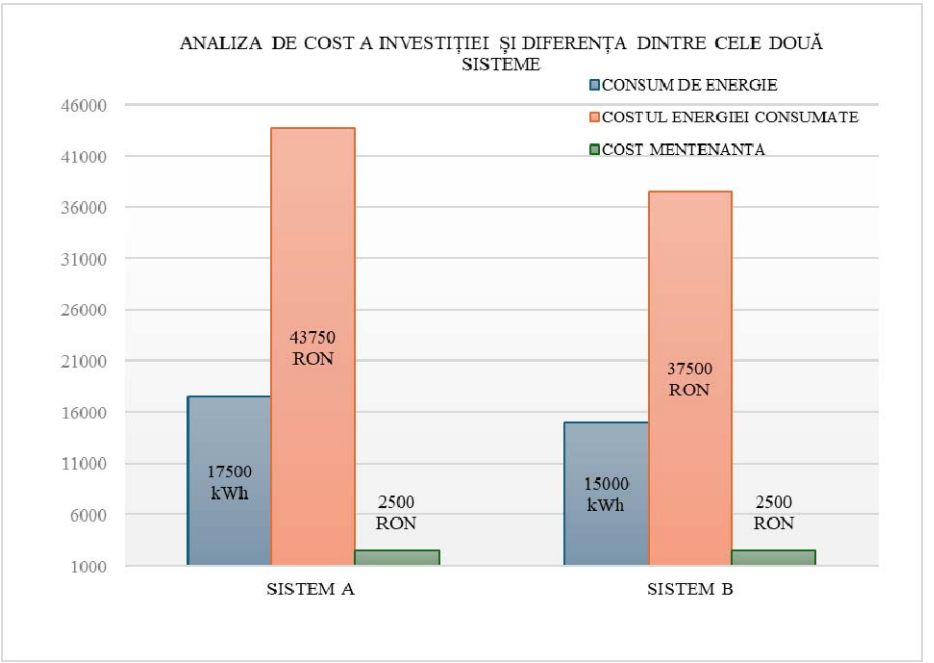

Fig. 5. Investment cost

The cost difference between the two systems (System A – traditional and System B – VRF) is 9.41%, with System B being more expensive at acquisition and commissioning.

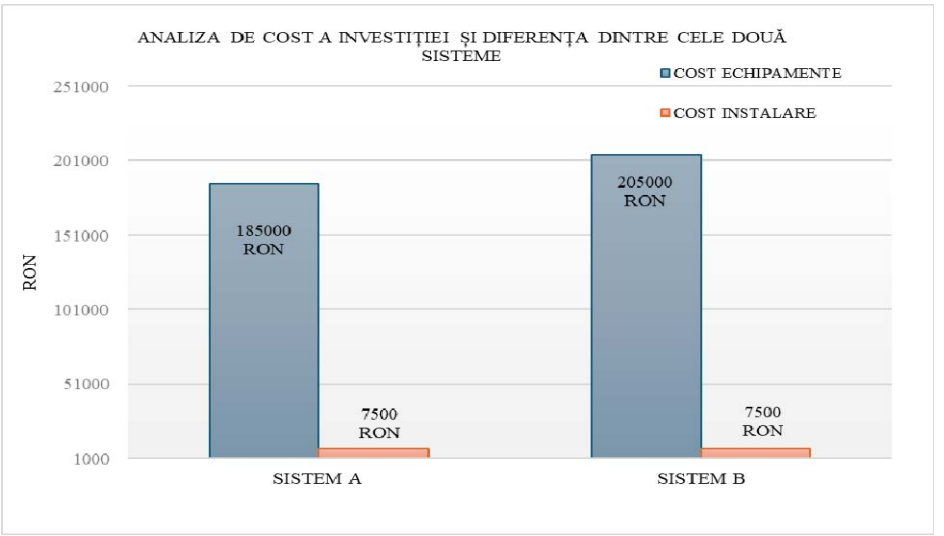

Fig. 6. Investment cost

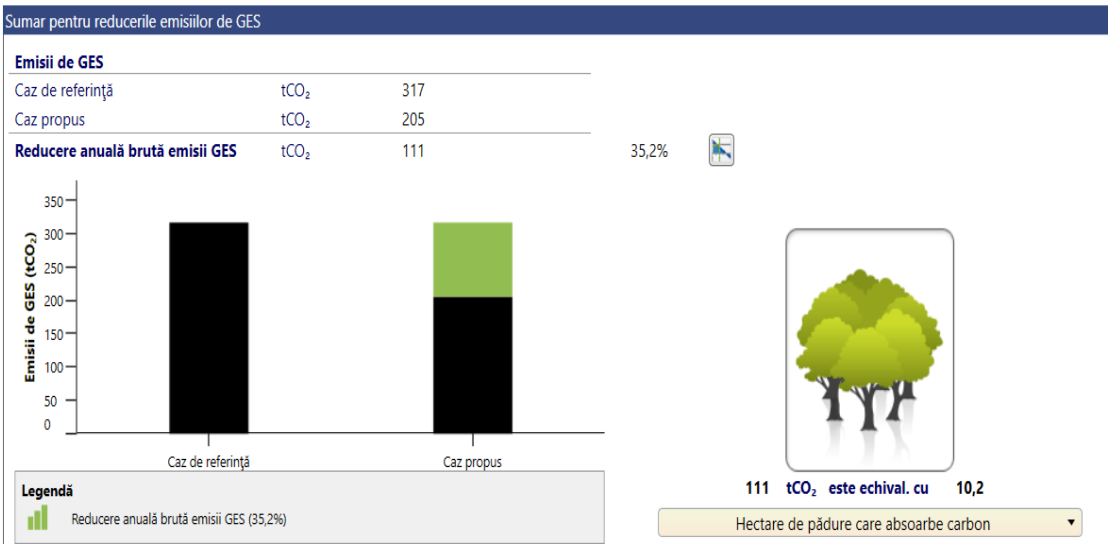

Fig. 7. Environment impact

References

[1] I5-2022 – Normativ pentru proiectarea, executarea si exploatarea instalatiilor de ventilatie si climatizare;
[2] I13-2023 - Normativ privind proiectarea, executarea si exploatarea instalatiilor de incalzire centrala;
[3] SR 1907/1/2014 – Instalatii de incalzire. Necesarul de incalzire de calcul. Prescriptii de proiectare;
[4] SR 6648/2:2014 - Instalatii de ventilare si climatizare. Parametri climatici exteriori;
[5] Soft CoolPack;
[6] Andrew C. Hernandez, Nelson Fumo, A review of variable refrigerant flow HVAC system components for residential application, International Journal of Refrigeration, Volume 110, 2020, Pages 47-57, ISSN 0140-7007
[7] Soft RETScreen Expert;
[8] https://www.daikin.eu
[9] 9 https://coolautomation.com

The choice of electricity storage systems to optimize the load curve. Case studies

Alegerea sistemelor de înmagazinare a energiei electrice pentru optimizarea curbei de sarcină. Studiu de caz

Danut Tokar [1], Adriana Tokar [1], Daniel Muntean [1], Daniel Bisorca [1], Alexandru Dorca[1], Marius Adam[1]

[1] University Politehnica Timisoara
Vctoriei Sq., No.2, 300006 Timisoara, Romania
E-mail: danut.tokar@upt.ro, adriana.tokar@upt.ro, daniel-beniamin.muntean@upt.ro, daniel.bisorca@upt.ro, alexandru.dorca@upt.ro, marius.adam@upt.ro

DOI: 10.37789/rjce.2026.17.1.7

Abstract. *The European Commission's (EC) policy to phase out fossil fuels from the energy system has forced the reconfiguration of electricity systems (ESS) as a result of the large-scale introduction of renewable energy systems (RES). Achieving these objectives while ensuring energy security must lead to a balanced energy mix capable of ensuring an energy price that can be borne by end consumers, a goal that can be achieved by installing energy storage systems.*

Key words: storage, energy, wind, photovoltaic, RES, energy securyty, cost

1. Introduction

Population growth, excessive urbanization, and the emancipation of the population have led to the development of a society based on consumption, determining the development of the means of production and the increase in energy consumption. Access to energy resources depends largely on technical, economic, political, cultural, geographical and military circumstances, highlighting the concept of energy poverty. [1-3].

The 1973 oil crisis highlights for the first time the energy vulnerability, including that of rich countries, and practically determines the start of research into renewable energy conversion systems. [1,4]. The attention of researchers, decision-makers, investors and last but not least, users has turned to energy sources capable of ensuring long-term sustainability. Research has been intensified into the use, in addition to waterfalls, of other renewable energy sources (RES): wind, solar, geothermal, tidal and biogas energy [5]. In the early 1980s, important research centers in Romania, under the coordination of the Research Center of the Traian Vuia

The article was received on 28.04.2025, accepted on 02.02.2026 and published on 24.02.2026

Polytechnic Institute in Timisoara, started a large-scale project to exploit the wind potential on Semenic Mountain [1,6].

Experts discuss the issue of depletion of energy resources but also the increase in greenhouse gas emissions (GHG). Thus, the end of the 20th century and the beginning of the 21st century mark the beginning of actions against global warming by reducing GHGs [2,3].

Even though Romania has the possibility of using a diversified range of primary energy resources (oil, natural gas, coal, hydropower, nuclear energy and renewable resources), in the current energy context, this sector is not immune to problems. În Fig. 1 este reprezentată evoluția producției de energie electrică pe surse de energie primară în perioada 2017-2050 [7].

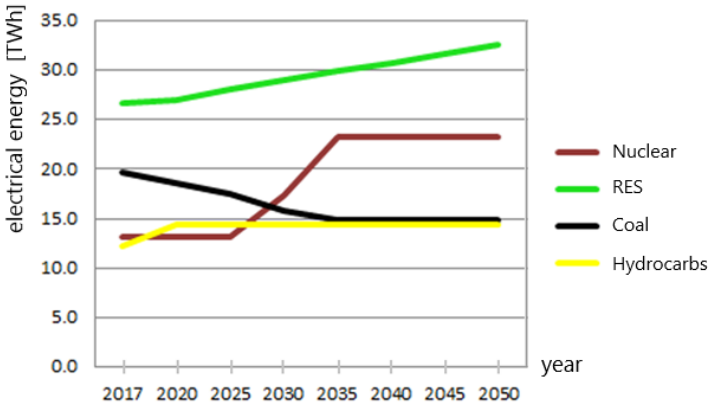

Fig. 1 Evolution of electricity production based on primary energy sources

On the other hand, in Fig. 2 it can be seen that a carbon-neutral Europe relies on solar and wind energy. Offshore wind technologies will become the most important source of electricity in the EU by 2040, complementing other renewable sources leading to a fully decarbonised energy system [8].

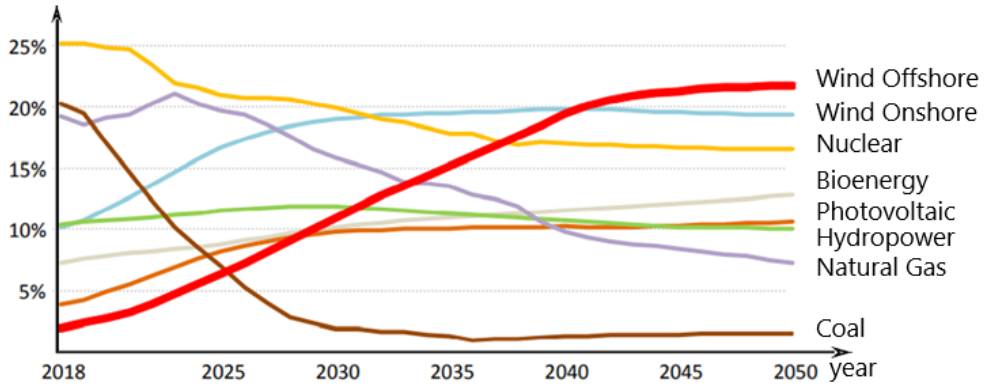

Fig. 2 Electricity production quotas in the EU according to the technologies used, in the scenario SDD [8]

The achievement of the objectives imposed by energy strategies at European level must be accelerated so that through the diversification of energy sources, energy security and an energy price that can be borne by end consumers are ensured.

2. Analysis of the National Energy System during the period 01.04.2025-21.04.2025

The announcements made by the Ministry of Energy proposing measures to support investments in new renewable electricity generation capacities [9,10] will increase the number of prosumers Table. 1, registered in the records of the National Energy Regulatory Authority (ANRE) [11]. All this confirms the trend towards the widest possible use of electricity from RES.

Table 1

Situation of the number of prosumers on 31.11.2023 versus 31.11.2024 [11].

Individual prosumers (IP)		Legal entity prosumers (PJ)		Total number of prosumers	
2023	2024	2023	2024	2023	2024
92569	172546	14432	22357	107001	194903

Analyzing the energy mix in the National Energy System (SEN) Fig.3, during the period 01.04.2025- 23.04.2025, its inability to ensure the energy needs was found, the positive balance is greater than the negative balance. It is worrying that with few exceptions Romania imported energy both on weekends and weekdays, Fig.4.

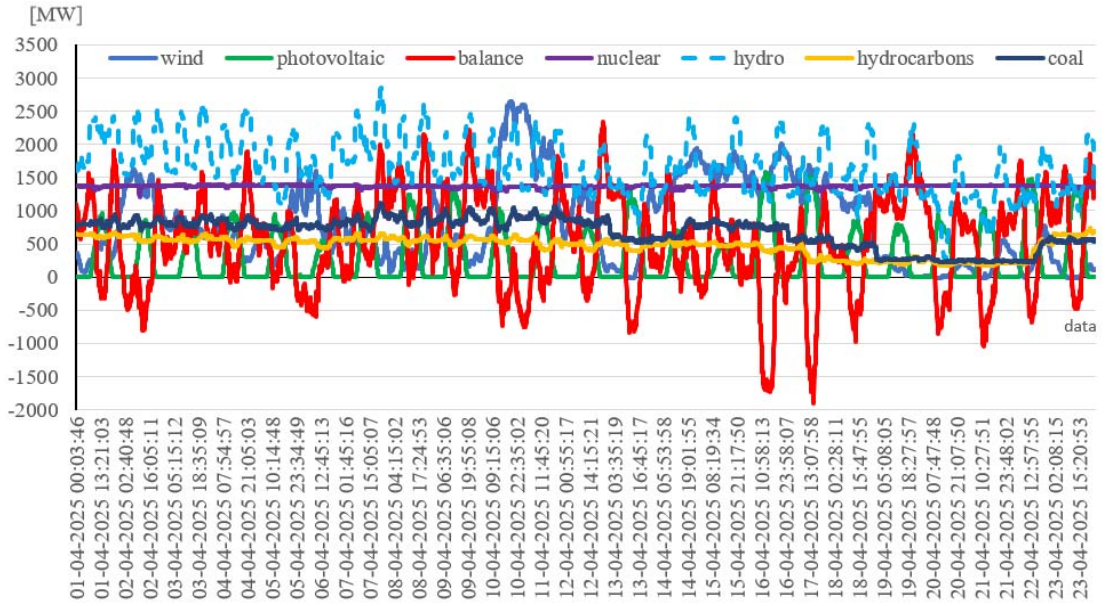

Fig. 3 Energy mix in the period 01.04.2025- 23.04.2025 [12]

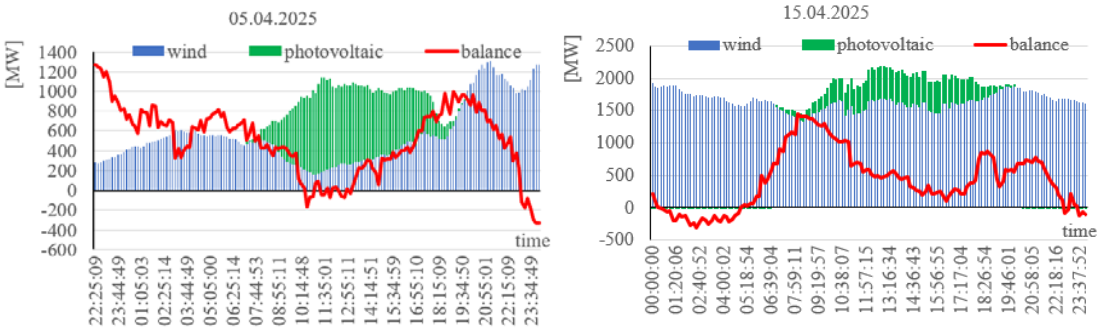

Fig. 4 SEN operation on 05.04.2025 and 15.04.2025 [12]

Even though the installed power in the NES increased by 4.52% in 2025 compared to 2024 [23], from a technical point of view, the failure to ensure the load curve, except for solar and wind systems, was due to the operation of classic conversion systems at 30.96% of the installed power [12], Table 2.

Table 2

Installed powers in NES [11,12]

Energy source	Installed capacity in 2024 [MW]	Installed capacity in 2025 [MW]	Average power charged in SEN in April 2025 [MW]
Wind	3026.91	3091.31	801.56
Photovoltaic	1626.74	2334.75	311.23
Hydropower	6639.06	6687.78	1658.78
Coal	2762.20	2762.20	676.18
Hidrocarbs	2684.43	2727.38	468.38
Nuclear	1413.00	1413.00	1368.40
Biomass	106.27	106.27	69.00

At the same time, it is noted that adopting only measures to increase the installed photovoltaic and wind power cannot ensure the ever-increasing demand for energy. Measures are required to improve the efficiency of coal-fired thermal power plants either by adopting Ultra-Supercritical (USC) technology or CO2 Capture and Storage (CCS) technologies [14], or by supplementing nuclear capacity [15] and electrical energy storage systems [16]. Practically, the optimization of hybrid energy systems that integrate RES is only possible by installing energy storage systems. All the more the storage systems are necessary for the optimization of small prosumer systems, which must be able to store the energy produced in favorable climatic conditions and return it to cover the load peaks during the day or when the production of renewable systems is not possible.

3. Electricity storage systems

The choice and sizing of electrical energy storage systems must take into account the nature and amplitude of fluctuations in the NES, the energy storage time,

the operating duration, the size of the storage system and, last but not least, the possibility of storing energy in natural environments or environments that do not generate electrotechnical waste.

Except for electrical and electrochemical storage systems, storing electrical energy with mechanical systems involves converting it into another form of energy. The classification of electrical energy storage systems is shown in Figure 5 [16].

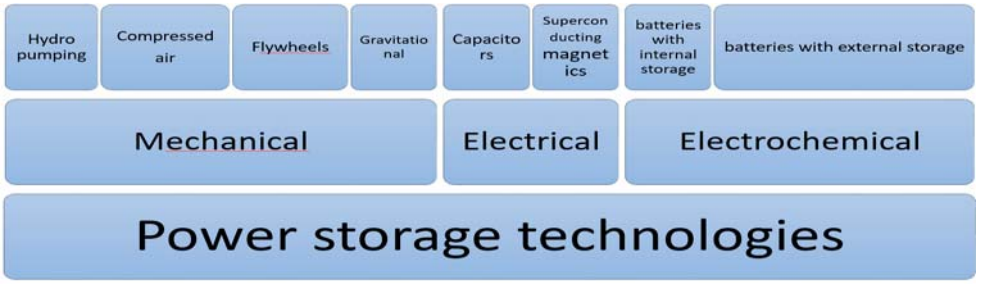

Fig. 5 Tehnologii de înmagazinare a energiei

In Fig. 6 shows the electrical energy storage systems ordered according to the power density (kW/kg), the energy density (kWh/kg) that it can store, but also according to the time in which the system can return the stored electrical energy to the SEN [5].

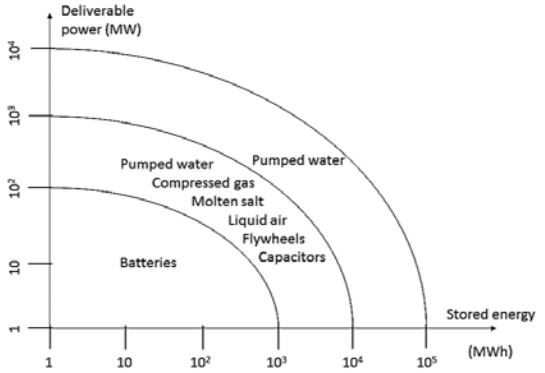

Fig 6 Systems of electrical energy storage [17]

The time in which an energy storage system returns the necessary energy can be in the order of seconds, minutes, hours, days, and the factors that influence the ability to return the stored energy are power density and energy density.

Mechanical energy storage systems are based on the transformation of kinetic and/or gravitational energy into electrical energy. Mechanical energy storage can be achieved in simple or complex systems, where the primary source can be water, compressed air, pressurized gases, thermal energy, etc. [18]. These systems have the advantage of qualitative and quantitative regulation of the NES, being able to return large amounts of energy in a very short time. The main electrochemical storage technologies presented in Fig. 7 refer to the storage of electrical energy in batteries, capacitors/supercapacitors and fuel cells, representing storage solutions in areas where

there are no storage possibilities in natural environments [1,16]. The electrochemical storage solution is compact, easy to install with fast charge/discharge cycles and is recommended for prosumers, but can also be adopted for large-scale RES systems.

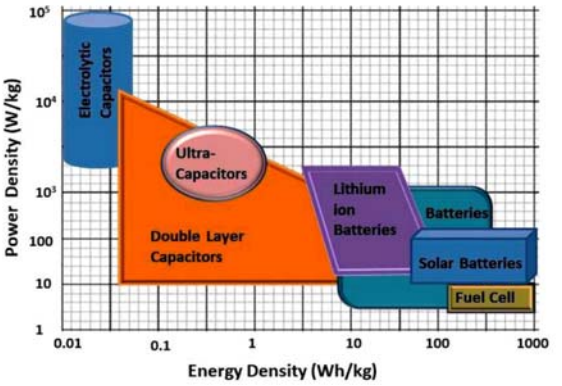

Fig. 7. Electrochemical storage systems [1]

3. Considerations regarding improving energy balance

The sizing of the storage system for the period analyzed in Fig. 8 must take into account the nominal voltage, maximum power, stored energy and the time in which it is stored and returned.

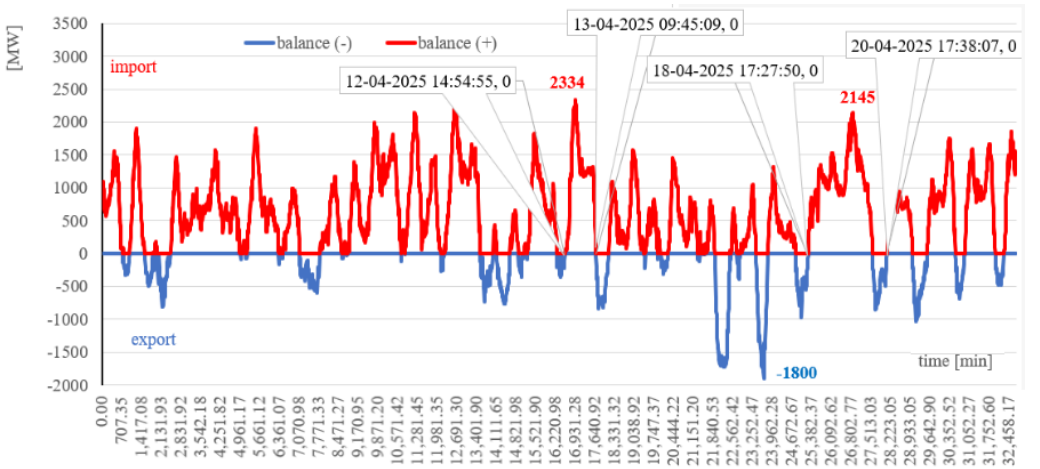

Fig. 8. NES balance in the period 01.04.2025- 23.04.2025 [12]

The value of the imported/exported energy E, in MWh, is obtained with the aid of rel.1:

$$E = \int_{t_1}^{t_2} P dt \tag{1}$$

Where: P is the electrical power in MW; t- time in h

For the period 04/01/2025- 04/23/2025, the energy required to cover the load curve calculated with rel, (1) is 11544MWh, at a maximum power of 2334MW (Fig.8). Assuming that we want to cover the load curve in Fig. 8, in the interval 18-04-2025 17:27:50 to 20-04-2025 17:38:07, i.e. 1128.59MWh with the energy produced up to that moment 1917.75MWh, a 2300MWh electrochemical storage system is proposed, the block diagram of which is presented in Fig. 9.

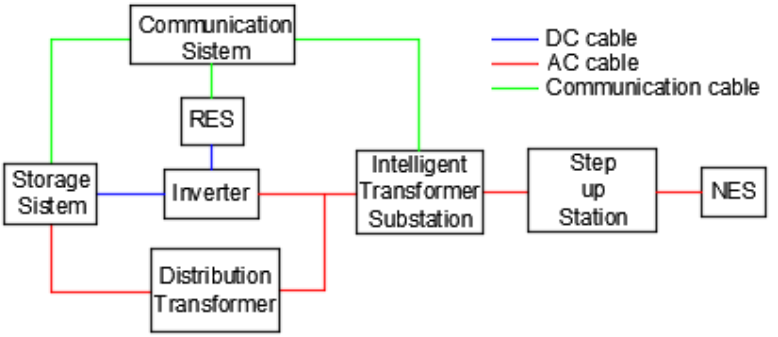

Fig. 9. Block diagram of the storage system

To size the storage system, the technical data sheet of the LUNA2000-4.5MWH-2H1 high-capacity battery, with 4.5MWh and 2h autonomy, was analyzed.. To store the energy produced during the analyzed period, 256 such batteries are required, each containing 104 cells of 280Ah/93.18kWh. Since the nominal power of the battery is 2236kW, peak loads will be covered from another source. The design of the system also involves the design of the site, which must take into account the fact that each unit is containerized, occupies an area of 17.55m^2 and a volume of 42.78m^3. For this reason, attention must be paid to the land areas occupied and to the design of the post-use phase of electrotechnical waste.

3. Conclusions

Without having a clear picture of the unavailability of already installed energy capacities, the inability of the NES to ensure consumption was observed even in the conditions in which there was an increase in installed power from RES compared to the previous year.

Thus, the targets assumed without careful analysis, the abandonment of fossil fuels without re-engineering thermoelectric plants based on the examples of good practices already on the table of the Ministry of Energy by Deloitte Touche Tohmatsu Limited, lead to massive imports of electricity to increase the price of electricity, to instability and energy poverty.

The need for electrical energy storage is accepted in all scientific and engineering circles, even by investors. The authors of this paper, analyzing the worrying situation of the NES, present the advantages of energy storage, but also draw attention to the occupied land areas and the obligation to design the post-use phase of electrotechnical waste.

References

[1] D. Tokar, A. Tokar, D. Muntean, D. Bisorca, A. Dorca, “Optimization of wind energy conversion systems”, Revista Română de Inginerie Civilă, vol. 15, Nr. 3, 2024, pp. 325-333.
[2] J. Kotcher, E. Maibach, WT. Choi, ”Fossil fuels are harming our brains: Identifying key messages about the health effects of air pollution from fossil fuels”, BMC Public Health, vol. 19, no.1079, 2019.
[3] J. Wang, L. Feng, X. Tang, Y. Bentley, M. Höök, ”The implications of fossil fuel supply constraints on climate change projections: A supply-side analysis”. Futures, vol.86, 2017, pp.58-72.
[4] W. Hafele, „Energy in a Finite World. Pathways to a viable future”, Editura Politică, Bucureşti, 1983.
[5] I.V. Dalea, I. Martin, A. Albu, ”Sustainable energy action plan monitoring report, Deva municipality, Hunedoara county”. Archistudio, Hunedoara, 2019.
[6] C. Zaharia, ” How the rust settled on the wind turbine project in communism”, Green Report, 2011, https://www.green-report.ro/cum-s-asezat-rugina-peste-eolienele/, Accessed: 07.02.2019.
[7] G.R., ” Romania's Energy Strategy 2019-2030 with a view to 2050”, Government of Romania, București, 2018.
[18] F. Birol, ”World Energy Outlook 2019”, International Energy Agency, Oslo, 2019.
[19] Ministry of Economy, "Applicant's Guide for Supporting Investments in New Electricity Production Capacities from Renewable Sources for Self-Consumption, for Applicants from the Private Sector, with Financing from the Modernization Fund - Key Programs 1 Renewable Energy Sources and Energy Storage, Related to the Second Round of the Call, to be Launched After the Approval of the Modified Programmatic Documents",https://energie.gov.ro/ Accessed: 09.04.2025.
[20] Ministry of Economy, ”OUG_URBAN-UP_29 Regarding the financing of condominium associations, social housing in condominium-type buildings under the administration of territorial administrative units and renewable energy communities, for the installation of photovoltaic panel systems for the production of electricity, with an installed power of at least 10 kWp, as well as for the purchase of electricity storage facilities produced from renewable sources, with a capacity of at least 50% of the installed power of the photovoltaic panel system", https://energie.gov.ro/proiectul-de-ordonanta-de-urgenta, Accessed: 09.04.2025.
[11] ANRE- Situation regarding the promotion of electricity produced by renewable electricity capacities belonging to prosumers as of 30.11.2024, https://anre.ro/consumatori/ energie -electrica/ cum-devin-prosumator/, Accessed: 09.04.2025.
[12] Transelectrica, ” The status of the National System in real time” https://www.transelectrica.ro/, Accessed: 24.04.2025.
[13] ANRE, ” The power installed in the production capacities", https://anre.ro/puteri-instalate/, https://www.transelectrica.ro/, Accessed: 09.04.2025.
[14] Deloitte Touche Tohmatsu Limited, „Study on the possibility of implementing advanced technologies in the exploitation and valorization of coal”, June, 2021-https://energie.gov.ro/ transparenta-si-integritate/ informatii-de-interes-public/, Accessed: 09.04.2025.
[15] F.A. Lunga, B.D. Toader, D. Tokar, Redemption of the lands occupied by the photovoltaic panels in the agricultural circuit, 33nd Edition International Conference, Building Facilitiesand Enviromental Comfort, Timisoara, 10- 11 April, 2024, pp.193-203.
[16] D. Tokar, C.Stroita, A.Tokar, A. Rusen, ”Hybrid System that Integrates the Lost Energy Recovery on the WaterWater Heat Pump Exhaust Circuit”, 4th International Conference World Multidisciplinary Civil Engineering-Architecture-Urban Planning Symposium (WMCAUS), IOP Conf. Series: Materials Science and Engineering vol.603, no. 042002 IOP Publishing, Prague, Czech Republic, 17- 21 June, 2019.
[17] T.M. Taylor, ”Energy storage”, in EPJ Web of Conferences, vol. 189, no. 00009, 2018.
[18] C. Cristescu, C. Dumitrescu, R. Rădoi, L. Dumitrescu, "New technological solutions for the conversion and storage of renewable energy", Buletinul AGIR, no. 3, 2018, pp. 56-62.
[19]*** LUNA2000-4.5MWH-2H1, https://vamat.nl/products/huawei-luna2000-4-5mwh-2h1, Accessed: 09.04.2025.

Vegetable origin-natural fibres for reinforcement of geopolymer composite

Fibre naturale de origine vegetală pentru armarea compozitului geopolimeric

Lucian Paunescu[1], Enikö Volceanov[2], Adrian Ioana[3], Bogdan Valentin Paunescu[4]

[1]Daily Sourcing & Research SA
95-97 calea Grivitei, sector 1, Bucharest 010705, Romania
E-mail: lucianpaunescu16@gmail.com

[2]National University of Science and Technology ”Politehnica”, Faculty of Engineering in Foreign Language
313 Independence Splai, sector 6, Bucharest 060541, Romania
E-mail: evolceanov@yahoo.com

[3]National University of Science and Technology ”Politehnica”, Faculty of Science and Materials Engineering
313 Independence Splai, sector 6, Bucharest 060541, Romania
E-mail: adyioana@yahoo.com

[4]Consitrans SA
56 Polona street, sector 1, Bucharest 010504, Romania
E-mail: pnscbogdan@yahoo.com

DOI: 10.37789/rjce.2026.17.1.8

Abstract. *The current trend to decrease greenhouse gas emissions through increasing the efficiency of fossil fuel consumption implies the use of lighter materials in building construction, with a lower carbon footprint compared to materials commonly applied in the present. Composites prepared from vegetable fibres constitute a viable solution to reach this objective. The precursors adopted for the production of the geopolymer composite were fly ash, granulated blast furnace slag, and rice husk ash, as alumina-silicate materials with cementitious properties, to which hemp fibres were added with a major role in reinforcing the composite. Results showed increasing the compression and flexure strength.*

Key words: *vegetable fibre, geopolymer composite, reinforcement, strength, hemp fibre.*

Rezumat. *Tendința actuală de a reduce emisiile de gaz cu efect de seră prin creșterea eficienței consumului de combustibil fosil implică utilizarea materialelor mai ușoare în construcția clădirilor, cu amprenta de carbon mai redusă, comparabil cu materialele aplicate în prezent în mod obișnuit. Compozitele preparate din fibre vegetale constituie o*

The article was received on 03.04.2025, accepted on 02.02.2026 and published on 24.02.2026

soluție viabilă pentru atingerea acestui obiectiv. Precursorii adoptați pentru producerea compozitului geopolimeric au fost cenușa zburătoare, zgura de furnal granulată și cenușa cojilor de orez, ca materiale aluminosilicatice cu proprietăți de cementare, la care au fost adăugate fibre de cânepă cu rolul major de armare a compozitului. Rezultatele au arătat creşterea rezistenței la compresiune și încovoiere.

Cuvinte cheie: fibră vegetală, compozit geopolimeric, armătură, rezistență, fibră de cânepă.

1. Introducere

The current trend to reduce greenhouse gas emissions by increasing the efficiency of fossil fuel consumption implies the use of lighter materials in the construction sector, with more reduced carbon footprint compared to the materials commonly used today. Composites made from natural plant-based fibres represent an interesting solution to achieve this objective. According to [1], this fibre type comes from renewable resources such as flax, hemp, jute, cotton, coconut, ramie, sisal, kenaf, etc. placed in a matrix derived from biomass.

The fibres contain variable proportions of cellulose, hemicellulose, and lignin. Cellulose and hemicellulose are polymers containing glucose and polysaccharides, respectively. Unlike these, lignin is an amorphous mixture of aromatic polymers and phenylpropane monomers [2].

Due to their excellent chemical and thermal resistance, high adhesion and mechanical strength properties, thermosets are widely used as matrices in bio-composites. Although it seems that thermoset matrices are more difficult to recycle at the end of their life, a more environmentally friendly matrix can be obtained by adding biodegradable fillers [3].

The prices of the main natural fibres available in the world vary according to [4] within quite wide limits between 200-4200 USD/ton. Among the cheapest, coir, kenaf, and pineapple are mentioned (between 200-550 USD/ton), followed by sisal and bamboo (600-900 USD/ton). Hemp fibre has values considered average (between 1000-2100 USD/ton), while cotton and flax reach the highest price ranges (between 1500-4200 USD/ton).

According to the literature [5], natural fibres exhibit high tensile strength, but their modulus of elasticity is slightly deficient. Several advantages of using natural fibres have been experimentally identified by researchers: the setting time of the composite cement is low as a result of releasing acidic components of fibres, the cement hydration is avoided due to the presence of hemicellulose and lignin, most natural fibres naturally decompose at end-of-life, the high availability and durability of resources from which natural fibres come, the low denseness of fibres favouring preparing lightweight materials, and the price of natural fibres mentioned above is much lower than that of glass, carbon or polymer fibres, the price of carbon fibres exceeding 12,000 USD/ton.

Traditionally, the techniques applied until recently were those based on reinforcing fibers from steel and synthetic materials. Currently, economic reasons make these fibre types no longer acceptable. Also, their manufacture is based on the consumption of non-renewable resources and emits CO_2 into the atmosphere [6].

Under the conditions in which of composite materials progress is in continuously growing, developing the new construction materials could not be left behind. In principle, the addition of fibres aims to prevent tensile cracking of materials, and improve other characteristics such as impact resistance and thermal insulation. Vegetable fibres whose structures include both crystalline and amorphous areas create problems related to porosity and water absorption, generating weak bonding between fibres and matrix [6].

A new challenge in the construction field in the last decade has emerged in the form of using vegetable materials as bio-aggregates in ecological concrete. As a result of recent research, innovative applications of natural fibres in construction have been promoted. Among the natural fibres mentioned above, hemp has been adopted for the manufacture of the new hemp concrete, considering its special peculiarities. Thus, fibres constitute about 33 % from the entire stem material, the remainder being the woody core. These components are processed into pieces with lengths between 2-25 mm called ”hurds”. Hemp does not need special protection against parasites because it does not contain nutrients. According to [7], the new hemp-based concrete is fireproof.

Results of research undertaken in the last two decades on the use of vegetable fibres as reinforcement in cement-matrix composites were presented in [8]. Applications of composites with reinforced vegetable fibre in structural and non-structural constructions to improve their mechanical properties were highlighted in this paper. It has been found that short vegetable fibres used as internal reinforcement increase the flexural and tensile strength as well as the hardness of cement-based composites. Long vegetable fibres are mainly used as external reinforcement, increasing the strength and ductility of composites. In accordance with authors, the information regarding the durability of fibres incorporated into cement matrices is still insufficient, leading to the deferral of their application in structural building components requiring high resistance to mechanical stress.

Reinforcing with hemp fibres (in weight ratios of 3 and 9 %, respectively) of a geopolymer material based on fly ash and red mud was experimentally tried [9]. The geopolymer matrix was made of 70 % fly ash with a grain size under 21 μm and 30 % red mud with a grain size under 75 μm. The aqueous solution including sodium silicate, sodium hydroxide in the form of pellets dissolved in deionized water, and hemp fibres was poured over the solid mixture. It has been observed that a hemp fiber content higher than 9 % adversely affects the homogeneity of the fibre distribution in the matrix, disturbing the mechanical properties of the geopolymer. Also, increasing the fibre content causes a decrease in workability, allowing air bubbles to enter and to be trapped in the geopolymer mass during the pouring of the paste into the mould. On the other hand, loading hemp fibres in the mentioned range of 3-9 % does not allow the formation of voids and uniform dispersion of fibres can be obtained. In general, it

was found that by increasing the proportion of added fibres, the compressive strength of the geopolymer composite tends to slightly decrease.

In another work [10], the effect of the binder type used to produce hemp-lime concrete on its mechanical strength and durability was investigated. The following types of binder were tested: hydrated lime, hydraulic lime, and Portland cement. Metakaolin and granulated blast furnace slag as pozzolanic materials were added to the manufacturing mixture due to their rapid setting and high reactivity. Due to its role on improving mechanical properties, hydroxymethyl cellulose has been used in optimal ratio of 0.8 % [11] as well as hemp fibres. The mixing procedure consisted in creating a slurry with binder and water before adding the fibres. The fresh concrete was poured into a mould and lightly pressed. Then, the material removed from the mould was placed in a curing chamber at about 16 ℃ and relative humidity between 50-60 %. The compression strength of the product had values in the range of 0.02-0.04 MPa after 5 days and 0.29-0.39 MPa after 28 days.

In a recent work [12], the influence of length and amount of hemp fibres on the properties of composite based on blast furnace slag reinforced with fibres was investigated. Thus, fibres with length of 10 and 20 mm, in proportions of 0.5; 1; 2; and 3 % from the cement weight were tested. Determining the compression and flexure strengths were carried out after 7 and 28 days. Values of the two resistance types after 28 days varies between 1.28-2.73 MPa (in the case of compression) and between 0.48-1.65 MPa (in the case of flexure), Determining the sample resistance to temperatures within the limits of 250-750 ℃ showed that the use of 20 mm hemp fibres led to increasing the compression and flexure strength, but also contributed to increase the heat conductivity.

An authors' team of the current paper recently investigated [13] a technique for manufacturing a reinforced concrete composite with hemp fibres using as a binder a mixture composed of alumina-silicate industrial by-products (fly ash and granulated blast furnace slag) as well as residual building concrete from demolition. Hemp fibres were added to the starting mixture, their weight proportion varying within the limits of 2.44-8.67 %. By mixing, a slurry resulted, being poured into a mould. Introduced into an laborator y electric oven, the mould containing the paste was heated with hot air at 80 ℃ for 4 hours. The hemp concrete specimen removed from the mould was subjected to the curing process at ambient temperature for 28 days. The experimental results indicated the following values: density between 303-350 $kg \cdot m^{-3}$, porosity in the range of 83.5-85.8 %, heat conductivity in the range of 0.084-0.102 $W \cdot m^{-1} \cdot K^{-1}$, compressive strength between 7.6-8.5 MPa, and water uptake in the range of 2.2-2.9 vol. %. The optimal version was identified as the one in which the hemp fibre amount was 5.66 g per 100 g solid mixture. The product corresponding to the optimal version had the density of 327 $kg \cdot m^{-3}$, heat conductivity of 0.094 $W \cdot m^{-1} \cdot K^{-1}$, and compression strength of 8.1 MPa.

The current work presented below brought several changes in the composition of the starting materials and the peculiarities of preparing and hardening process of the geopolymer composite reinforced with vegetable fibres, aiming to improve its mechanical properties.

2. Materials and methods

Materials adopted for manufacturing geopolymer composite reinforced with vegetable fibres were coal fly ash, ground granulated blast furnace slag, and rice husk ash, all being cementitious materials with pozzolanic properties, suitable for producing geopolymers. The combination of fly ash and granulated blast furnace slag in this process type is quite frequently used, according to the literature, while the addition of rice husk ash to this mixture is much less applied.

Coal fly ash was the main material used in the solid mixture of the geopolymer composite, coming as a by-product of the energy producing industry. Fly ash is the result of burning the coal in boilers of the Paroseni thermal power plant, being captured in its electrostatic precipitators. The grain size of this by-product is below 250 μm. The ash was purchased by authors about 10 years ago, at a period when anthracite was the used coal type. For this reason, the fly ash is classified as class F, characterized by low proportion of calcium oxide. The waste purchased from Paroseni was subjected to mechanical processing for reducing its grain size under 80 μm. The chemical composition of the ash was determined through analysis in the AXIOS type X-ray fluorescence spectrometer from the Romanian Metallurgical Research Institute. The oxide composition of fly ash included the following components: 50.2 % SiO_2, 25.6 % Al_2O_3, 3.5 % CaO, 3.3 % MgO, 5.9 % Na_2O, 4.0 K_2O, 6.9 % Fe_2O_3.

Granulated blast furnace slag procured from ArcelorMittal Galati (Romania) 12 years ago is a by-product of the metallurgical industry. Granulated slag is obtained by pouring hot slag into a water bath, resulting in the form of spheres with diameter between 2-6 mm. For use in the manufacture of the geopolymer composite, the granulated slag was ground in a ball mill to particle size below 70 μm. The chemical composition of the slag includes 36.5 % SiO_2, 11.7 % Al_2O_3, 41.5 % CaO, 5.7 % MgO, 0.5 % MnO, 0.9 % Fe_2O_3, 0.3 % Na_2O, 0.4 % K_2O.

Rice husk ash is a by-product of the rice milling industry, resulting from the burning or incineration of rice husks at high temperature. The process of controlled burning in a furnace or reactor reduces the rate of silica crystallization, simultaneously increasing the amorphous silica content. Burning at temperatures between 550-800 ℃ favours the formation of amorphous silica, while higher temperatures lead to the formation of crystalline silica. The particle size of rice husk ash is within the limits of 5-10 μm and the silica content of the ash varies between 84.4-93.1 % [14].

The alkaline activation of the above-mentioned alumina-silicate materials involved the formation of a liquid mixture including NaOH in the form of pellets dissolved in distilled water (the molarity of the solution being 12M) and a sodium silicate solution (38 % concentration). Also, short hemp fibres were introduced and mixed into the alkaline liquid solution.

NaOH pellets were purchased from the market. The basic properties of NaOH pellets are high solubility, high alkalinity, non-volatility, and hygroscopic nature [15]. Also, sodium silicate solution with 38 % concentration was procured from the market. Sodium silicate or water glass is produced by melting quartz sand together sodium carbonate. Most commonly, water glass is a silicate binder dissolved in water. The

main suppliers of water glass are in Germany (Bockling GmbH, Caldic Deutschland Chemie B.V.), Poland (Chematex Sp.z.o.o.), Austria (Deuring GmbH), China (MC Glass). Short hemp fibres originating from the United States were also commercially purchased. Hemp production has significantly increased in the last decades due to the intense demand for environmentally friendly and sustainable products. Hemp fibres are concentrated in the stem of the plant, so harvesting the stems and separating the fibres are the main fibre recovery operations.

The method of turning alumina-silicate waste as inert materials into geopolymer composites was based on their alkaline activation with a liquid mixture of NaOH and water glass. Through alkaline activation, the geopolymerization reaction is initiated and developed leading to the formation of a geopolymer, according to the discovery of the French researcher J. Davidovits [16].

Peculiarities of the geopolymerization process of alumina-silicate minerals are presented in [17]. Geopolymers having an amorphous microstructure are formed through co-polymerization of individual aluminum and silicates species that come from the dissolution of precursor materials containing silicon and aluminum in the presence of soluble alkali-metal silicates. Alumina-silicate materials are largely soluble in the alkaline activator solution, the dissolution degree being higher in NaOH solution compared to KOH solution. It was found that materials with a higher dissolution degree facilitate to obtain higher compression strength after geopolymerization. On the other hand, the use of KOH solution instead of NaOH solution favours the development of the geopolymerization process.

Geopolymerization involves a non-homogeneous chemical reaction between the alkaline solution and alumina-silicate oxides. Thus, conditions are created for the formation of semi-crystalline polymer systems containing Si-O-Si and Si-O-Al bonds. Poly(sialates) are known as ring polymers and chain with Al^{3+} and Si^{4+} [18]. J. Davidovits, the inventor of geopolymer, has found that the by-product of the reaction of alkaline activator with aluminum and silicon could be used for producing geopolymers.

The methods used for investigating the composite specimen features were the following. The geopolymer composite density was determined by Archimedes' method through the water intrusion technique (ASTM D792-20). Porosity was calculated as a percentage of the difference between the estimated density of vegetable fibre composite without voids and the measured density including the void volume related to the composite density without voids, in accordance with NE 012-99 (Code 1999). The compression strength was measured with a 2000 kN-compression fixture Wyoming Test Fixture [19] and the flexural strength was determined by carrying out the three-point bend test on the specimen (SR EN ISO 14125:2000). Heat conductivity at room temperature was determined with HFM 446 Lambda apparatus using the heat-flow method (SR EN 1946-3:2004). Water uptake was determined by the immersion method of the sample under water for 24 hours (ASTM C948) at the end of the curing process (28 days) and the specimen mass was identified through weighing. The microstructural appearance of geopolymer composite specimens was investigated with the Biological Microscope model MT5000.

3. Results and discussion

Four experimental versions were chosen for making the hemp fibre reinforced geopolymer composite. The quantity and composition of materials that composed up the starting mixture are shown in Table 1.

Table 1

Composition of experimental versions

Composition	Experimental version (g)			
	1	2	3	4
Coal fly ash	45.2	44.0	42.8	41.6
Granulated blast furnace slag	29.5	29.0	28.5	28.0
Rice husk ash	22.7	22.3	21.9	21.5
Hemp fibre	2.6	4.7	6.8	8.9
Total solid	100.0	100.0	100.0	100.0
Water glass solution	30.5	30.5	30.5	30.5
12M NaOH solution	12.0	12.0	12.0	12.0
Water addition	7.5	7.5	7.5	7.5
Total liquid	50.0	50.0	50.0	50.0
Total slurry	150.0	150.0	150.0	150.0

In accordance with the data in Table 1, the amount of coal fly ash varied between 41.6-45.2 g, granulated blast furnace slag had values between 28.0-29.5 g, and rice husk ash within the limits of 21.5-22.7 g, all being decreasing, while hemp fiber had increasing values between 2.6-8.9 g. The total solids of the mix in all four versions were set to be 100 g. Liquid components were kept at constant values: Water glass solution (30.5 g), 12M NaOH solution (12 g), and water addition (7.5 g), and the total of their value was 50 g. The water glass/NaOH ratio was also constant for all versions, i.e. 2.54.

Applying the requirements of the adopted production method, including also the parameters of the curing process of the fresh materials (at 28 days), four cured specimens of hemp fiber geopolymer composite were obtained, shown in Fig. 1.

a b

c d

Fig. 1. Images of the surface of geopolymer composite specimens reinforced with hemp fibre
a – version 1; b – version 2; c – version 3; d – version 4.

Physio-mechanical and heat characteristics of composite specimens are presented in Table 2.

Table 2

Physio-mechanical and heat characteristics of the hemp fibre geopolymer composite specimens

Characteristic	Version 1	Version 2	Version 3	Version 4
Density ($kg \cdot m^{-3}$)	352	335	317	300
Porosity (%)	83.0	83.9	84.8	85.9
Heat conductivity ($W \cdot m^{-1} \cdot K^{-1}$)	0.105	0.098	0.091	0.083
Compression strength (MPa)				
- after 7 days	2.5	2.6	2.1	1.5
- after 28 days	6.3	6.8	5.5	4.7
Flexural strength (MPa)				
- after 7 days	1.2	1.0	0.9	0.6
- after 28 days	1.7	1.6	1.2	0.8
Water uptake (vol. %)	3.0	2.8	2.7	2.5

Table 2 presents the evolution of geopolymer composite features between the four experimental versions made by slight decrease in the proportion of the main components of the mix (fly ash, slag, and rice husk ash) and the quite pronounced increase in the amount of hemp fibre. A significant decrease in the density of specimens (from 352 to 300 $kg \cdot m^{-3}$) was observed simultaneously with an increase in their porosity (between 83.0-85.9 %). Interesting effects on the compressive strength were felt after 28 days of curing. Thus, first, the strength value slightly increased, then in the case of the last two versions it had a clear decreasing trend, still remaining in remarkably high value range (up to 4.7 MPa). The improvement in compressive strength at early age (after 7 days) was achieved slowly in all tested versions with values of 2.5-2.6 MPa in the case of the first two versions and 1.5-2.1 MPa in versions

3-4. On the other hand, the flexure strength value registered a decrease from 1.7 to 0.8 MPa after 28 days in the ascending order of experimental versions. The measurement results carried out at early age showed that the flexure strength values reached high levels compared to the values at the end of the curing process (between 62.5-75 %). Water uptake measured in the case of geopolymer composite reinforced with hemp fibres was in the range of 2.5-3.0 vol. %, being considered at a normal level for this material type.

Microstructural peculiarities of geopolymer composite specimens reinforced with hemp fibre are shown in Fig. 2.

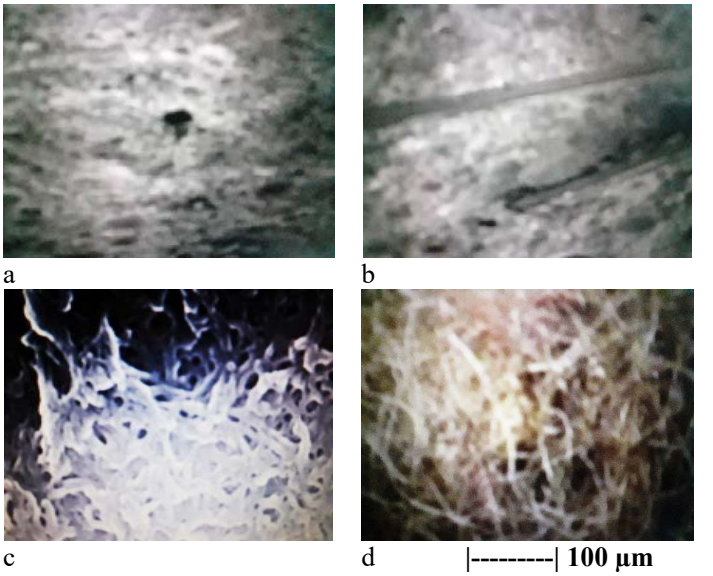

Fig. 2. Microstructural peculiarities of geopolymer composite specimens reinforced with hemp fibre
a – version 1; b – version 2; c – version 3; d – version 4.

The length of fibres used in this experiment was within the limits of 13-19 mm. The pictures in Fig. 2 show the increase conditions of hemp fibres ratio between versions 1-4.

The environmentally friendly and economic role of using various alumina-silicate industrial by-products in the production process of geopolymer composites as substitutes for traditional cementitious and pozzolanic materials (Portland cement) has already been evaluated in recent decades. These wastes, as well as other natural alumina-silicate materials nominated and claimed by the inventor of geopolymers J. Davidovits, have allowed the manufacture, through various combinations in the starting mixture, of new construction materials with excellent physical, mechanical, chemical, and thermal features.

Vegetable fibres have already confirmed their effect on increasing the strength of these composites. In the current work, coal fly ash, granulated blast furnace slag, and rice husk ash were adopted as precursor materials and hemp fibres as reinforcing

vegetable fibres. Regarding hemp fibre, this type of vegetable fibre is probably one of the most appreciated materials for reinforcing geopolymer composites.

Of course, it is well known that vegetable fibsres do not have a reinforcing effect comparable to that of steel, glass, or carbon fibres, which were used intensively until recently, but the price of these fibres is very high, incomparable to that of vegetable fibres. This is the main reason why there is a clear trend in the world to adopt vegetable fibres in manufacturing processes of composites.

According to [5], natural fibres show high tensile strength, although their modulus of elasticity is deficient. Based on experimental determinations, several advantages of using natural fibres should be mentioned: availability and durability of resources containing natural fibres, setting time of the composite cement is low, cement hydration is avoided due to hemicellulose and lignin presence, most natural fibres decompose at end-of-life, contributing to environmental protection.

4. Conclusions

The paper aimed at the production of a geopolymer composite based on alumina-silicate precursor materials (fly ash, granulated blast furnace slag, and rice husk ash) from industrial by-products. The composite was reinforced with vegetable fibres (hemp fibres). The inert material mixture was activated with a liquid alkaline solution containing NaOH dissolved in deionized water and water glass (sodium silicate). Therefore, the work fell within the modern trend of using cheap residual materials, including also vegetable reinforcement fibres, incomparably less expensive than steel, glass or carbon fibres intensively utilized until now. Among the many types of vegetable fibre available in the world, short hemp fibres with a length between 19-29 mm were chosen. The advantages of their use include some peculiarities such as durability, versatility, and availability. Lately, the interest in this plant and especially, the recovery of its fibres is growing. The method for producing the hemp fibre-geopolymer composite tried in this experiment generally adopted the principles expounded and claimed by the inventor of geopolymers the French researcher J. Davidovits at the end of the 20th century and the beginning of the new millennium. The coal fly ash as well as the metallurgical slag are industrial by-products suitable for the manufacture of geopolymers, being recommended by the French inventor. The rice husk ash used by authors in the experiment described in this paper constitutes another adequate, but less applied, waste type. Apart from the particular combination of material precursors, another element of originality of the work is represented by the adopted ranges of their quantity values. The test results showed the possibility of obtaining relatively high values of compressive strength after the 28-day curing process (6.8 MPa in the case of experimental version 2). The peculiarity of the flexural strength was the high level of the values of this resistance at early age (after only 7 days) compared to its final values after 28 days.

References

[1] I. Elfaleh, F. Abbassi, M. Habibi, F. Ahmad, M. Guedri, M. Nasri, C. Garnier, „A Comprehensive Review of Natural Fibers and their Composites: An Eco-Friendly Alternative to Conventional Materials", in Results in Engineering, Elsevier, vol. 19, 2023. https://doi.org/10.1016/j.rineng.2023.101271

[2] V.M. John, M.A. Cincotto, C. Sjöström, V. Agopyan, C.T.A. Oliveira, „Durability of Slag Mortar Reinforced with Coconut Fibre", in Cement and Concrete Composites, Elsevier, vol. 27, no. 5, 2005, pp. 565-574. https://doi.org/10.1016/j.cemconcomp.2004.09.007

[3] G.F. Smith, „New Development in Producing More Functional and Sustainable Composites", in Management Recycling and Reuse of Waste Composites, Elsevier, 2010. pp. 425-439. https://doi.org/10.1533/9781845697622.4.425

[4] P. Peças, H. Carvalho, H. Salman, M. Leite, „Natural Fibre Composites and their Applications: A Review", in Journal of Composites Science, MDPI, vol. 2, no. 4, 2018. https://doi.org/10.3390/jcs2040068

[5] F. Pacheco-Torgal, S. Jalali, „Vegetable Fibre Reinforced Concrete Composites: A Review", in Materials Science and Engineering, vol. 527, no. 1-2, 2009. https://repositorium.sdum.uminho.pt/bitstream/1822/10453/1/Materials_2009.pdf

[6] A. Arvizo-Montes, M.J. Martinez-Echevarria, „Vegetable Fibers in Cement Composites: A Bibliometric Analysis, Current Status, and Future Outlooks", in Materials, MDPI, Sun, L. (acad.ed.), vol. 18, no. 2, 2025. https://doi.org/10.3390/ma18020333

[7] M. Brűmmer, M.P. Sâez-Pérez, J.D. Suârez, „Hemp Concrete: A High Performance Material for Green-Building and Retrofitting", 2017. https://urbannext.net/hemp-concrete/

[8] V. Laverde, A. Marin, J.M. Benjumea, M.R. Ortiz, „Use of Vegetable Fibers as Reinforcements in Cement-Matrix Composite Materials: A Review", in Construction and Building Materials, Elsevier, vol. 340, 2022. https://doi.org/10.1016/j.conbuildmat.2022.127729

[9] E.A. Taye, J.A. Roether, D.W. Schubert, D.T. Redda, A.R. Boccaccini, „Hemp Fiber Reinforced Red Mud/Fly Ash Geopolymer Composite Materials: Effect of Fiber Content on Mechanical Strength", in Materials, MDPI, A. Mohajerani, F.J. Espinach Orus (acad. eds.), vol. 14, no. 3, 2021, pp. 511-519. https://doi.org/10.3390/ma14030511

[10] R. Walker, S. Pavia, R. Mitchell, „Mechanical Properties and Durability of Hemp-Lime Concretes", in Construction and Building Materials, Elsevier, vol. 61, 2014, pp. 340-348. https://doi.org/10.1016/j.conbuildmat.2014.02.065

[11] Y. Cui, H. Hao, J. Li, W. Chen, „Effect of Adding Methylcellulose on Mechanical and Vibration Properties of Geopolymer Paste and Hybrid Fiber-Reinforced Geopolymer Composite", in Journal of Materials of Civil Engineering, American Society of Civil Engineering, vol. 32, no. 7, 2029. https://doi.org/10.1916/(ASCE)MT.1943-55.33.000.3236

[12] O.Y. Bayraktar, D.E. Tobbala, M. Turkoglu, G. Kaplan, B.A. Tayeh, „Hemp Fiber Reinforced One-Part Alkali-Activated Composites with Expanded Perlite: Mechanical Properties, Microstructure Analysis and High-Temperature Resistance", in Construction and Building Materials, Elsevier, vol. 363, 2023. https://doi.org/10.1061/j.conbuildmat.2022.129716

[13] L. Paunescu, E. Volceanov, B.V. Paunescu, „Reinforced Concrete Composite with Vegetable Fibre", in Academic Journal of Manufacturing Engineering, Technical University of Cluj-Napoca, Romania, Academic Association of Manufacturing Engineering, vol. 21, no. 1, 2023, pp. 120-125, ISSN: 1583-7904.

[14] A.H. Ismail, A. Kusbiantoro, Y. Tajunnisa, J.J. Ekaputri, I. Laory, „A Review of Aluminosilicate Sources from Inorganic Waste for Geopolymer Production: Sustainable Approach for Hydrocarbon Waste Disposal", in Cleaner Material, Elsevier, vol. 13, 2024. https://doi.org/j.clema.2024.100259

[15] *** Understanding the Chemistry of Sodium Hydroxide Pellets, Atlas Pellets Industies, Gujarat, India, 2024. https://www.causticpellets.com/chemistry-of-sodium-hydroxide-pellets/

[16] J. Davidovits, „Geopolymers: Inorganic Polymeric New Materials", in Journal of Thermal Analysis Calorimetry, Springer Link Publishing, vol. 37, no. 8, 2008, pp. 1633-1656. https://doi.org/10.1007/BF01912193

[17] H. Xu, J.S.J. Van Deventer, „The geopolimerisation of alumino-silicate minerals", in International Journal of Mineral Processing, Elsevier, vol. 59, no. 3, 2000, pp. 247-266. https://doi.org/10.1016/S0301-7516(99)00074-5

[18] J. Davidovits, „Geopolymers: Ceramic-Like Inorganic Polymers", in Journal of Ceramic Science and Technology, vol. 8, no. 3, 2017, pp. 335-350. https://doi.org/10.4416/JCST2017-00038

[19] A.A. Dyg Siti Quraisyah, K. Kartini, M.S. Hamidah, „Water Absorption of Incorporating Sustainable Quarry Dust in Self-Compacting Concrete", 4th International Symposium on Green and Sustainable Technology (ISGST), Kampar, Malaysia, October 3-6, 2021, IOP Conf. Series: Earth Environmental Science, vol. 945, IOP Publishing Ltd., 2021. https://doi.org/10.1088/1755-1315/945/1/012037

Latest solutions in optimizing electrical energy consumption in water supply systems

Water losses in the water supply system

Soluţii de ultimă oră în optimizarea consumului de energie electrică în sistemele de alimentare cu apă

Pierderile de apă ale sistemului de alimentare cu apă

Dragoș – Vasile Ille[1], Coita Flaviu-Glad[1], George – Lucian Ionescu [2]

[1]University of Oradea, PhD student, Energy Engineering Field
4 Delavrancea Str., Oradea, Bihor, Romania
E-mail: illedragos@yahoo.com, gladflaviu@gmail.com
[2] University of Oradea, 4 Delavrancea Str., Oradea, Bihor, Romania
E-mail: lucian.ionescu1985@yahoo.com

DOI: 10.37789/rjce.2026.17.1.9

Abstract. *The main source of energy loss within water supply systems is found within the loss of water from within said systems.Understanding the reasons for these losses and taking the proper steps in curtailing their occurence while also reinforcing the reliability of the systems will ensure not only the optimal operational regime for the system but also increase the energy economy.*

Key words: water losses, water supply systems, energy consumption

1. Introduction

Water losses in water supply systems are the most common phenomena that lead to large energy losses.

Water losses in water supply systems of populated centers and industries, i.e. water that does not bring in revenue (Non Revenue Water) is understood as the amount of water that leaves the installations without a specific use, due to leaks in pipe joints, the operation of reservoir overflows, etc. and must represent a percentage as small as possible of the total volume of water distributed [6], [8], [16], [17].

Upon a deeper analysis of the phenomenon of water losses, it is found that these losses are divided into three categories:

A) Technological water loss, referring to the water used to ensure the proper functioning of the water treatment process.

The article was received on 08.12.2025, accepted on 02.02.2026 and published on 24.02.2026

According to IWA (International Water Association) this is a loss of water because it does not bring in income. However, this loss of water should not be quantified as water that does not bring in income, due to the fact that if a treatment plant is not maintained in proper operating condition, we will have nothing to sell, so we will have no income. However, there is also a component of this water that can be perceived as a loss of water, namely, the part of the technological consumption used independently of the water strictly necessary for the maintenance of the plant.

For example, if the operator washes the filter with 4 $l/s \cdot m^2$ in a time interval of 20 minutes instead of 15 minutes as would be necessary, although normally, the filter can be washed with 2 $l/s \cdot m^2$, then the difference between the actual consumption required and the actual consumption used constitutes a loss of water. In addition, the tank is washed until the resulting water at the spillway is clear, or washing could be stopped when the resulting water has a turbidity equivalent to the decanted water.

By proceeding in this way, washing water can be saved, thus reducing the loss of technological water. This additional water consumption is considered a real loss, as is the water for discharging the sludge when it is very diluted. In the end, it can be concluded that water loss is only the amount of water used irrationally in the station.

B) Physical loss of water that occurs through leaks in pipes, basins, overflows, hydrants, etc. located on the water circuit between the point of capture and the consumer.

These constitute effective water losses and can be divided into two categories:

- technically admissible loss – refers to the "losses" (consumptions) of water necessary to ensure the technological process. The logical question would be: who and how establishes the limit from which the costs are exaggerated, given that the amount of water required for the technological process is related to local conditions and especially to the real cost of water;
- real water loss in addition to the technically admissible loss; is in fact the true water loss; this depends on many elements that will be detailed below.

C) Water waste is considered to be the loss of water at the user, a loss of water that also produces income; it is metered water (carrying fictitious lost water) or not (but accepted and sold at a flat rate) but water that is actually a real loss of water.

If the garden is irrigated with tap water, even if it is paid for, this is lost water considering that it is used for a completely different purpose than the one for which it was intended; this forces the entire system to introduce more water into the locality, therefore, to increase the pressure in the pipes, inevitably leading to a greater real loss from group B. Although it is metered water, it still falls into the category of water loss.

Washing hands is another common operation. We can imagine how much water flows when we wash our hands under the water jet in contradiction to the amount normally used. In the same way, the question arises: what happens if the tap is used at a higher water pressure? If we are more responsible with water, we open the tap less and in this way, apparently, the washing time is extended. How significant is this? It should not be. We can imagine how water is used in an apartment on the ground floor

of a 10-story building and how water is used in a similar apartment on the 10th floor. The risk of water waste is all the greater the higher the pressure at the tap.

Waste can be fought through permanent control of external and internal buildings and installations and by measuring the quantities of water actually consumed, using water meters.

The own needs of the water supply system objects are calculated analytically, based on the following elements:

- The technology used, as well as the components of the treatment plant; the admissible technological losses in the treatment plant should not exceed 6% of the quantity of water produced; in situations where the recirculation of the supernatant from the waters from cleaning the decanters and washing the filters is ensured, the technological losses can be reduced to 3%; for groundwater, the increase must be provided on a case-by-case basis;
- based on an operational plan for cleaning the network sections, the water requirement for periodic cleaning of the distribution network can be established; this depends on the pipe material, water quality and the affinity of the materials to form biofilm; the quantities of water used should not exceed 1...2‰ of the volume of water distributed;
- the water requirement for washing and sanitizing the system tanks; Once or twice a year, each tank in the system's tanks will be emptied, washed and disinfected; the quantities of water required for washing the tanks do not exceed 0.4...0.5% of the annual water volumes consumed.

Technically permissible water losses in the distribution network must be classified as water losses. In distribution networks less than 5 years old, it is estimated that losses will be less than 15% of the volume of water distributed ($K_p^* = 1,15$); these may be the result of improper execution, daily pressure variations or due to defective materials. In the case of existing distribution networks, where renovation and/or expansion works are being carried out, losses can reach values of up to 35% (Kp = 1.35). Percentages exceeding 35% as a value of water losses are considered abnormal, in which case appropriate measures must be adopted.

Solutions to reduce water losses exist, but they must be applied with the help of water users and equipment manufacturers. In the following, I will highlight a series of aspects that require reflection and to impose ourselves on finding solutions step by step. In order to quantify the magnitude of the phenomenon and adopt a solution based on certain data, not on assessments, it is necessary to have clear evidence of achievements.

---

* *K_p este un coeficient de majorare a necesarului de apă, pentru a ţine seama de pierderile tehnic admisibile în obiectele sistemului de alimentare cu apă* $\left(1{,}15 \le K_P \le 1{,}35\right)$.

A series of proposals, some of which have already been applied in practice, although not in all countries, are:

- Faucets with smaller diameters;
- The obligation to install flow control valves at the entrance to the internal installation;
- Installing check valves to allow the flow to be regulated in the internal installation (against water losses by maintaining the flow in the area where the meter does not react);
- Pressure control in the general network or in restricted areas;
- Two-speed toilets;
- Variable speed pumps,
- Leak detection equipment,
- Relining technologies, etc.

All of these have repercussions on the functioning of the water supply system, but also on the proper functioning of the sewage system (sewage network, as well as the treatment plant) by reducing the flow of wastewater.

Water supply companies can obtain viable solutions and communicate them to others for efficient use of information. The costs cannot be stopped, but over time, they will contribute to reducing social efforts, while also ensuring a quality service.

2. Detection of water losses in the water supply network

An important economic task is to reduce water losses in its distribution. Through the methods of detection of losses, resources are saved, quality is ensured and costs are reduced.

The strategy of any operator managing water resources in a locality must be a good management of the detection of water losses. To achieve this goal, it is necessary to use specialized personnel or experienced companies.

Fig. 1. – Illustration of water losses

The results obtained through the water loss detection process will be recorded in a breakdown statistics and thus will represent the basis for the systematic renewal of

the distribution network. It is recommended that the initiation of loss detection and personnel training be done in cooperation with equipment manufacturing companies.

It is not uncommon for losses greater than 50% to be found, which represents a significant waste of resources and even one of the essential points from an economic point of view for water distribution operators.

Water supply can be organized in the following six stages: capture, pumping, transport, treatment, storage, distribution. In general, each step is equipped with technical equipment, which depends on the availability of energy (pumps, compressors, etc.). In this way, each drop of water can be accounted for both economically and energetically. In locations where water availability is limited, water losses will jeopardize the security of supply, or will generate new costs for the construction of efficient capture facilities.

In locations where water leaks from the supply network, it leads, under low pressure conditions, to infiltration of foreign water, endangering the health of the population. It can be mentioned that in 2008 such conditions led to a devastating cholera epidemic in Harare (Zimbabwe) with numerous deaths.

Water that is introduced into the distribution network but is not metered is considered a loss in the balance sheet. In the event that the metering instruments are missing or lack precision, as well as in the event that the water is used for the benefit of the municipality (network washing, irrigation of green spaces, firefighters, washing roads), it is not metered and falls into the category of apparent losses.

Also in the category of apparent losses are illegal uses of water.

Real losses also occur if water leaks uncontrollably through a crack and the connections between pipes or hydrants as well as the tanks are not tight.

In conclusion, the water distributor has the obligation to maintain only real losses. Apparent water losses must be correctly cataloged from an economic perspective, so that the water supply is not overloaded. Detecting cracks in the network and fixing them is the responsibility of the distributor and must be done with the utmost seriousness.

Knowledge of all equipment and the network as a whole is vital for all maintenance work.

Lately, most distributors recognize the need for this technique, even having switched to mapping water networks in digital form.

A continuous update of the documents is required, in parallel with having a coherent action plan to avoid any failures in time.

There must be as accurate information as possible between the company managers so that the management of changes in the network can be operated on time.

From the design phase of a water plant, the fight against network losses must be taken into account, which is why the design must be entrusted only to qualified engineers. It is of great importance both the correct location of the network, as well as the correct choice of materials to be used, according to the hydraulic and construction conditions.

In addition to the own control service that most companies have, it is imperative to ensure their own site management through their own personnel trained in this direction or by hiring people for this purpose. This way, mistakes during the work can be avoided, which can be repaired more difficult later (collection and provision of evidence, trial, digging again, additional costs).

Both the operation and maintenance of the network and the equipment require a series of maintenance and periodic inspection works for which inspection programs and procedures will be drawn up.

Based on these programs and procedures, the work of the operating personnel will be organized. Periodic inspection of tanks, hydrants and flushing of the network, as well as continuous supervision and inspection of pumping equipment and treatment stations are among the important tasks.

Water leak detection must be done systematically and with great responsibility, thus guaranteeing the formation of a complete picture of the entire network. For this purpose, specially trained personnel must be employed in this direction.

Taking into account the fact that any leak discovered and repaired must be documented, it is necessary to draw up damage statistics, which will allow to establish the vulnerabilities of certain areas of the network in time and thus to avoid losses by drawing up programs for replacing the respective part of the network. Emergencies, such as a cracked pipe, must be immediately identified and remedied, in order to avoid additional damage to streets and other nearby utilities.

According to the IWA (International Water Association), inspections will be carried out regularly at the following intervals:

- annually, in the case of large leaks;
- once every three years, in the case of medium leaks;
- once every six years, in the case of small leaks.

The detailed detection of water losses involves:

- a reduction in water losses due to leaks in raw water pipes, connections or any cracks in the supply pipes;
- a reduction in the costs incurred in paying for damages caused by cracks or even burst pipes;
- ensuring appropriate water quality in accordance with current regulations;
- a reduction in costs by increasing the reliability of the networks;
- a reduction in the costs of maintaining and repairing pipes;
- a reduction in the energy required for the proper functioning of the networks.

Through a competent inspection of the pipe networks, possible blockages and damages can be prevented, thus increasing the safety of distribution. The Water Companies are responsible for the annual inspection of the networks, with the obligation to comply with the imposed norms. It is mandatory to use competent and well-trained personnel for such work, and it is also advisable to contract external specialized companies.

The methods used to detect water losses are:
- flow analysis;
- measurement correlation;
- geophone listening;
- reinforcement verification techniques.

Quantifying water losses through percentage reports can lose their value when the following are not known: the length of the network, the number of consumers or the conditions in which the water distribution takes place.

For illustration, the following simulation example will be given:

A consumption of 1000 m3 of water per day is estimated for a small town.

A loss of 10% is found, equivalent to 100 m3/day. The respective town is also about to open an industrial park that will consume an additional 1000 m3 of water.

If water losses continue to remain at the value of 100 m3, this quantity will now represent only 5% of the total. The conclusion is that a qualitative characterization of the network status cannot be made only in percentage terms. The recommendation is as follows: the estimated losses will be counted quantitatively per unit of time, in relation to the network length. The calculation of the loss value can be done with the following formula:

$$q_v = \frac{Q_v}{8760} x L_R \qquad (3.1.)$$

where:
q_v – loss value
Q_v – annual loss volume
L_R – network length
8760 – number of operating hours per year

The approximation of the network condition is determined by the specific loss depending on the soil conditions.

For the detection of polymer pipes, it is possible to use a shear probe or a device with a magnetic field transmitter. The proposed methods can be used in the case of detection of leaks in non-metallic pipes. Manufacturers of polymer pipes and pipes can provide more information on drinking water distribution networks.

Fig. 2. – Illustration of how to use metal rods to listen to consumer connections and network fittings

3. Conclusions

Applying polymer coatings to the surface of the pipes – necessarily protected from any sharp stones – will lead to better anti-corrosion protection of the networks. Correct insulation of the connections after installation is mandatory.

The classic principle on which the aforementioned technologies for detecting water leaks are based is based on the fact that water produces noise when it gushes out of a pipe under pressure.

English specialists, 100 years ago, used metal rods with a wooden funnel to listen to consumer connections and fittings on the network (Fig. 3.2.).

Later, in the 1960s, electronic sticks (ground microphones) also known as "electronic ears" appeared. These instruments proved to be useful by amplifying the sound produced by a water leak, thus allowing easier detection. Noise correlators, similar to today's sonic equipment, only appeared in the late 1970s. The evolution of the noise correlator materialized over the next 20 years, moving from the size of a box with appreciable weight and with which it took half a day to locate a water leak, to a small device that can identify a leak in just a few minutes.

A chronological evolution of water loss detection technologies looks like this [15]:

- 1850 – Use of the rod listening method;
- 1880 – Use of water meters;

- 1920 – transition to helical water meters with paddles;
- 1930 – Implementation of the "step by step" test - zero consumption;
- 1965 – Use of the ground microphone;
- 1978 – Use of noise correlators;
- 1980 – Sectorization;
- 2001 – Use of a combined method – loggers-correlator;
- 2002 – Use of ground penetrating radars - Acoustic loggers;
- 2002 – Digital correlator;
- 2003 – Introduction of advanced detection microphones;
- 2006 – use of leakage indicators.

Due to the exponential development of localities and implicitly of water distribution networks, the need to introduce zonal metering was imposed, which included between 500 and 3,120 connections. As a measure to increase the efficiency of detecting water losses, it is necessary to introduce pressure and flow monitoring points in these areas.

The most modern methods of detecting water losses, which due to their high costs are still quite rarely applied, would be: the isotope method, ground radar, infrared measurement methods, the use of tracer gas, the air pressure method, the air piston press, etc.

Starting from May 2011, the General Urban Planning Regulation was implemented in our country, approved by Government Decision number 525/2008, which provided in paragraph (2), "The construction and expansion of municipal networks provided for in paragraph (1) letter c), including for their crossing of public roads, shall be carried out in the underground location variant, in compliance with the specific technical regulations in force."

"On the routes of municipal networks located underground, non-destructive identification systems, namely markers, shall be provided for the operative detection of the position of municipal networks in the horizontal and vertical plane, for the purpose of carrying out intervention works on them." (paragraph 7).

A major problem was the accurate location of underground networks due to the large amount of time that had to be allocated for detecting the fault and the additional costs. It was important to note that excavation was no longer necessary to detect the underground water network.

3M systems (www.3M.ro/MarcareSiLocalizare) offer solutions for more accurate location of the municipal network in a relatively short time and at low costs. The localization process is as follows:

1. 3M markers are inserted during the execution or maintenance process of the municipal network in the ground. These markers can be with or without iD. The difference is that iD markers contain a chip inside that stores information, such as: the type of network, its depth, the date of its installation, etc. Writing and reading data was allowed precisely because of the iD function. The only supplier of iD markers on the Romanian market is 3M.

2. To detect the marker and implicitly the water network, the 3M Dynatel TM localization device is passed over the marker, at the surface of the ground.

A detection method used by locators is based on capturing the signal, having a certain frequency, emitted by radio waves, generated by a transmitter.

GPS communication is characteristic of 3M systems and has applicability to GIS maps for cable/locator devices and markers.

The advantages of the 3M solution are: low costs, simple applicability and durability.

References

1. BÎRSAN, E., IGNAT, C. – O modalitate de realizare a controlului reţelelor de distribuţie a apei. Conferinţa de Instalaţii pentru Construcţii, Iaşi, 2008.
2. FELEA, I., IONESCU, GH. C. – Consideraţii privind fiabilitatea previzională a sistemelor de alimentare cu apă a centrelor urbane. Analele Universităţii din Oradea, Fascicula de Energetică, nr. 8, vol.I, 2002.
3. GAVRILAŞ, M., GEORGESCU, G. – Utilizarea algoritmilor genetici pentru determinarea schemei optime de funcţionare a reţelelor de distribuţie urbană. Rev. Energetica, nr. 6B, 2008.
4. IBA, K. – Reactive Power Optimization by Genetic Algorithm, In: IEEE Transactions on Power Systems, Vol. 9, No. 2, May 2006, pp. 685-692.
5. IONESCU, DANIELA-SMARANDA; IONESCU, GH. C. – Similitudinea şi modelarea în hidraulică – A 42-a Conferinţă Naţională de Instalaţii – 17-20 octombrie 2007 – Sinaia, România.
6. IONESCU, G. L. – The optimization of energy consumption in water supply systems – Conferinţa Naţională (cu participare internaţională) „TEHNOLOGII MODERNE PENTRU MILENIUL III" – Analele Universităţii din Oradea – Fascicula Construcţii şi instalaţii hidroedilitare, 2009.
7. IONESCU, GH. C. – Contribuţii la studiul şi optimizarea fiabilităţii instalaţiilor hidraulice din cadrul sistemelor de alimentare cu apă a centrelor urbane – Teză de doctorat, Universitatea din Oradea, martie, 2003.
8. IONESCU, GH. C. – Optimizarea configuraţiei reţelelor de distribuţie urbană a apei prin utilizarea algoritmilor genetici – Conferinţa Naţională (cu participare internaţională) „TEHNOLOGII MODERNE PENTRU MILENIUL III" – Analele Universităţii din Oradea – Fascicula Construcţii şi instalaţii hidroedilitare, 2007.
9. IONESCU, GH. C. – Creşterea siguranţei funcţionării sistemelor de alimentare cu apă – Conferinţa Naţională (cu participare internaţională) „TEHNOLOGII MODERNE PENTRU MILENIUL III" – Analele Universităţii din Oradea – Fascicula Construcţii şi instalaţii hidroedilitare, 2007.
10. IONESCU, GH. C. – Consideration regarding the wastewater biological treatment – Tiszántúli Mezőgazdagsági Tudományos Napok – Környezetvédelmi Szekcio – Debrecen, 28 – 29 octombrie 2011.

11. IONESCU, GH. C., IONESCU, G. L. – Sisteme de Alimentare cu apă. Editura Matrix Rom, Bucureşti, 2010.
12. IONESCU, GH. C. – Optimizarea fiabilităţii instalaţiilor hidraulice din cadrul sistemelor de alimentare cu apă – Editura Matrix Rom, Bucureşti, 2004.
13. IONESCU, GH. C.; GLIGOR, E. – Probleme de fiabilitate generală a sistemelor de alimentare cu apă – Conferinţa Naţională (cu participare internaţională) „TEHNOLOGII MODERNE PENTRU MILENIUL III" – Analele Universităţii din Oradea – Fascicula Construcţii şi instalaţii hidroedilitare, 2008.
14. IONESCU, GH. C.; IONESCU, DANIELA-SMARANDA – Increasing the efficiency of water supply systems by optimizing the electrical energy consumption - The 19th DAAAM INTERNATIONAL SYMPOSIUM "Intelligent Manufacturing & Automation" 22-25th, October 2008 – Trnava, SLOVAKIA-ISI.
15. IONESCU, GH. C.; IONESCU, DANIELA-SMARANDA – Phisycal and Chemical Techniques for Removing Nitrogen and Phosphorus from Residual Waters – International Symposia Risk Factors for Environment and Food Safety & Natural Resources and Sustainable Development, Faculty of Environmental Protection, Nov. 6-7, Oradea, 2009.
16. IONESCU, GH. C.; IONESCU, DANIELA-SMARANDA – Advanced Water Treatment Technologies – International Symposia Risk Factors for Environment and Food Safety & Natural Resources and Sustainable Development, Faculty of Environmental Protection, Nov. 6-7, Oradea, 2009.
17. IONESCU, GH. C.; GLIGOR, E. – Optimizarea funcţionării decantoarelor suspensionale cu ajutorul modelului matematic – Conferinţa Naţională (cu participare internaţională) „TEHNOLOGII MODERNE PENTRU MILENIUL III" – Analele Universităţii din Oradea – Fascicula Construcţii şi instalaţii hidroedilitare, 2008.
18. IONESCU, GH. C.; GLIGOR, E. – Probleme de fiabilitate generală a sistemelor de alimentare cu apă – Conferinţa Naţională (cu participare internaţională) „TEHNOLOGII MODERNE PENTRU MILENIUL III" – Analele Universităţii din Oradea – Fascicula Construcţii şi instalaţii hidroedilitare, 2008.
19. IONESCU, GH. C., IANCULESCU, O., IONESCU DANIELA. – Fiabilitatea instalaţiilor hidraulice. Editura Treira – Oradea, 2012.
20. ROTBERG, R., COTOROBAI, V. – Utilizarea microconvertizoarelor de frecvenţă la variaţia turaţiei pompelor. Conferinţa de Instalaţii pentru Construcţii, Iaşi, 2008.
21. SOARE DAVID (Bursașiu Arghir) – Analiza cauzelor de defectare a sistemelor de alimentare cu apă – Lucrare prezentată la a 42-a Conferinţă Naţională de Instalaţii – 17-20 octombrie 2007 – Sinaia – România.
22. SOARE DAVID (Bursașiu Arghir) – Probleme de fiabilitate generală a sistemelor de alimentare cu apă – Lucrare prezentată la Conferinţa Naţională (cu participare internaţională) „TEHNOLOGII MODERNE PENTRU MILENIUL III" – Oradea, 2008
23. SOARE DAVID (Bursașiu Arghir) – Making good use frequency converters for increasing the efficiency of water supply systems – Lucrare prezentată la Conferinţa Naţională (cu participare internaţională) „TEHNOLOGII MODERNE PENTRU MILENIUL III" – Oradea, 2011.
24. MĂNESCU, AL. – Manual pentru detectarea şi controlul pierderilor de apă în sistemele de alimentare cu apă. ARA/ MUDP II, Bucuresti 2012.
25. MĂNESCU, AL. – Alimentări cu apă – Aplicaţii. Editura *H*G*A, Bucureşti,
2010.
26. RÎŞTEIU M. – Elemente de tehnologia informaţiei. Editura Universitas, Petroşani, 2012.
27. RÎŞTEIU M. – Sisteme dinamice asistate de calculator. Editura Universitas, Petroşani, 2001
28. KOVACS TIBERIU, GH. CONSTANTIN IONESCU – Optimization of electrical energy consumption in water supply systems - 19th edition of The National Tehnical-Scientific Conference „Modern Technologies for the 3rd Millenium, April 5-6, 2020, Oradea, România

http://www.arhiconoradea.ro/Conferinta/HOME.htm
ISBN 978-88-7587-724-8 Published: 2020 ISI PROCEEDINGS
29. SZABO STEFAN, KOVACS TIBERIU, IONESCU GEORGE – LUCIAN, CZISZTER K. ISTVAN – ANDRAS, IONESCU DANIELA – SMARANDA, SĂRĂCUȚ-ARDELEAN ANDREI-FLORIN - Comparative studies and research on optimizing electric consumption of water supply systems - JOURNAL OF APPLIED ENGINEERING SCIENCES, VOL. 12(25)1-2022 B+ by the same C.N.C.S.I.S. Our journal is accepted in five International Databases (IDB), (WOS) Web of Science (see: http://mjl.clarivate.com/cgi-bin/jrnlst/jlresults.cgi?PC=MASTER&Full=Journal%20of%20Applied%20Engineering%20Sciences)
30. CZISZTER K. ISTVAN – ANDRAS, IONESCU GHEORGHE – CONSTANTIN, SĂRĂCUȚ-ARDELEAN ANDREI-FLORIN, SZABO STEFAN, KOVACS TIBERIU, IONESCU GEORGE – LUCIAN - Comparative studies and research on energy optimization of non-residential buildings - JOURNAL OF APPLIED ENGINEERING SCIENCES, VOL.
12(25)1-2022 B+ by the same C.N.C.S.I.S. Our journal is accepted in five International Databases (IDB), (WOS) Web of Science
(see: http://mjl.clarivate.com/cgi-bin/jrnlst/jlresults.cgi?PC=MASTER&Full=Journal%20of%20Applied%20Engineering%20Sciences)
31. DEPARTMENT OF ENERGY U.S, U.S. ENVIRONMENTAL PROTECTION AGENCY- Roof product list, list current as of January 2, 2009,
http://www.energystar.gov/ia/products/prod_lists/roofs_prod_list.pdf, March 2021, 18:15
32. EIA - International Energy Outlook 2010, Report #:DOE/EIA-0484 (2010). http://www.eia.doe.gov/oiaf/ieo/ world.html, Vizualizat 2020/07/25, 16:45
33. EUROPEAN PARLIAMENT - Tackling climate change.
http://europa.eu/legislation_summaries/environment/tackling_climate_change/index_en.htm, vizualizat 2020/07/10, 11:00
34. EUROPEAN PARLIAMENT - Energy efficiency: energy performance of buildings,
http://europa.eu/legislation_ summaries/energy/energy_efficiency/l27042_en.htm, vizulizat 2020/07/10, 12:30
35. EUROPEAN PARLIAMENT - EU energy in figures 2010.
http://ec.europa.eu/energy/publications/doc/statistics/part_2_energy_pocket_book_2010.pdf, vizualizat 2020/11/09, 12:00
36. EUROPEAN PARLIAMENT - The EU climate and energy package.
http://ec.europa.eu/environment/climat/ climate_action.htm,
vizualizat 2020/10/07, 19:00
37. EUROPEAN PARLIAMENT - Green Paper on the security of energy supply. http://europa.eu/legislation_summaries/energy/external_dimension_enlargement/l27037_en.htm, vizulizat 2020/11/08, 19:30
38. EUROPEAN PARLIAMENT - Proposal for a Directive of the European Parliament and of the Council on the energy performance of buildings (recast) {SEC(2008) 2864} {SEC(2008) 2865} of document: 13/11/2008 of transmission: 19/12/2008.
http://eurlex.europa.eu/LexUriServ/LexUriServ.do?uri=CELEX:52008PC0780:EN:NOT, vizualizat 2020/11/10, 14:00
39. EUROPEAN PARLIAMENT - Energy Efficiency in Buildings.
http://ec.europa.eu/energy/efficiency/buildings/ buildings_en.htm, vizualizat 2021/07/03, 10:00
40. X X X – Revista "Instalaţii pentru construcţii" – colecţie.
41. X X X – Revista "Instalatorul" – colecţie.
42. X X X – Revista "Detectivii apei pierdute" – colecţie 2012-2021.
43. X X X – SR 1343-1 iunie 2006.
44. X X X – Legea 311- 28 iunie 2004.
45. X X X – Standarde şi normative în vigoare.

Comparative Analysis of a Photovoltaic System's Performance: Simulation vs. Reality

Analiza comparativă a performanței unui sistem fotovoltaic: Simulare vs. realitate

Norbert Gocz

Universitatea Transilvania din Brașov, Facultatea de Construcții
Str. Turnului 5, 500152, Brașov, Romania
E-mail: norbert.gocz@student.unitbv.ro

DOI: 10.37789/rjce.2026.17.1.10

Abstract. *This paper provides a comparative analysis of the estimated versus actual energy production of a residential photovoltaic system installed on a single-family home. The aim is to assess the accuracy of simulations conducted using PV*Syst and PVGIS software, using different climatic data sources. The system under study has a total installed capacity of 6.56 kWp and it is equipped with monocrystalline panels and an on-grid inverter. By comparing the simulated results with real data recorded monthly, the differences between the estimated and observed performance during operation are highlighted. The findings emphasize the importance of validating simulations through practical measurements and the relevance of selecting appropriate meteorological data for accurately sizing a photovoltaic system and estimating the return on investment.*

Key words: *residential photovoltaic system, simulation, renewable energy*

Rezumat. *Lucrarea prezintă o analiză comparativă între producția estimată și cea reală a unui sistem fotovoltaic rezidențial instalat pe o locuință unifamilială. Scopul este evaluarea acurateței simulărilor realizate cu ajutorul software-urilor PV*Syst și PVGIS, utilizând diverse baze de date climatice. Sistemul analizat are o putere instalată de 6.56 kWp și este echipat cu panouri monocristaline și un invertor on-grid. Prin compararea rezultatelor simulate cu datele reale înregistrate lunar, se evidențiază diferențele dintre performanța estimată și cea observată în exploatare. Rezultatele subliniază importanța validării simulărilor prin măsurători practice și relevanța alegerii corecte a datelor meteorologice pentru dimensionarea corectă a unui sistem fotovoltaic și estimarea rentabilității investiției.*

Cuvinte cheie: sistem fotovoltaic rezidențial, simulare, energie regenerabilă

1. Introducere

Schimbările climatice devin tot mai evidente la nivel global, iar impactul acestora asupra mediului și societății este din ce în ce mai resimțit. Aceste fenomene sunt strâns legate de încălzirea globală, care s-a intensificat considerabil în ultimele

The article was received on 28.04.2025, accepted on 02.02.2026 and published on 24.02.2026

decenii. Creșterea temperaturii medii anuale este determinată, în principal, de emisiile crescânde de gaze cu efect de seră, în special dioxidul de carbon .[1,2]

Pentru a contracara aceste efecte, se impune o tranziție rapidă către surse de energie regenerabilă, care să reducă dependența de combustibilii fosili și să contribuie la limitarea emisiilor de gaze cu efect de seră. În acest context, energia solară fotovoltaică reprezintă una dintre cele mai promițătoare soluții pentru producerea de electricitate curată și sustenabilă.

În România, în special, panourile fotovoltaice au devenit o componentă esențială a pieței de energie regenerabilă, având un impact semnificativ în creșterea capacităților de producție de energie din surse regenerabile . Numărul instalațiilor fotovoltaice, în majoritate sisteme de tip On-Grid, montate pe acoperișurile locuințelor unifamiliale, este în continuă creștere, datorită accesului la fonduri guvernamentale și scăderii costurilor de implementare și întreținere .[3]

În proiectarea sistemelor fotovoltaice, una dintre cele mai importante întrebări pe care le pun oamenii este, într-adevăr, câtă energie pot produce cu sistemul respectiv și cât de mult din aceasta poate acoperi consumul lor de energie.

Răspunsul la aceste întrebări este esențial pentru a evalua atât eficiența, cât și rentabilitatea unei investiții fotovoltaice. Astfel, lucrarea de față își propune să analizeze performanța unui sistem fotovoltaic instalat pe o locuință unifamilială din România, comparând rezultatele obținute prin simulare cu cele înregistrate în exploatarea reală.

2. Descrierea sistemului fotovoltaic

Sistemul fotovoltaic analizat este instalat pe o locuință unifamilială situată în orașul Covasna, România. Acoperișul casei are o orientare predominant sud-sud-est (S-SE), cu un azimut de -17°, ceea ce înseamnă o abatere de 17° spre est față de direcția sud ideală. Înclinația acoperișului este de aproximativ 39°, un unghi foarte apropiat de valoarea optimă pentru latitudinea locală, ceea ce favorizează o captare eficientă a radiației solare pe tot parcursul anului.

Sistemul este compus din 16 panouri fotovoltaice Longi LR5-55HIH-410M, fiecare având o putere nominală de 410 W, rezultând o putere totală instalată de 6.56 kWp. Panourile utilizează tehnologie monocristalină Half-Cut, recunoscută pentru eficiența ridicată și performanța superioară în condiții de umbrire parțială și radiație solară difuză. Panourile sunt conectate în două stringuri egale, fiecare format din 8 panouri, ceea ce asigură o distribuție echilibrată a curentului și o mai bună compatibilitate cu invertorul utilizat. (Fig.1)

Pentru conversia energiei electrice, sistemul este echipat cu un invertor Huawei SUN2000-5KTL-L1 de tip on-grid, monofazat, cu o putere nominală de 5 kW.

Fig. 1. Sistemul fotovoltaic studiat

3. Metodologia de lucru

Pentru analiza performanței sistemului fotovoltaic propus, au fost utilizate două instrumente software specializate: **PV*Syst** și **PVGIS**. Scopul acestei abordări a fost compararea rezultatelor obținute din simulări, precum și evaluarea influenței bazei de date climatice asupra estimării producției de energie electrică.

a. Simularea în PV*Syst 8.0.9 (Fig.2)

În cadrul software-ului PV*Syst[4], au fost realizate trei scenarii de simulare, fiecare bazat pe o altă bază de date meteorologică. Acestea sunt:

i. **Meteonorm** - Bază de date meteorologică cu acoperire globală, generată pe baza datelor din peste 8000 de stații meteo din întreaga lume. Utilizează metode statistice pentru completarea și interpolarea datelor lipsă.

ii. **PVGIS TMY (Typical Meteorological Year)** - Este o bază de date disponibilă în cadrul platformei PVGIS, care oferă un an meteorologic tipic (sintetic), calculat pe baza unei perioade istorice de referință. Acesta combină cele mai frecvente condiții climatice lunare într-un set standardizat de date, util pentru estimări de producție anuale.

iii. **NASA-SSE (Surface meteorology and Solar Energy)** - Bază de date globală, dezvoltată de NASA, care oferă informații despre radiația solară și alți parametri meteorologici pe baza observațiilor satelitare. Are o rezoluție spațială medie și o acoperire istorică amplă, fiind Ade sea folosită în zone cu acces limitat la date locale detaliate.[5]

iv.

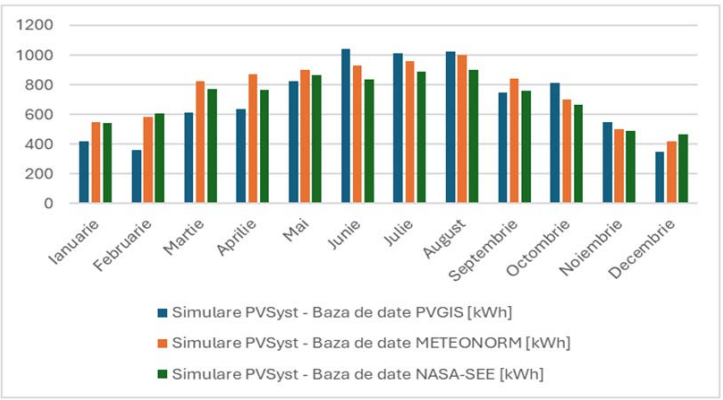

Fig. 2. Rezultate obținute prin simulare in PVSyst

b. Simularea în PVGIS (Fig.3)

În paralel, au fost efectuate simulări și pe platforma online PVGIS[6] (Photovoltaic Geographical Information System), dezvoltată de Comisia Europeană. În acest caz, au fost analizate două scenarii, fiecare corespunzător unei baze de date diferite:

i. **SARAH (Surface Solar Radiation Data Set – Heliosat)** – Set de date de înaltă rezoluție privind radiația solară, furnizat de EUMETSAT. Informațiile sunt obținute pe baza imaginilor captate de sateliții Meteosat și prelucrate cu ajutorul algoritmului Heliosat. SARAH este recunoscut ca una dintre cele mai precise surse pentru analiza resurselor solare în Europa și Africa.[7]

ii. **ERA5** - este o reanaliză climatică globală furnizată de Centrul European pentru Prognoze pe Termen Mediu (ECMWF), în cadrul programului Copernicus. Aceasta combină observații din multiple surse cu modele numerice atmosferice, oferind date orare privind radiația solară, temperatura, vântul și alți parametri, la o rezoluție spațială de aproximativ 31 km. Este ideală pentru analize pe termen lung și estimări în regiuni cu date meteo limitate.[8]

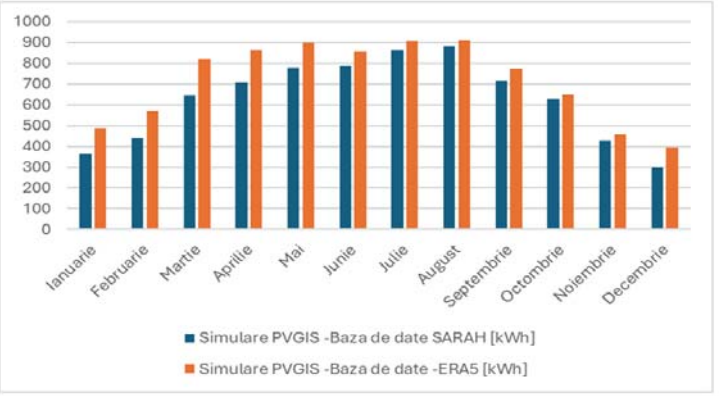

Fig. 3. Rezultate obținute prin simulare in PVGIS

Ambele baze de date sunt disponibile direct în interfața PVGIS și permit estimarea producției anuale și lunare pe baza parametrilor specificați ai sistemului.

Producția de energie reală a sistemului fotovoltaic a fost monitorizată și înregistrată lunar prin intermediul invertorului. Acesta a colectat date detaliate privind energia produsă de panourile fotovoltaice pe parcursul anului 2024, oferind informații precise despre performanța sistemului în fiecare lună.

4. Rezultate și discuții

Compararea producției de energie estimată cu cea înregistrată în exploatarea reală a sistemului fotovoltaic, prezentată în Tabelul 1, a evidențiat diferențe semnificative între valorile simulate și cele măsurate în anul 2024. În timpul iernii, producția reală scade semnificativ din cauza zăpezii care se acumulează pe panouri, un efect ce nu este luat în calcul de software. În perioadele cu precipitații reduse, performanța sistemului a fost afectată de depunerile de praf și alți factori atmosferici,

care reduc eficiența panourilor fotovoltaice. Pe de o altă parte, trebuie menționat că pot exista abateri de la un an la altul în ceea ce privește producția de energie, deoarece softurile folosesc date climatice ideale, bazate pe medii multianuale. Din acest motiv, simulările oferă doar o estimare orientativă, iar performanța reală trebuie analizată în funcție de condițiile specifice fiecărui an. Aceste aspecte evidențiază importanța monitorizării continue și a întreținerii regulate a sistemului, pentru a asigura o funcționare cât mai eficientă.

Tabelul 1

Compararea rezultatelor simulate și reale ale sistemului fotovoltaic

Luna	Energia produsa de sistemul fotovoltaic in 2024 (kWh)	Simulare PVSyst - Baza de date PVGIS (kWh)	Simulare PVSyst - Baza de date METEONORM (kWh)	Simulare PVSyst - Baza de date NASA-SEE (kWh)	Simulare PVGIS - Baza de date SARAH (kWh)	Simulare PVGIS - Baza de date - ERA5 (kWh)
Ianuarie	329	415	549	542	367	484
Februarie	427	361	586	605	439	570
Martie	627	611	823	771	646	822
Aprilie	817	635	868	764	707	863
Mai	908	821	901	866	780	901
Junie	984	1042	928	835	788	859
Julie	1000	1013	957	887	861	909
August	920	1022	998	899	883	912
Septembrie	772	746	842	761	717	774
Octombrie	724	813	702	665	629	649
Noiembrie	391	546	502	491	429	457
Decembrie	150	345	416	468	297	396
Total anual	8050.18	8369.4	9071.5	8553.6	7542.5	8594.8

6. Concluzii

Analiza comparativă dintre producția estimată și cea reală a sistemului fotovoltaic instalat pe o locuința unifamilială evidențiază importanța validării simulărilor prin măsurători reale și a implementării unor strategii eficiente de monitorizare și întreținere. Rezultatele obținute subliniază că software-urile specializate, cum ar fi PV*Syst și PVGIS, tind să supraaprecieze producția de energie în sezonul de iarnă, dar subapreciază ușor producția de energie în sezonul de vară.(Fig.4) Acest lucru se datorează faptului că fiecare regiune și fiecare sistem au o configurație și o locație unică, care nu pot fi complet reflectate de modelele standardizate utilizate în simulări. Astfel, estimările generate de aceste instrumente trebuie considerate orientative și nu ca predicții exacte ale performanței reale.

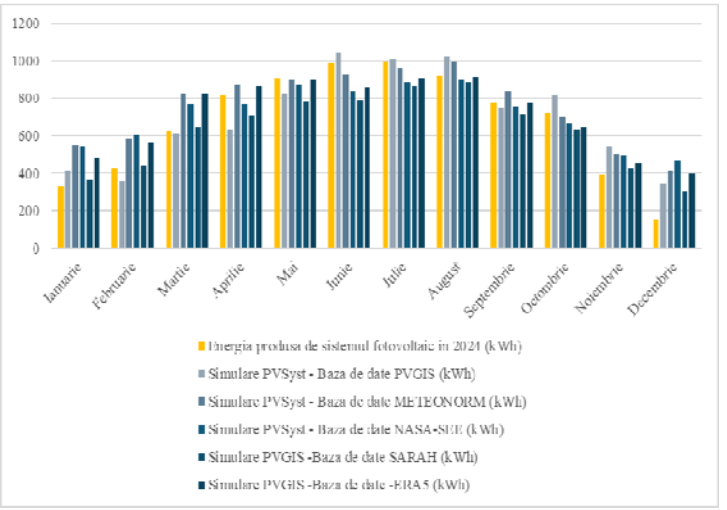

Fig. 4. Comparația între producția reală și producția modelată a sistemului fotovoltaic

Referințe

[1] B. G. Vuțoiu, M. B. Tăbăcaru, G. A. Beșchea, Ștefan I. Câmpean, A. M. Bulmez, and G. Năstase, 'Seven continents. 737 One sky', 2024

[2] M. Azhar Khan, M. Zahir Khan, K. Zaman, L. Naz, „Global estimates of energy consumption and greenhouse gas emissions", in Renew. Sustain. Energy Rev., 29,2014, pp.336-344

[3]https://energie.gov.ro/ministerul-energiei-relanseaza-doua-apeluri-de-proiecte-care-privesc-bateriile-si-panourile-fotovoltaice-suma-totala-depaseste-278-milioane-euro/

[4]https://joint-research-centre.ec.europa.eu/photovoltaic-geographical-information-system-pvgis_en

[5] https://ntrs.nasa.gov/citations/20080012200

[6]https://www.pvsyst.com/

[7]https://joint-research-centre.ec.europa.eu/photovoltaic-geographical-information-system-pvgis/pvgis-data-download/sarah-solar-radiation_en

[8] https://cds.climate.copernicus.eu/datasets/reanalysis-era5-single-levels?tab=overview

Prospects for sustainable development of the energy sector in the Republic of Moldova through energy efficiency programs and projects

Perspectivele de dezvoltare durabilă a sectorului energetic în Republica Moldova prin programe și proiecte de eficiență energetică

Alexandrina Berzerdeanu[1], Mihai Lupu[2], Galina Uzun[3], Vasile Daud[4]

[1]Universitatea Tehnică a Moldovei, Facultatea Energetică și Inginerie Electrică
Adresa: Str. 31 August1989, 78, Chisinau, Republica Moldova
E-mail: alexandrina.berzedeanu@en.utm.md

[2,3,4]Universitatea Tehnică a Moldovei, Institutul de Energetică
Adresa: Str. Academiei, 5, Chisinau, Republica Moldova
E-mail: mihai.lupu@if.utm.md; galina.uzun@if.utm.md; vasile.daud@if.utm.md

DOI: 10.37789/rjce.2026.17.1.11

Abstract. *The paper analyzes the impact of the EcoVoucher Program on the sustainable development of the energy sector in the Republic of Moldova. Launched in November 2023 with the support of UNDP (United Nations Development Programme) Moldova and funded by the European Union, through the former Energy Efficiency Agency-now the National Center for Sustainable Energy (CNED) -the program aimed to support vulnerable households in replacing old household appliances with modern, energy-efficient ones. During the pilot stage, carried out between October 2023 and July 2024, a total of 198,685 vouchers were distributed, of which 39,084 were redeemed, resulting in annual energy savings of approximately 1.6 million kWh or 7 million MDL, and contributing to a reduction of over 830 kg of CO_2 emissions annually. Subsequently, the program was fully taken over by CNED, which in 2024 issued 17,305 vouchers, of which 7,223 were used, achieving additional savings of 1.5 million kWh or 6.6 million MDL, and contributing to a reduction of 789.6 kg of CO_2 emissions annually.*

Keywords: *Energy sector, programs, EcoVoucher, sustainable development, energy efficiency.*

Rezumat. *Lucrarea analizează impactul Programului EcoVoucher asupra dezvoltării durabile a sectorului energetic din Republica Moldova. Lansat în noiembrie 2023 cu sprijinul PNUD (Programul Națiunilor Unite pentru Dezvoltare) Moldova si finanțat de Uniunea Europenea, prin intermediul fostei Agenții pentru Eficiență Energetică, actualul Centru Național de Energie Durabilă (CNED), programul a avut drept scop sprijinirea gospodăriilor vulnerabile în procesul de înlocuire a echipamentelor electrocasnice vechi cu unele moderne, eficiente energetic. În etapa pilot, desfășurată între octombrie 2023 și*

The article was received on 17.12.2025, accepted on 02.02.2026 and published on 24.02.2026

iulie 2024, au fost distribuite 198.685 de vouchere, dintre care 39.084 au fost valorificate, ceea ce a generat economii anuale de circa 1,6 milioane kWh sau 7 milioane lei, contribuind la reducerea emisiilor cu peste 830 kg CO_2 anual. Ulterior, programul a fost preluat complet de către CNED , care în 2024 a emis 17.305 vouchere, dintre care 7.223 au fost utilizate, obținându-se economii suplimentare de 1,5 milioane kWh sau 6,6 milioane lei, contribuind la reducerea de emisii cu 789,6 kg CO_2 anual.

***Cuvinte cheie**: Sectorul energetic, programe, EcoVoucher, dezvoltare durabilă, eficiență energetică.*

Introducere

Sectorul energetic al Republicii Moldova trece printr-un proces amplu de transformare, determinat atât de contextul geopolitic regional, cât și de necesitatea alinierii la obiectivele europene de dezvoltare durabilă [1]. Criza energetică din 2022 a evidențiat vulnerabilitatea dependenței de resurse externe și a subliniat necesitatea consolidării securității energetice prin diversificarea surselor și creșterea eficienței consumului [2] [3]. Un exemplu concret în această direcție este Programul de Vouchere pentru Electrocasnice („EcoVoucher”), adoptat prin Hotărârea Guvernului nr. 533/2024 [4], o inițiativă guvernamentală, menită să sprijine gospodăriile vulnerabile în înlocuirea echipamentelor vechi cu electrocasnice moderne și eficiente. Prin acoperirea a până la 70% din costul de achiziție, programul contribuie la reducerea facturilor, la diminuarea consumului de energie și la scăderea emisiilor de gaze cu efect de seră. Aceste măsuri sunt esențiale într-un context în care producerea energiei electrice prin centrale termoenergetice, bazate în mare parte pe combustibili fosili, continuă să fie una dintre principalele surse de poluare, generând emisii considerabile de CO2, SO2 și particule în suspensie. Astfel, Republica Moldova se află la intersecția dintre provocări și oportunități: pe de o parte, gestionarea vulnerabilităților legate de securitatea energetică și impactul poluant al sistemului tradițional; pe de altă parte, valorificarea programelor și proiectelor de eficiență energetică, care constituie instrumente-cheie pentru consolidarea rezilienței și pentru atingerea obiectivelor de dezvoltare durabilă [5].

1. Programului EcoVoucher și perspectivele de dezvoltare durabilă

Programul EcoVoucher (*în continuare Program)* reprezintă una dintre inițiativele guvernamentale inovatoare din Republica Moldova, orientată spre promovarea unui comportament ecologic responsabil și a utilizării eficiente a resurselor energetice la nivelul gospodăriilor casnice. Programul a fost lansat oficial la 15 noiembrie 2023, și constituie un instrument practic de aplicare a politicilor publice în domeniul eficienței energetice și al reducerii emisiilor de gaze cu efect de seră. Obiectivele principale ale

prezentului articol vizează o analiză comparativă privind reducerea consumurilor de energie electrică în sectorul rezidențial, a emisiilor de gaze cu efect de seră, creșterea gradului de conștientizare privind consumul sustenabil și îmbunătățirea calității vieții beneficiarilor.

Resursele financiare ale programului provin din bugetul de stat și din fonduri externe, fiind direcționate atât către subvenționarea achizițiilor, cât și către campanii de promovare și instruirea comercianților autorizați. Programul generează efecte pozitive pe mai multe planuri: scăderea cheltuielilor energetice la nivel de gospodărie, impulsionarea pieței echipamentelor eficiente, sprijinirea grupurilor vulnerabile și reducerea presiunii asupra infrastructurii energetice. Totodată, programul contribuie la atingerea angajamentelor Republicii Moldova privind agenda de dezvoltare durabilă până 2030 și Pactul Verde European. Din perspectiva dezvoltării durabile, extinderea programului ar putea include noi tehnologii verzi (boilere eficiente, pompe de căldură, termostate), consolidarea mecanismelor financiare și digitalizarea monitorizării rezultatelor. Astfel, Programul EcoVoucher poate deveni un model de bună practică regională în tranziția energetică, cu beneficii simultane economice, sociale și ecologice.

2. Provocări în procesul de implementare a programului

Programul EcoVoucher a fost inițial implementat ca proiect-pilot în perioada 26 octombrie 2023 – 22 iulie 2024. La această etapă au fost distribuite un total de 198 685 de vouchere energetice către beneficiarii eligibili, dintre care vouchere pentru becuri LED și echipamente electrocasnice. Repartizarea statistă a acestora este prezentată în tabelul 1. Distribuirea a fost organizată în 29 de sesiuni, cu valabilitate de două-trei săptămâni, fiecare etapă fiind atent monitorizată pentru a gestiona volumul mare de solicitări și pentru a asigura o repartizare echitabilă. O sesiune de distribuire a voucherelor debutează cu identificarea potențialilor beneficiari eligibili, selectați conform criteriilor de eligibilitate, din platforma compensatii.gov.md, unde aceștia au fost înregistrați în sezonul rece precedent. Ulterior, lista beneficiarilor propuși și bugetul aferent sesiunii sunt examinate și aprobate în cadrul ședinței Comitetului de Finanțare și Risc (CFR), fiind stabilită data oficială a lansării sesiunii [6] [7].

În ziua lansării, beneficiarii sunt informați printr-un mesaj SMS, poștă electronică sau prin cabinetul personal din platforma compensatii.gov.md cu privire la disponibilitatea voucherului. Sesiunea are o durată medie de aproximativ trei săptămâni, iar cu cinci zile înainte de expirare, beneficiarii sunt notificați suplimentar privind termenul limită de utilizare a voucherului.

După încheierea sesiunii, magazinele partenere prezintă rapoartele financiare aferente, care sunt ulterior evaluate individual de către persoanele responsabile, în vederea efectuării plăților către comercianți pentru voucherele valorificate.

Tabelul 1

Vouchere emise, valorificate, retrase

Vouchere	Emise	Valorificate	Retrase
Becuri LED	182300	31838	150462
Electrocasnice	16385	7246	9139
TOTAL	198685	39084	159601

Implementarea programului a scos în evidență o serie de provocări. Unii beneficiari nu au reacționat la mesajele inițiale privind disponibilitatea voucherelor, ceea ce a necesitat reluarea procesului de distribuire pentru a garanta accesul tuturor persoanelor eligibile. În acest context, centrul de suport al programului a avut un rol crucial, gestionând 11.664 apeluri telefonice (cu o durată medie de aproximativ două minute) și 425 de solicitări scrise prin e-mail.

Interacțiunile au vizat atât clarificări privind utilizarea voucherelor, cât și informații legate de criteriile de eligibilitate, interesul ridicat demonstrând relevanța și utilitatea acestui instrument. Statistica acestora este prezentată în fig. 1.

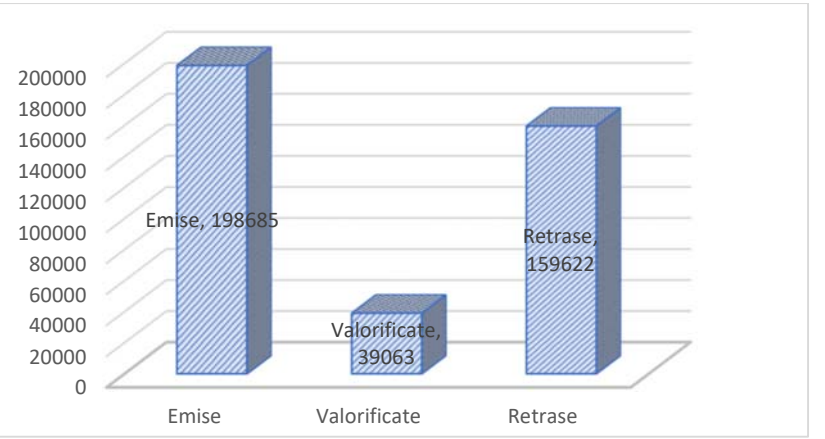

Fig. 1. Statistici privind voucherele emise, valorificate și retrase

După cum se poate observa din figura 1, un număr important de vouchere nu au fost utilizate. Motivele neutilizării au fost cauzate de diferiți factori. Cele mai frecvente motive, conform apelurilor primite, au fost:

- Beneficiarii nu se aflau în țară;
- Beneficiarii nu au avut posibilitatea să meargă la magazinele partenere din cauza că erau prea bătrâni, imobilizați la pat;
- Persoanele care s-au înregistrat au greșit date esențiale pe platforma compensații, IDNP-ul nu corespundea cu numele, prenumele.

După etapa de pilotare a programului a urmat faza de implementare, care a fost inițiată in august 2024. Prima sesiunea s-a lansat pe 30 septembrie cu o durată de o lună. În total au fost două sesiuni gestionate de CNED [8], iar în total în anul 2024 au fost lansate două sesiuni de vouchere, conform tabelului 2.

Tabelul 2

Vouchere emise, valorificate, retrase

Vouchere	Emise	Valorificate	Retrase
Electrocasnice	17 305	7 223	10 082

3. Analiza economiilor de energie obținute și reducerea emisiilor de CO_2

3.1. Calculul economiilor de energie obținute de la faza de pilotare a Programului

Conform datelor, disponibile pe perioada pilotării, în cadrul Programului au participat in familiile vulnerabile care au achiziționat cu ajutorul voucherelor 7.246 de electrocasnice mari (3.819 de frigidere, 3.391 de mașini de spălat, 36 de aragaze) și 303.336 becuri de tip LED. Totodată, prin intermediul programului au fost transmise pentru reciclare 7.246 echipamente vechi și uzate. Conform estimărilor, o familie poate economisi aproximativ 1.618 lei pe an la factura de energie electrică doar prin înlocuirea becurilor incandescente cu cele economice de tip LED. Economia anuală în urma înlocuirii unui singur bec incandescent de 60 W cu un bec LED de 7 W a fost estimat la 323 lei anual.

În tabelul 3 este prezentată informația comparativă privind consumul de energie electrică pentru echipamentele vechi versus cele noi, iar tabelul 4 reflectă economiile totale de energie, ca rezultat al înlocuirii echipamentelor vechi pe cele noi. Totodată, economiile financiare și reducerea emisiilor de CO2, sunt reflectate în tabelul 5, respectiv 6.

Tabelul 3

Informații privind consumul de energie echipamente vechi și noi

Echipament	Consumul specific de energie echipament vechi, kWh/an	Echipament nou	
		Clasa energetică	Consumul specific, kWh/an
Frigider, inclusiv cu congelator integrat	-	A	-
	450	B	110
	450	C	140
	450	D	180
Mașină de spălat, inclusiv cu uscător	200	A	45,5
	200	B	56
Aragaze electrice	12	A	8

Tabelul 4

Economiile totale de energie

Echipament	Clasa energetică	Nr.	Economii de energie la unitatea de produs, kWh/an	Economii de energie totale, kWh/an
Frigider, inclusiv cu congelator integrat	A	-	-	-
	B	60	340	20 400
	C	1437	310	445 470
	D	2 322	270	626 940
Total		3 819	920	1 092 810
Mașină de spălat, inclusiv cu uscător	A	2123	155	329 065
	B	1268	144	182 592
Total		3391	299	511 657
Aragaz electric	A	36	4	144
Total		36		144
Becuri LED		303 336	48	14 560
Total		303 336	48	14 560
Total Frigidere + Mașini de spălat + Aragaze electrice		7 246		1 604 611

Tabelul 5

Economiile financiare determinate

Echipament	Nr.	Economii de energie, kWh/an	Tarif mediu, lei/kWh	Economii financiare, lei/an
Total Frigidere + Mașini de spălat+ Aragaze electrice	7 246	1 604 611	4,39	7 051 488, 29
Becuri LED	303 336	14 560	4.39	63 918, 4
Total				7 115 406, 7

Tabelul 6

Reducerea emisiilor de CO2

Echipament	Nr.	Economii de energie, kWh/an	Factorul de emisie utilizat, CO2/kWh	Reducerea emisiilor de CO2, kgCO2
Total Frigidere + Mașină de spălat + Aragaze electrice	7 246	1 604 611	0,522	837,6
Becuri LED	303 336	14 560	0,522	7, 6

3.2. Calculul economiilor de energie obținute la faza de implementare a Programului

Pe baza datelor colectate și analizate, economiile de energie obținute ca urmare a înlocuirii echipamentelor au fost estimate în mod detaliat, fiind prezentate în tabelele de mai jos. La faza de implementarea s-a demonstrat impactul concret pe care îl are Programului în termeni de consum redus de energie, economii financiare pentru gospodării și contribuția acestuia la reducerea emisiilor de CO_2 [9].

Tabelul 7

Informații privind consumul de energie echipamente vechi și noi

Echipament	Consumul specific de energie echipament vechi, kWh/an	Echipament nou	
		Clasa energetică	Consumul specific, kWh/an
Frigider, inclusiv cu congelator integrat	-	A	-
	450	B	110
	450	C	140
	450	D	180
Mașină de spălat, inclusiv cu uscător	200	A	45,5
	200	B	56

Tabelul 8

Economiile totale de energie

Echipament	Clasa energetică	Nr.	Economii de energie la unitatea de produs, kWh/an	Economii de energie total, kWh/an
Frigider, inclusiv cu congelator integrat	A	-	-	-
	B	45	340	15 300
	C	725	310	224 750
	D	2 453	270	662 310
Total		3 223	920	902 360
Mașină de spălat, inclusiv cu uscător	A	3 276	155	506 142
	B	724	144	104 256
Total		4 000	299	610 398
Total Frigidere + Mașini de spălat		7 223		1 512 758

Tabelul 9

Economiile financiare determinate

Echipament	Nr.	Economii de energie, kWh/an	Tarif mediu, lei/kWh	Economii Financiare, lei/an
Total Frigidere + Mașini de spălat	7 223	1 512 758	4,39	6 641 008

Tabelul 10

Reducerea emisiilor de CO2

Echipament	Nr.	Economii de energie, kWh/an	Factor de emisie utilizat, CO2/kWh	Reducerea emisiilor de CO2, kgCO2
Total Frigidere + Mașină de spălat	7 223	1 512 758	0,522	789,6

Prin înlocuirea a peste 7.223 de echipamente vechi și ineficiente – în special frigidere și mașini de spălat – cu aparate moderne, cu clasă energetică superioară, programul a adus beneficii concrete și imediate în viața de zi cu zi a beneficiarilor. Familiile care au accesat voucherele au beneficiat nu doar de aparate mai performante,

ci și de un consum mai redus de energie electrică, fapt ce s-a tradus în facturi mai mici și un confort sporit în locuință.

Economiile totale de energie, calculate pe baza datelor disponibile, depășesc 1,5 milioane kWh pe an – o cantitate semnificativă ce reflectă eficiența măsurilor adoptate. La nivel financiar, acest consum evitat înseamnă economii anuale de peste 6,6 milioane de lei pentru beneficiari – bani care pot fi redirecționați spre alte nevoi ale gospodăriilor.

Totodată, reducerea consumului de energie electrică a avut un efect pozitiv asupra mediului. Calculele efectuate arată o reducere a emisiile de dioxid de carbon cu peste 750 de tone anual, contribuind astfel la eforturile țării noastre de combatere a schimbărilor climatice și de tranziție către un viitor mai verde.

Dincolo de cifre, programul a generat și un impact social important: a stimulat un comportament mai responsabil în rândul populației cu privire la consumul de energie, a contribuit la o mai bună înțelegerea etichetei energetice și a stimulat achiziția electrocasnicelor care consumă mai puțină energie.

Pentru a face o apreciere asupra reducerii consumurilor energetice in urma implementării Programului, in tabelul 11 de mai jos, sunt aduse datele comparative pe perioada anului 2024 [10] , unde sunt reflectate economiile financiare si de emisii la faza de pilotare și implementare a Programului.

Tabelul 11

Totalul economiilor pentru anul 2024

PNUD		
Echipament	Economii Financiare, lei/an	Reducerea emisiilor de CO2, kgCO2
Total Frigidere + Mașini de spălat+ Aragaze electrice	7 051 488	837,6
Becuri LED	63 918	7,6
CNED		
Echipament	Economii Financiare, lei/an	Reducerea emisiilor de CO2, kgCO2
Total Frigidere + Mașini de spălat	6 641 008	789,6
TOTAL 2024	13 756 414	1 634,8

Concluzie

Programul EcoVoucher a demonstrat un impact semnificativ asupra eficienței energetice și a sustenabilității în Republica Moldova privind reducerea consumului de energie electrică în sectorul rezidențial. În etapa pilot, desfășurată sub coordonarea PNUD, Programul EcoVoucher a generat economii anuale de aproximativ 1,6 milioane

kWh, ceea ce a însemnat beneficii financiare de circa 7 milioane lei pentru gospodării și o reducere a emisiilor de dioxid de carbon cu peste 837,6 de tone. Ulterior, în etapa de implementare gestionată de CNED, au fost obținute economii suplimentare de 1,5 milioane kWh, echivalent a 6,64 milioane lei, iar emisiile de CO2 au fost reduse cu 789,6 de tone anula. În total, pe parcursul anului 2024, programul a asigurat economii de peste 3,1 milioane kWh, o reducere a facturilor gospodăriilor cu aproximativ 13,75 milioane lei și o diminuare a emisiilor cu 1 634,8 kg CO2 anual.

Rezultatele confirmă faptul că EcoVoucher reprezintă un instrument eficient atât pentru sprijinirea categoriilor vulnerabile, cât și pentru accelerarea tranziției energetice, contribuind direct la atingerea obiectivelor Agendei de Dezvoltare Durabilă până în 2030 și ale Pactului Verde European [11] [12].

Bibliografie:

[1] *Ministerul Energiei al Republicii Moldova*, Site oficial, Chișinău, Republica Moldova: Disponibil la:– https://energie.gov.md;
[2] *Ministerul Energiei al Republicii Moldova*, Raport privind securitatea energetică 2022, Chișinău, 2023;
[3] *European Commission*, EU Energy Security and Green Transition in Eastern Partnership Countries, Brussels: European Union, 2023;
[4] Hotărârea Guvernului nr. 533/2024 privind aprobarea Strategiei Energetice a Republicii Moldova până în anul 2050; Disponibil la: – https://www.legis.md/;
[5] Hotărârea Guvernului nr. 953/2022 pentru aprobarea Regulamentului privind performanța energetică a clădirilor. Disponibil la: – https://www.legis.md/;
[6] *Centrul Național pentru Energie Durabilă (CNED)*, Raport de implementare a Programului EcoVoucher – Etapa pilot (2023–2024), Chișinău, 2024;
[7] *Centrul Național pentru Energie Durabilă (CNED)*, Manual Operațional Programul de Vouchere pentru Electrocasnice;
[8] *Centrul Național pentru Energie Durabilă (CNED)*, Site oficial, Chișinău, Republica Moldova. Disponibil la: – https://cned.gov.md;
[9] USAID / MESA. Assessment of the Grid Emission Factor of Moldova's Electricity System (Final Report). Chișinău: *Ministry of Energy of the Republic of Moldova, 2024.* https://energie.gov.md/sites/default/files/document/attachments/usaid_mesa_grid_emission_factor_of_moldova_electricity_system_assessment_final.pdf ;
[10] *Centrul Național pentru Energie Durabilă (CNED)*, Raport de activitate IP CNED, 2024;
[11] *United Nations (UN),* Agenda 2030 for Sustainable Development, 2015;
[12] *European Commission*, The European Green Deal, 2019.

Analysis of the computer simulation for optimizing the evacuation of people in an event hall

Analiza simulării computerizate pentru optimizarea evacuării persoanelor într-o sală de evenimente

Emanuil-Petru Ovadiuc[1], Răzvan Calotă[2], Ilinca Năstase[2], Ion Anghel[1], Manuel Șerban[1]

[1] Fire Officers Faculty, Police Academy "Alexandru Ioan Cuza", Romania
3 Morarilor Road, Bucharest, Romania

[2] Technical University of Civil Engineering of Bucharest, Romania
121-126 Bvd Lacul Tei, Bucharest, Sector 2, Romania

E-mail: emanuil-petru.ovadiuc@phd.utcb.ro, razvan.calota@utcb.ro, ilinca.nastase@utcb.ro, ion.anghel@gmail.com, manuel.serban@gmail.com

DOI: 10.37789/rjce.2026.17.1.12

Abstract. *The article presents the development and analysis of an evacuation simulation for the ground floor of a building intended for conferences and events, using geometric modeling in SketchUp and occupant behavior simulation in Pathfinder. A total of 31 rooms and 41 doors (11 used as evacuation exits) were defined, along with a population of 524–526 occupants, assigned with variable profiles regarding speed, behavior, and anthropometric dimensions. Three scenarios were analyzed: normal evacuation, evacuation including persons with disabilities and one blocked exit, and a severe scenario with seven exits unavailable. The results show increases in evacuation time up to 121.8 seconds and the occurrence of congestion zones caused by uneven occupant distribution and reduced evacuation paths. The study highlights the importance of redundancy in evacuation routes, optimal furniture arrangement, and assistance for vulnerable individuals.*

Key words: *evacuation simulation, Pathfinder, SketchUp, fire safety, occupant behavior, people flow.*

Rezumat. *Articolul prezintă realizarea și analiza unei simulări de evacuare pentru nivelul parter al unei clădiri destinate conferințelor și evenimentelor, folosind modelarea geometrică în SketchUp și simularea comportamentului ocupanților în Pathfinder. Au fost definite 31 de încăperi, 41 de uși (11 de evacuare), și o populație compusă din 524–526 ocupanți, incluși cu profiluri variabile privind viteză, comportament și dimensiuni antropometrice. Au fost analizate trei scenarii: evacuare normală, evacuare cu persoane cu dizabilități și blocarea unei uși, respectiv scenariu sever cu 7 uși blocate. Rezultatele indică creșteri ale timpului de evacuare până la 121,8 s și apariția zonelor de congestie cauzate de distribuția neuniformă și restrângerea căilor de evacuare. Studiul evidențiază*

The article was received on 19.01.2026, accepted on 02.02.2026 and published on 24.02.2026

importanța redundanței căilor de evacuare, configurării optime a mobilierului și asistenței pentru persoane vulnerabile.

Cuvinte cheie: *simulare evacuare, Pathfinder, SketchUp, securitate la incendiu comportament ocupanți, flux de persoane.*

1. Introduction

The evaluation of the performance of evacuation systems in emergency situations is a fundamental element in the analysis of the fire safety of modern buildings. The progress of computer simulation tools today allows the detailed reproduction of occupant behavior and the dynamics of evacuation flows, thus contributing to the substantiation of technical decisions and the validation of compliance with regulatory provisions. In this context, the use of specialized software, such as SketchUp to create geometry and Pathfinder to simulate the evacuation, offers the possibility of generating realistic and reproducible scenarios, which reflect both the architectural conditions of the building and the behavioral variability of the people involved.

This article presents the process of realizing a complex evacuation simulation for the ground floor level of a building with conference, event and catering functions. The modeling of the space included the faithful representation of the partitions, furniture, level differences and escape routes, and subsequently, the configuration of the population was made based on individualized profiles, differentiated according to anthropometric, behavioral characteristics and functional role. In addition, three distinct scenarios were analysed, including both the normal configuration of use and situations of constraint generated by the blocking of escape doors or the presence of people with disabilities requiring assistance.

By comparatively approaching these scenarios, the study aims to identify the determinants of evacuation times, highlight critical congestion areas and assess the capacity of the evacuation network to manage highly complex situations. The results obtained contribute to an in-depth understanding of the interactions between the architecture, the behavior of the occupants and the limitations of the evacuation infrastructure, while providing support for the optimization of fire safety measures and for the improvement of intervention strategies.

2. Methodology for conducting the simulation

Geometric modeling and plane import into the simulation environment

The realization of a credible simulation of the evacuation process requires the construction of a geometric model that faithfully reproduces the spatial configuration of the analyzed building. In this sense, the ground level of the objective, intended for conferences and events, was modeled using the SketchUp software, thanks to its

ability to quickly generate three-dimensional geometries compatible with the format used by Pathfinder. The model includes partitions, furniture, escape routes, doors and access areas, all of which are necessary to obtain a realistic simulation.

Subsequently, the plan was exported to the .dae format (Collada), natively compatible with Pathfinder, and imported into the simulation mediator. At this stage, scale and positioning adjustments were made to ensure the exact correspondence between the model and the actual escape routes, avoiding geometric overlaps that could affect the behavior of the simulated agents.

Definition of rooms and parameterization of escape doors

After importing the geometric model, the 31 rooms used in the simulation were delimited: conference rooms, event rooms, hallways, public catering areas, changing rooms, toilets, offices and corridors. This step is essential because it allows the attribution of specific characteristics to each space, such as the maximum permissible density and the behaviour of the occupants in relation to obstacles.

Similarly, 41 doors have been defined, of which 11 constitute exhaust exits to the outside. The doors were classified by color codes: orange for the interior doors, green for the exhaust doors, respectively red for the unavailable doors. The parameters introduced – effective width, direction of circulation and direction of opening – complied with the requirements of the P118/1 [1] standard on the dimensioning of escape routes. The existing level differences in the plan also required the introduction of two stairs with 16 steps, necessary to achieve the transition between the -1.50 m and +0.00 m elevations.

Location and characterization of the simulated population

In order to reproduce the real conditions of use of the building, the population distribution was made based on the functions of the rooms and the maximum densities allowed according to the provisions of P118/1. In total, 524 occupants were introduced: 279 men, 159 women, 40 children and 46 employees. They were evenly positioned or concentrated in relevant areas (around tables, near the bar, in conference spaces) using the "Add an occupant" function in Pathfinder.

For each simulated agent, individual anthropometric characteristics (height, shoulder width, body mass) and mobility parameters (travel speed) were defined, thus ensuring a realistic heterogeneity of the population. The initial position of the occupants is a determining factor in the occurrence of congestion, temporary blockages and in the general evolution of the evacuation process.

Behavioral profiles and inclusion of persons with disabilities

To reflect real behavioral diversity, distinct profiles have been created for each category of occupants: men, women, children, employees and people with disabilities. These profiles include parameters regarding travel speed, evacuation priority, anthropometric characteristics and the associated 3D model.

A special profile was assigned to people with locomotor disabilities, represented by "polygon" models configured with wheelchair animations. These

people were set as not being able to leave the building autonomously, requiring the support of evacuation teams. To this end, two additional behaviors were defined – "evacuation team" and "person in need of help" – implemented through the "Assisted evacuation teams" module. Designated employees (one for each person with disabilities) start the action with a reduced delay, reflecting specific training in evacuation procedures.

Simulation of evacuation in different scenarios

Scenario 1 – Evacuation under normal conditions

The first scenario simulates the evacuation of the 524 occupants under normal operating conditions, using all 11 available escape doors. The general behavior attributed to the agents was "go to any exit", they would go to the nearest door.

The prioritization given to the categories of occupants is as follows:

- Children
- Women
- Men
- Employees

A uniform delay of 20 s has been introduced for the perception of the alarm signal, and the capacity of the doors has been set to 1–2 persons/s, depending on the width of each door. The simulation does not involve artificial bottlenecks, except for those naturally generated by flow congestions.

Total evacuation time: 102.8 s.

Scenario 2 – Presence of people with disabilities and locking a door

Two people with disabilities were introduced in this scenario, bringing the total number of occupants to 526. At the same time, an escape door (door 41) has been deactivated, reducing the number of available exits to 10.

People with disabilities received the behavior "Wait for assistance", and the employees designated as companions – the behavior "Assist" followed by "go to any exit". The reaction time for these employees has been reduced to 10 s, and the travel speed during assistance has been set to 1 m/s.

Evacuation priorities become:

- people with disabilities
- Children
- Women
- Men
- Employees
- The rest of the parameters remain similar to the previous scenario.
- Total evacuation time: 107.3 s.

Scenario 3 – Locking the doors on the north side of the building

The third scenario involves a severely disrupted situation: 7 of the 11 escape doors (doors 24, 23, 07, 25, 10, 08 and 09) were blocked, with only 4 doors on the

south side being functional. This configuration forces all occupants in the northern half of the building to travel longer routes, negatively affecting the total evacuation time.

The simulation further includes the two persons with disabilities and the related evacuation teams, with the same characteristics as in scenario 2. The remaining factors (densities, delays, priorities) are identical.

Total duration of the evacuation: 121.8 s.

3. Analysis of the results obtained

The analysis of the 3 scenarios is necessary to observe and highlight certain factors that lead to the lengthening of evacuation times, the creation of congestion areas, as well as the comparison of evacuation times between them and the degree of use of each evacuation door according to their availability.

Scenario 1 Analysis

In scenario 1, a scenario in which the evacuation occurs normally, without unforeseen events, the evacuation time is 102.8 seconds. The arrangement of the occupants in the first second of the simulation is shown in Figure no. 1. A filter has been applied to be able to visualize the density of people per m2, thus making it possible to identify the busiest areas in the building and the most used doors and escape routes.

Fig.1. Arrangement of the occupants in the first second of the simulation for scenario 1

According to the specifications made at the presentation of the first scenario, the evacuation starts at the 20th second.

There are 4 large areas with a high density of users and an arrangement very close to each other. As can be seen in Figure no. 2, this resulted in the creation of large queues towards the exhaust outlets starting at 23 seconds, just 3 seconds after the start of the exhaust and thus lengthening the exhaust time. The busiest doors at the beginning of the evacuation are door 25 which connects to the outside and interior doors 26, 12 and 42 which connect the rooms and corridors leading to the exits to the outside.

Fig. 2. 23 seconds, 3 seconds after the start of the evacuation for scenario 1

Starting with the 28th second, the maximum value of the density of persons/m^2 supported by the program is reached, which is highlighted in the dark red color shown in Figure no. 3. This demonstrates that in order to accommodate in a room that will have a high density of users, it is advisable to use access doors in that room as wide as possible to allow people to leave the room quickly and avoid possible blockages until they enter the escape routes.

Fig. 3.Areas with very high density of people for scenario 1

A notable aspect is found at 68.8 seconds where a congestion area is observed near door no. 13. Here it can be seen that it is the last door at which a waiting line made up of the last 68 occupants is formed.

The situation in question presents a major deficiency in the distribution of doors intended for external evacuation because for the last 68 users another 34 seconds are allocated to leave the building compared to the rest of the users who up to 68.8 seconds managed to evacuate in a very short time, which is due to the correct sizing of the width of the interior doors and the correct placement of the escape doors.

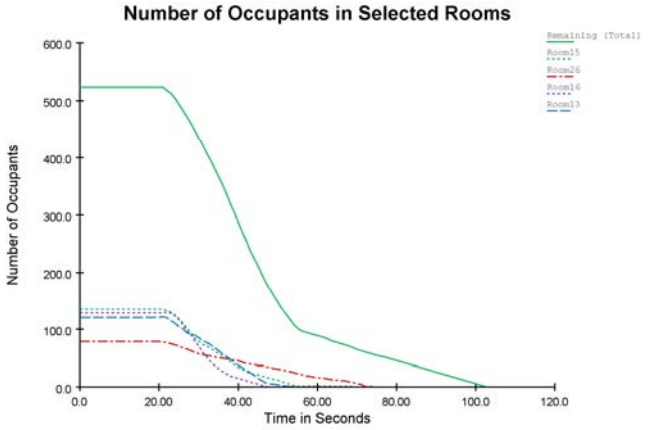

Fig. 4. Graph of users remaining in the rooms after moving to the escape doors in unit time for scenario 1

The graph in Figure no. 4 presents the number of users left in the 4 crowded rooms following their departure in time and states the situation presented in the previous paragraph, room no. 26 having a very long time for the evacuation of all occupants. This aspect can also be correlated with the Graph in Figure no. 5 which shows no. of occupants evacuated in time.

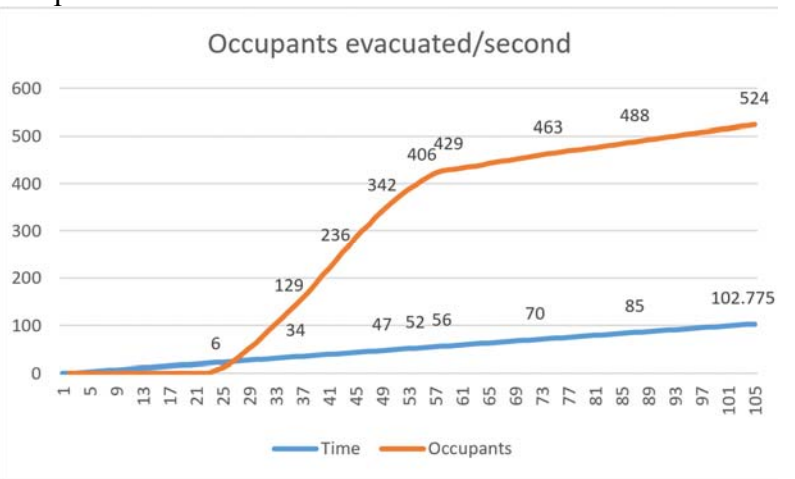

Fig. 5.Graph with users evacuated in time for scenario 1

The most used exhaust door for this scenario was door no. 13 with 157 evacuated users, and the least used door was door no. 9 with only 7 occupants evacuated.

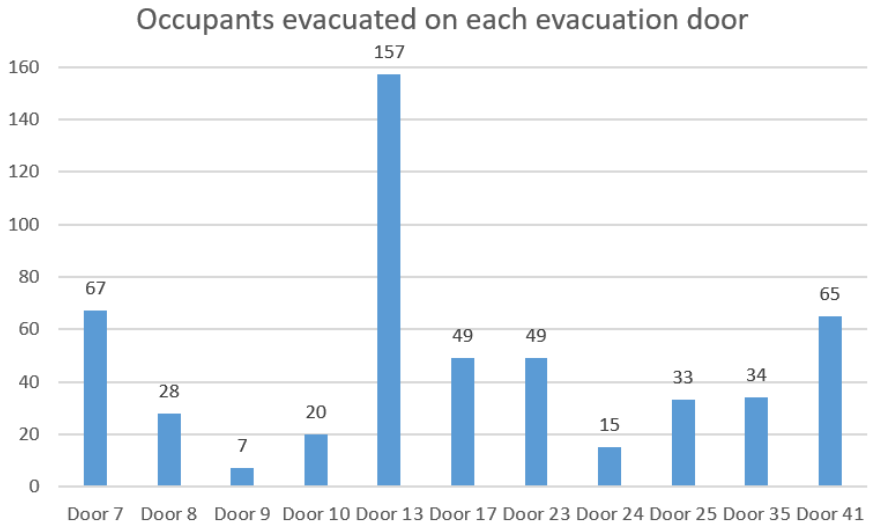

Fig. 6.Graph with the total number of users evacuated on each door for scenario 1

Scenario 2 Analysis

In scenario 2, a scenario in which the evacuation does not occur under normal conditions, the evacuation time is 107.3 seconds, a time 4.38% longer compared to that in scenario 1. This increase is due to door lock no. 41 as well as the addition of persons who cannot evacuate themselves. The arrangement of the occupants in the first second of the simulation is shown in Figure no. 7. A filter has been applied to putea visualize the density of people per m^2 thus making it possible to identify the busiest areas in the building and the most used doors and escape routes.

Fig. 7. Occupant arrangement in the first second of the simulation for scenario 2

The new situations imposed by the locking of a door and the introduction of two occupants who cannot evacuate themselves are, on the one hand, the increase of the evacuation time by 4.5 seconds compared to the previous scenario and on the other hand, the formation of new congestion zones (found in Figure no. 8), as well as the change in the number of people evacuated over time and the number of people evacuated on each escape door.

The first people to be evacuated were the people who cannot evacuate themselves due to the staff who consider themselves trained in this regard and act 10 seconds before the other users.

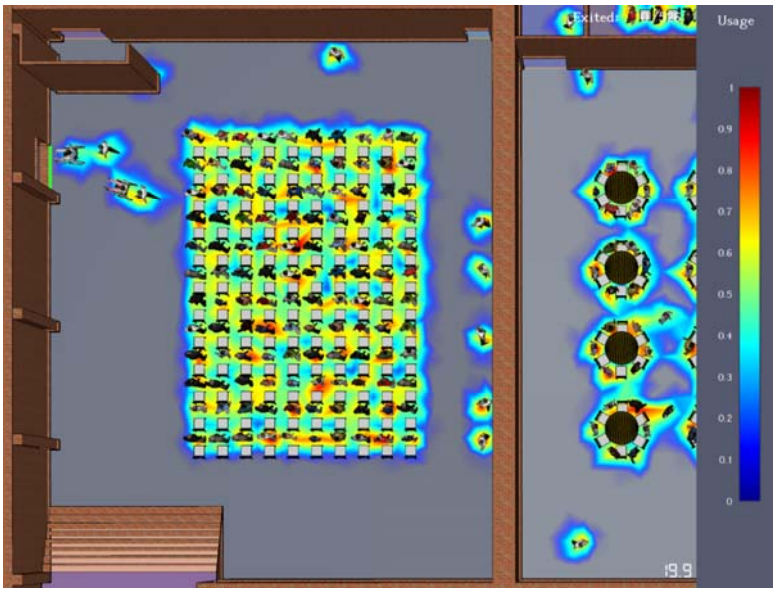

Fig. 8. 20 seconds, rapid evacuation of people who cannot evacuate themselves for scenario 2

Fig. 9. New area with increased density of people for scenario 2

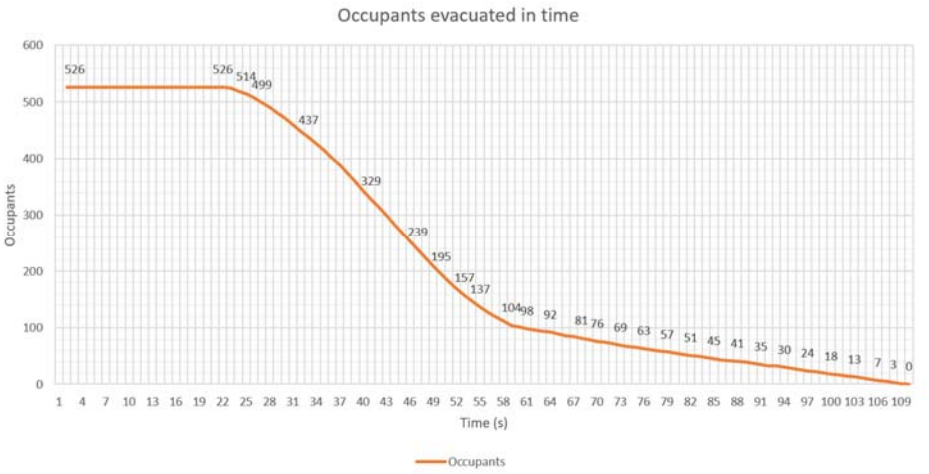

Fig. 10. Graph of users evacuated in time for scenario 2

Compared to scenario 1, there is a significant increase in users evacuated through door no. 9 (from 7 users to 25), but also an increase of 6 users for door no. 13 which was already very crowded.

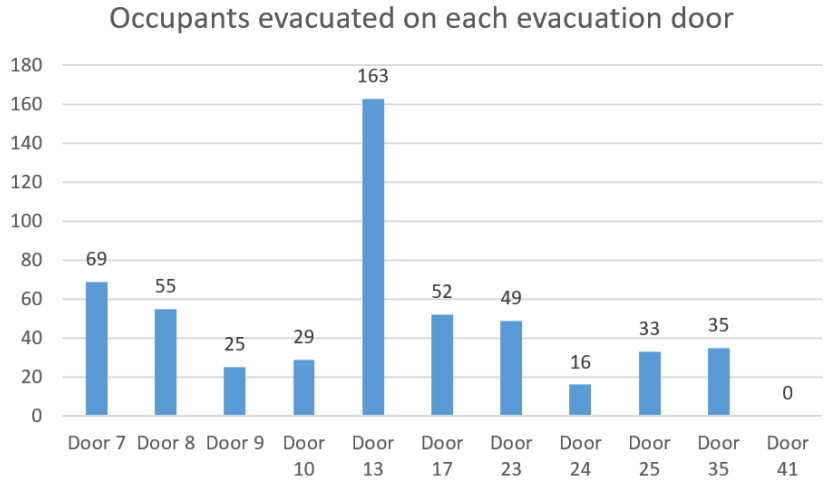

Fig. 11. Graph with the total users evacuated to each door for scenario 2

Scenario 3 Analysis

In scenario 3, a scenario in which the evacuation does not occur under normal conditions, the evacuation time is 121.8 seconds, a time 18.48% longer compared to that in scenario 1. The arrangement of the occupants in the first second of the simulation is shown in Figure no. 11. A filter has been applied to be able to visualize the density of people per m2, thus making it possible to identify the busiest areas in the building and the most used doors and escape routes.

Fig. 12. Occupant arrangement in the first second of the simulation for scenario 3

The blocking of 7 doors led to a significant increase in evacuation time (19 seconds more than scenario 1) and also an increase in the number of people evacuated on the few remaining doors that had around 50 users evacuated on each door (doors 17, 41, 13 and 35). Another effect is the creation of new congestion areas, as well as the much higher use of stairs leading to the south side of the building.

Fig. 13. New areas with high density of people for scenario 3

The first people to be evacuated were the people who cannot evacuate themselves due to the staff who consider themselves trained in this regard and act 10 seconds before the other users.

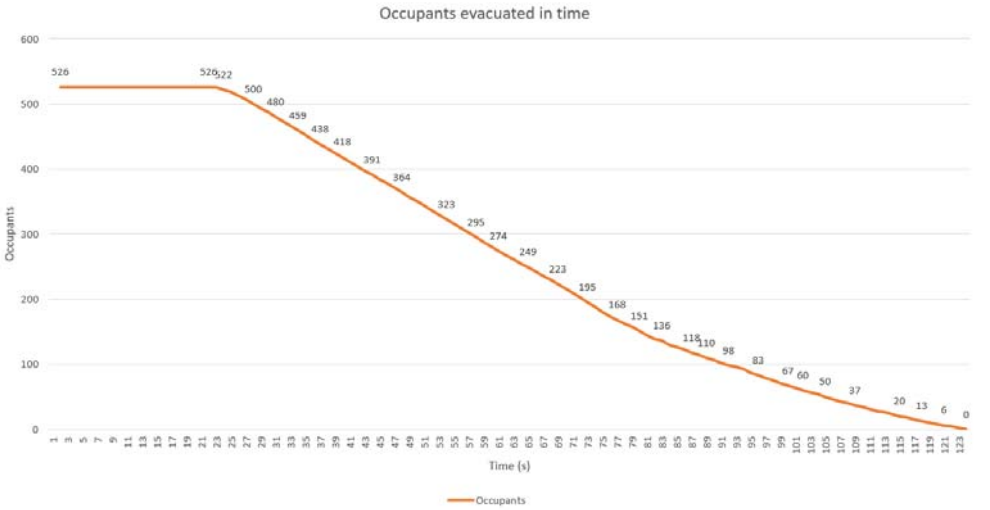

Fig. 14. Graph of users evacuated in time for scenario 3

Compared to scenario 2, the curve is no longer so steep as users from the northern part of the building have to cross the building to the southern part of it, making it impossible to use the doors closest to the main entrance.

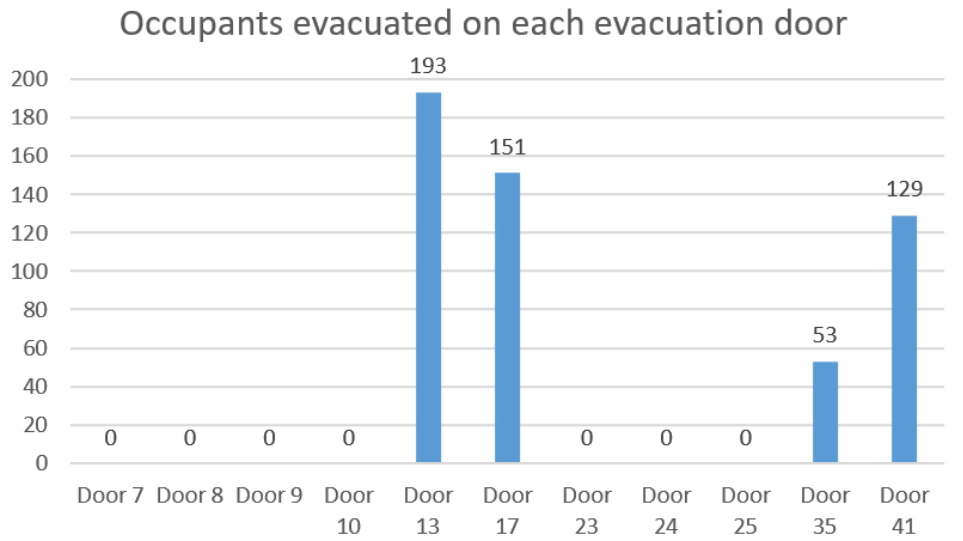

Fig. 1. Graph with the total users evacuated to each door for scenario 2

Compared to scenarios 1 and 2, only 4 escape doors are used, and the number of evacuated users on each door is considerably higher, in the case of the door no. 17 being about triple.

The scenario considered is a totally fictitious one, in practice it is impossible to decommission 7 escape doors. A special mention is that it is impossible to pregătit o

building for such a scenario with such exaggerated elements. For this case, the time obtained is a very good one, being an evacuation executed in ideal time.

Solutions to make the evacuation more efficient

The analysis of the three simulated scenarios showed a significant increase in the evacuation time when one of the escape doors was blocked (scenario 2) and, in particular, when the doors at the main entrance became inaccessible (scenario 3). The evacuation time increased from 103.8 seconds (scenario 1) to 122.8 seconds (scenario 3), which represents an increase of more than 18%, indicating a vulnerability of the system in the absence of redundancy.

Based on these results, the following technical and organizational measures are proposed:

1. Reconfiguring the furniture in event rooms and hallways

In the simulations carried out, accumulations of people were observed in the vicinity of tables and chairs, especially in the areas between furniture and escape routes. It is recommended to reposition or group furniture more airy, so as not to reduce the width of the escape aisles and to allow a more fluid flow of people.

2. Resizing or supplementing secondary escape doors

The blocking of a single door led to an overload of the other exits. It is recommended to consider the possibility of extending the width of secondary doors or introducing a new direct exit to the outside from areas with high occupancy density (e.g. breakfast room or conference room).

3. Installation of additional directional exhaust signs

In scenarios with blocked exits, occupants initially continued to orient themselves towards inaccessible exits, wasting time. The implementation of dynamic signaling panels, capable of indicating in real time the fastest available outputs (voice alarm or sequential LEDs), can route flows adaptively and reduce local bottlenecks.

4. Provision of assistance for persons with reduced mobility

In scenario 2, the introduction of occupants who cannot evacuate themselves generated delays in areas where they crossed paths with groups of mobile evacuees. It is proposed to allocate dedicated routes for these trained occupants and/or companions, as well as to clearly mark these routes in the evacuation plan.

5. Implementation of an evacuation plan differentiated by areas

The simulation showed that the uneven distribution of the population leads to the overloading of some outputs and the underutilization of others. It is recommended to draw up an evacuation plan by sectors, with the advance assignment of pre-established routes for each functional area (e.g. restaurant area → side door; bar area → secondary main exit).

The proposed measures aim not only at geometric compliance with evacuation requirements, but also at optimizing the collective behavior of occupants under stress, ensuring a high level of safety even in situations with partial restriction of exits or in the presence of people with special needs. The implementation of these solutions directly contributes to shortening evacuation time and reducing the risk of congestion at critical points.

4.Conclusions

The computer simulation of the evacuation using the Pathfinder program was a key step in assessing the performance of the evacuation routes of the analyzed building, providing a dynamic perspective on how users react and move in emergency situations. Building the 3D model in SketchUp and importing it into Pathfinder allowed the faithful rendering of the architectural, functional and furniture configuration, factors that directly influence the trajectories and speed of movement of people.

The configuration steps – delimiting the spaces, defining the escape doors, setting the exit points and assigning the various occupant profiles – ensured the generation of extremely realistic evacuation scenarios. The differentiated distribution of occupants and the introduction of individualized characteristics (speed, reaction time, behavior) allowed the precise identification of areas with a high risk of congestion and vulnerable sections of the exhaust network.

The three scenarios tested demonstrated that relatively small changes in initial conditions – the appearance of people with reduced mobility or the blocking of doors – can have a major influence on overall evacuation times. The blocking of the main access generated a forced redistribution of flows to secondary exits, causing dangerous accumulations in constriction zones and confirming the need for effective redundancy of escape routes, as well as the importance of maintaining the permanent functionality of the doors.

The analysis of the results allowed the identification of key vulnerabilities, such as areas with dense furniture, insufficiently sized routes and high dependence on certain exits. The proposals formulated – resizing or supplementing the doors, reorganizing the furniture, installing additional directional signs and training the staff – directly contribute to increasing the level of safety.

Main conclusions of the study:

- evacuation times can increase by more than 18% in the absence of redundancy of escape routes;
- the uneven distribution of occupants is one of the main factors in the occurrence of congestion;
- people with disabilities significantly influence the dynamics of flows if the routes are not adapted;
- the width of the doors and the arrangement of the furniture are decisive elements for the efficiency of the evacuation;
- Trained staff can reduce times for vulnerable occupants.

Applicability to other types of buildings:

The principles and conclusions obtained are also valid for other buildings with large flows of people – conference centers, restaurants, hotels, shopping centers, clădiri administrative sau educaționale. Comportamentul mulțimii, influența furniture, the importance of redundancy and correct door sizing remain constant regardless of the

type of construction, which confirms the generalizable nature of the methodology used.

Recommendations for occupants in case of evacuation:

- follow the signage and instructions of the staff without stopping or turning;
- Use the closest functional output, not just the input originally used.
- keep calm, walk orderly and avoid running;
- not to block doors and aisles;
- parents to keep their children close;
- people who can help vulnerable occupants to do so without exposing themselves to risks.

Strictly forbidden actions during the evacuation:

- the use of elevators;
- returning for personal belongings;
- pushing or forming compact masses that can generate panic;
- blocking of escape doors or corridors;
- ignoring signage or moving to locked doors.

In conclusion, the use of Pathfinder has proven to be a valuable tool for validating, optimizing and generalizing technical evacuation solutions. The results obtained support both architectural adaptations and operational improvements regarding occupant response and emergency management, contributing to increasing the overall level of fire safety.

References

[1] P118/1-2025 Romanian Norm
[2] Wang, Yiyu, Jiaqi Ge, and Alexis Comber. "An Agent-Based Simulation Model of Pedestrian Evacuation Based on Bayesian Nash Equilibrium." Journal of Artificial Societies and Social Simulation, vol. 26, no. 3, 2023, p. 6, https://doi.org/10.18564/jasss.5037
[3] Muhammed, Danial A., et al. "An Improved Simulation Model for Pedestrian Crowd Evacuation." Mathematics, vol. 8, no. 12, 2020, p. 2171, https://doi.org/10.3390/math8122171.
[4] Răduică, Ion-Cătălin, Ion Anghel, Adrian Simion, and Horaţiu Gabriel Dragne. Simulări de evacuare ale persoanelor dintr-un cămin cultural în contextul pandemiei SARS-COV-2 = Simulations of evacuation of people from a cultural home in the context of the SARS-VOC-2 pandemic. INCD URBAN-INCERC.
[5] NFPA 101 – Life Safety Code

The concept of an installation for testing, monitoring and efficient management of complex systems equipped with a heat pump for heating / cooling and preparing hot water in buildings

Conceptul unei instalații pentru testarea, monitorizarea și gestionarea eficientă a sistemelor complexe dotate cu pompe de căldură pentru încălzirea / răcirea și prepararea apei calde în clădiri

Daniel Bisorca[1], Adriana Tokar[1], DănuțTokar[1], Daniel Muntean[1], Alexandru Dorca[1]

[1] University Politehnica Timisoara
Victoriei Square, no.2, Timisoara, Romania
E-mail: daniel.bisorca@upt.ro, adriana.tokar@upt.ro, danut.tokar@upt.ro, daniel-beniamin.muntean@upt.ro, alexandru.dorca@upt.ro

DOI: 10.37789/rjce.2026.17.1.13

Abstract: *Articolul prezintă propuneri de eficientizare energetică a sistemelor complexe de încălzire/răcire și preparare apă caldă de consum prin conceptualizarea a două sisteme pentru testarea și gestionarea eficientă din punct de vedere energetic aplicate unui ansamblu mixt format din două pompe de căldură de tip apă-apă, respectiv aer-apă.*

Key words: heating/cooling, heat pumps, energy efficiency

Rezumat: *The article presents proposals for energy efficiency of complex heating/cooling and domestic hot water systems by conceptualizing two systems for energy-efficient testing and management applied to a mixed ensemble consisting of two water-to-water and air-to-water heat pumps, respectively.*

Cuvinte cheie: încălzire/răcire, pompe de căldură, eficientizare energetică

1. Introducere

Având în vedere politica Uniuni Europene de tranziție spre un sistem de preparare și de furnizare a energiei termice eficiente energetic și cu cât mai puține emisii de gaze cu efect de seră [1, 2], în ultima perioadă de timp se sesizează o creștere a utilizării pompelor de căldură ca și surse de energie termică în componența acestor sisteme. Energia termică produsă cu ajutorul pompelor de căldură este considerată energie verde și cu emisii reduse de CO_2 deoarece se poate considera că energia

The article was received on 28.04.2025, accepted on 02.02.2026 and published on 24.02.2026

electrică consumată de pompe de căldură poate proveni din surse regenerabile sau din surse cu emisii reduse de gaze cu efect de seră [3, 4].

În cazul utilizării pompelor de căldura ca și surse de energie termică sau surse pentru prepararea apei calde în instalații aferente unor clădiri publice sau ansambluri de locuințe, în majoritatea cazurilor este necesară instalarea mai multor pompe de căldură, de același tip aer-apă sau apă-apă. Sunt întâlnite însă și unele cazuri în care avem chiar o combinație a acestor surse. În sistemele de încălzire ale clădirilor eficiente energetic, în majoritatea cazurilor avem nevoie de temperaturi reduse ale agentului termic în sistemul de încălzire și din acest considerent agentul termic este distribuit spre a fi încălzit în mai multe pompe de căldură conectate în paralel. Având în vedere că sarcina termică necesară la utilizatorii finali este dependentă în general de temperatura exterioară, modul de cascadare și de încărcare a pompelor de căldură trebuie gestionat astfel încât consumul de energie electrică al sistemului să fie cât mai redus. Cu alte cuvinte, se impune o automatizare a întregului proces astfel încât randamentul energetic al pompelor de căldură să fie cât mai ridicat posibil. Automatizarea modului de prioritizare și încărcare a pompelor de căldură trebuie să țină cont de mai mulți factori dintre care cei mai importanți sunt: temperatura necesară a agentului termic la consumator, temperatura aerului exterior, temperatura apei de suprafață sau a apei freatice, curbele de putere și de randament ale pompelor de căldură, energia electrică consumată de pompa de căldură în funcție de gradul de încărcare a acesteia. Dacă furnizorul de pompe de căldură nu furnizează informații complete pentru toate regimurile de funcționare, beneficiarul va fi nevoit să își ridice singur aceste curbe de funcționare înregistrând datele caracteristice în toate punctele posibil a fi întâlnite în funcționarea acestora. Astfel, ținând cont de eficiența energetică a fiecărei pompe din componența sistemului de încălzire determinată printr-un bilanț energetic aplicat pe conturul fiecărui echipament se poate concepe o configurație optimă de încărcare succesivă a pompelor de căldură. Sistemul de automatizare trebuie să aibă implementat sistemul de pornire și folosire succesivă a tuturor echipamentelor astfel încât uzura acestora să fie cât mai uniformă.

2. Conceptul sistemului format din pompe de căldură apă-apă și aer-apă

În Figura 1 se prezintă conceptul unui sistem pentru testarea și gestionarea eficientă din punct de vedere energetic aplicat unui ansamblul mixt format din două pompe de căldură de tip apă-apă respectiv apă-aer, montate în paralel, în care se pot observa toate elementele necesare sistemului (contoare de energie, senzori, placa de achiziție și calculator de proces) pentru ridicarea curbelor caracteristice și pentru optimizarea încărcării celor două pompe de căldură.

Pompele de căldură apă – apă au și capacitatea de a crește potențialul termic al sistemelor de încălzire care folosesc energia geotermală ca și sursă regenerabilă de energie. În cazul acestor sisteme, pompele de căldură au și rolul de a răci apa geotermală astfel încât aceasta să poată fi deversată în siguranță la emisar sau să fie reintrodusă în sol prin forajul de reinjecție.

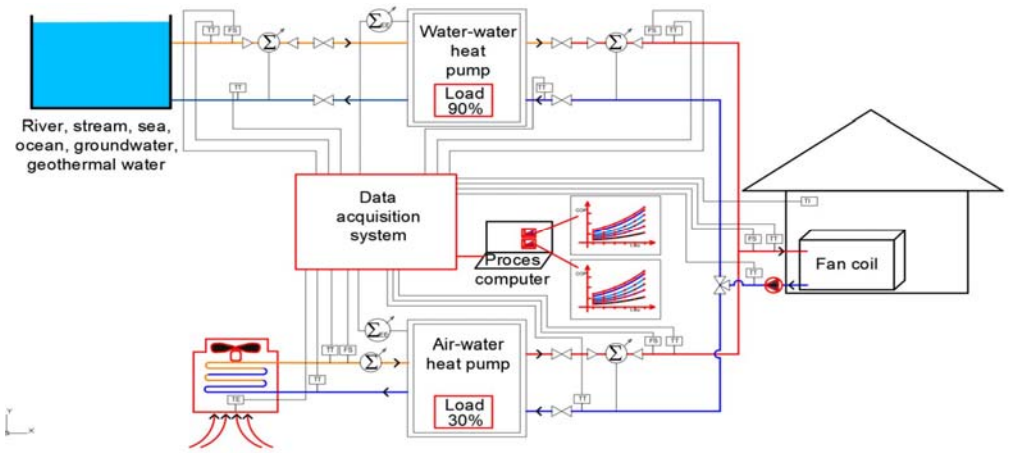

Fig. 1. Schema conceptuală cu pompe de căldură montate în paralel

Pentru a răci suficient această apă geotermală și pentru a folosi cât mai mult din potențialul termic al acesteia, atât apa geotermală, cât și agentul termic parcurg circuitul pompelor de căldură înseriate (de obicei două/trei pompe de căldură).

În figura 2 se prezintă conceptul unui sistem pentru testarea și gestionarea eficientă din punct de vedere energetic aplicat unui ansamblul format din trei pompe de căldură de tip apă-apă înseriate, în care se pot observa toate elementele necesare sistemului (contoare de energie, senzori, placa de achiziție și calculator de proces) pentru ridicarea curbelor caracteristice și pentru optimizarea încărcării celor două pompe de căldură.

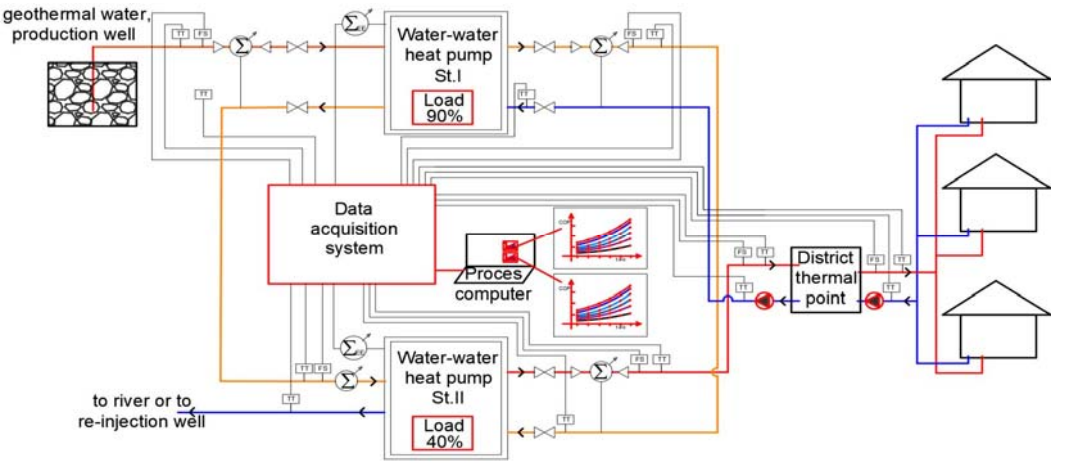

Fig. 2. Schema conceptuală cu pompe de căldură montate în serie

Și în acest caz ținând cont de eficiența energetică a fiecărei pompe din componența sistemului de încălzire determinată tot printr-un bilanț energetic aplicat pe conturul fiecărui echipament se poate concepe o configurație optimă de încărcare succesivă a pompelor de căldură. Sistemul de automatizare trebuie să aibă implementat

și acel sistem de pornire și folosire succesivă a tuturor echipamentelor astfel încât uzura acestora să fie una cât mai uniformă.

6. Concluzii

Eficientizarea energetică a sistemelor de încălzire a clădirilor, în majoritatea cazurilor, se face la temperaturi reduse ale agentului termic. Agentul termic este distribuit spre a fi încălzit în mai multe pompe de căldură conectate în serie/paralel. Având în vedere că sarcina termică necesară la utilizatorii finali este dependentă în general de temperatura exterioară, modul de prioritizare și de încărcare a pompelor de căldură trebuie gestionat astfel încât consumul de energie electrică al sistemului să fie cât mai redus, adică se impune o automatizare a întregului proces astfel încât randamentul energetic al pompelor de căldură să fie cât mai ridicat posibil. Prin urmare, articolul propune dezvoltarea a două concepte care se bazează pe testarea si gestionarea a două tipuri de pompe de căldură și prioritizarea funcționării instalației în funcție de parametrii stabiliți (temperatură interioară, temperatură exterioară, etc) prin integrarea unui sistem de automatizare. Autorii articolului intenționează să realizeze la scară pilot o instalație care să integreze conceptele propuse. Un avantaj care trebuie exploatat în viitor este acela că pompele de căldura pot furniza eficient energetic și apă rece în sistem de răcire pasivă / activă. Apa răcită se poate furniza consumatorilor, prin conductele de termoficare, în perioada verii ca și agent de răcire în sistemele dotate cu ventiloconvectoare. Conceptele propuse în aceasta lucrare sunt valabile și pentru modul de furnizare apă răcită pentru răcirea clădirilor.

References

[1] S. Tagliapietra, G. Zachmann, O. Edenhofer, J.M. Glachant, P. Linares, A. Loeschel "The European union energy transition: Key priorities for the next five years", Energy, vol. 132, September 2019, pp. 950-954.

[2] S. Potrč, L. Čuček, M. Martin, Z. Kravanja "Sustainable renewable energy supply networks optimization – The gradual transition to a renewable energy system within the European Union by 2050", Renewable and Sustainable Energy Reviews, vol.146, August 2021, ID Article: 111186.

[3] A. David, B. V. Mathiesen, H. Averfalk, S. Werner and H. Lund, "Heat Roadmap Europe: Large-Scale Electric Heat Pumps in District Heating Systems", Energies, 22 April 2017.

[4] A. S. Gaur, D. Z. Fitiwi, J. Curtis, "Heat pumps and our low-carbon future: A comprehensive review", Energy Research & Social Science, vol. 71, January 2021, ID Article: 101764.

Considerations regarding the impact of artificial lighting on health

Considerații privind impactul iluminatului artificial asupra sănătății

Iasmina-Daiana Holecică[1], Andreea-Miruna Tokar[2]
Coordinator: Dănuț Tokar[3]

[1] University Politehnica Timisoara
2, Victoriei Square, Timisoara, Romania
E-mail: iasmina.vig@upt.ro

[2] Faculty of Medicine and Pharmacy-University of Oradea
1, Universitatii Street, Oradea, Romania
E-mail: tokar.andreeamiruna@student.uoradea.ro

[3]University Politehnica Timisoara
2, Victoriei Square, Timisoara, Romania
E-mail: danut.tokar@upt.ro

DOI: 10.37789/rjce.2026.17.1.14

Abstract. *The article presents quantitative and qualitative aspects of lighting, its influence on activities carried out in educational and health spaces, and the impact of artificial lighting through its effects, especially blue light, on health.*

Key words: artificial lighting, blue light, LED, health

1. Introduction

The role of lighting in buildings is to ensure the quantity and quality of light, natural or artificial, so that activities can be carried out in hygienic and healthy conditions throughout the day. Although, from the point of view of the positive effect on the mental state of the occupants, but also on the properties of the rooms, natural lighting is preferred, due to the multitude of uncontrollable factors (seasonal and daily variation of brightness, limitation of glazed surfaces, etc.) artificial lighting is the one that replaces daylight. In this context, artificial lighting, depending on the purpose of the buildings, must allow the occupants to easily perceive the visual task, improve precision for a better performance of the activities carried out, not to have a risk of accident (too weak light), not to damage the vision through glare or generate visual

The article was received on 28.04.2025, accepted on 02.02.2026 and published on 24.02.2026

fatigue. Thus, optimal lighting levels are defined for a wide range of spaces, activities/areas or visual tasks.

Table 1 presents the level of illumination, and Table 2 presents a selection of recommended values for the design of general lighting systems that refer to buildings intended for educational and public health institutions (hospitals and clinics) [1].

Table 1

Lighting level [1]

Lightings level (lx)	**Type of activity/Visual perception**	**Examples of destinations**
20-30-50	Areas intended for circulation, storage	Secondary corridors, dryers in industry **)
50-100-150	Areas for circulation, simple orientation or temporary visits	Corridors, halls, warehouses, storerooms
100-150-200	Rooms where work activity is not continuous	Main halls, stairs, escalators
200-300-500	Simple visual perception	Theater, concert halls, canteens, industrial machine rooms, general factory lighting
300-500-750	Medium visual perception	Gymnasiums, classrooms, on library shelves, assembly areas
500-750-1000	Imposed visual perception	Offices (writing, reading, with computers), laboratories (where precise measurements are made)
750-1000-1500	Difficult visual perception	Fine assembly (mechanics, electronics), sewing, knitting rooms, final inspection
1000-1500-2000	Special visual perception	Precision work (electronics), color control, jewelry workshop
Peste 2000	Very accurate visual perception where high performance is required	Boxing rings, medical operating tables

**) Where color identification is not required

Table 2

Recommended values for the design of general lighting systems [1]

Types of destinations, activities or visual perception	**E_m**		**UGR_L**	**R_a**	**H_u**	**U_0**	**Remarks**
	minimum	**compensation**					
Educational institutions							
Playrooms	300	500	22	80	0.00	0.40	
Nursery and kindergarten classrooms	300	500	22	80	0.00	0.40	
Consultation rooms	300	500	19	80	0.70	0.60	
Classrooms	500	1000	19	80	0.70	0.60	For classrooms intended for young children, the minimum lighting level can be reduced to 300 lx.

Types of destinations, activities or visual perception	E_m		UGR_L	R_a	H_u	U_0	Remarks
	minimum	compensation					
Classrooms for evening classes or for adults	500	750	19	80	0.70	0.60	
Reading rooms	500	750	19	80	0.70	0.60	
Blackboard	500	750	19	80		0.70	On the board. To be avoid veiling reflections
Demonstration board in lecture halls Workshops	500	750	19	80		0.70	On the board. To be avoid veiling reflections
Workshops	500	750	19	80	1.0	0.60	
Art workshops in art schools	750	1000	19	90	0.7	0.70	4000 K $\leq T_{cp} \leq$ 6500 K
Technical drawing rooms	750	1000	19	80	0.7	0.60	Pe planșetă
Laboratories	500	750	19	80	0.7	0.60	
Amphitheaters	500	750	19	80	0.7	0.60	
Music rooms	300	500	19	80	0.7	0.60	
Computer rooms	300	500	19	80	0.7	0.60	
Language laboratories	300	500	19	80	0.7	0.60	
Study Rooms Sports	500	750	22	80	0.7	0.60	
Student Common Rooms and Meeting Rooms	200	300	22	80	0.7	0.40	
Teacher's room	300	500	19	80	0.7	0.60	
Halls and Swimming Pools	300	500	22	80	0.0	0.60	For public access areas, the values are correlated with the SR EN 12193:2019 standard.
Entrance halls	200	300	22	80	0.00	0.40	
Corridors, circulation areas	150	200	25	80	0.00	0.40	
Stairs	150	200	25	80	-	0.40	Lighting is done at the level of the stairs.
Teaching material warehouses	100	150	25	80		0.40	On the shelves.
Hospitals and clinics							
Waiting rooms	200	300	22	80	0.00	0.40	-
Corridors, day	-8î	200	22	80	0.00	0.40	-
Corridors, night	50	-	22	80	0.00	0.40	-
Staff offices	500	1000	19	80	0.7	0.60	-
Staff rooms	300	500	19	80	0.7	0.60	-
General lighting in the rooms	100	200	19	80	0.00	0.40	Floor-level lighting. By local lighting on the
- reading in the rooms	300	750	19	80		0.70	

Types of destinations, activities or visual perception	E_m		UGR_L	R_a	H_u	U_0	Remarks
	minimum	compensation					
- simple examination in the rooms	300	500	19	80		0.60	usable surface.
- examinations and treatments	1000	1500	19	90		0.70	
- nighttime/observation lighting	5		-	80		-	
Patient bathrooms and toilets	200	300	22	90		0.40	At the mirror
General lighting in consulting rooms	500	750	19	90	0.70	0.60	4000 K ≤ T_{cp} ≤ 6500 K
Eye and ear examinations	1000	1500	-	90	-	-	4000 K ≤ T_{cp} ≤ 6500 K
Vision tests (reading and color)	500	750	16	90		0.70	On the test surface 4000 K ≤ T_{cp} ≤ 6500 K
Dialysis rooms	500	750	19	80	0.70	0.60	-
Dermatology rooms	500	750	19	90	0.70	0.60	-
Endoscopy rooms	300	500	19	80	0.70	0.60	-
Dressing rooms	500	750	19	80	0.70	0.60	-
Massage and radiotherapy rooms	300	500	19	80	0.70	0.60	-
Saloane preoperator și de reanimare	500	750	19	90	0.70	0.60	-
Operating rooms: - general lighting;							3 x 3 m^2 around the table
- general lighting;	500		19	90	0.70		
- general lighting around the operating table;	1000		19	90	0.70		
Local lighting operating table.	10000-100000		16	90			On the operating field
Intensive care:							
- general lighting;	300	500	19	90	0.00	0.60	At floor level
- simple examinations;	500	750	19	90	0.00	0.60	
- examinations and treatments;	1000	1500	19	90	0.00	0.70	At bed level
- nighttime surveillance.	20	-	19	90	0.00	-	On examination surface
Dentistry:							Lighting must not present a risk of blinding the patient
- general lighting	500	750	19	90	0.70	0.60	
- local patient lighting	1000	1500	-	90		0.70	Local examination lighting
- local lighting operation	5000			90			On the operator

Types of destinations, activities or visual perception	E_m		UGR_L	R_a	H_u	U_0	Remarks
	minimum	compensation					
							field. Values higher than 5000 lx may be required
- jointing, adjustment white teeth	5000			90			T_{cp} at least 6000 K
Laboratories and pharmacies	500	750	19	80	0.7	0.60	-
Color control (laboratories)	1000	1500	19	90	0.7	0.60	4000 K ≤ T_{cp} ≤ 6500 K
Sterilized/disinfected rooms	500	750	22	80	0.7	0.60	-
Autopsy rooms and morgues	500	750	19	90	0.7	0.60	-
Autopsy and dissection table	5000	7500	-	90	0.7	0.60	Values higher than 5000 lx may be required

Note: E_m represents the recommended illumination level on the reference surface, in lx; UGR_L – the limit value of the UGR index (unified glare index) corresponding to the type of destination, activity or visual load; R_a – the general color rendering index; H_u – the height of the reference surface when it is parallel to the floor/useful plane, in m; U_0 - the minimum value of the illumination uniformity coefficient on the surface of the useful plane.

In the specialized literature, it is estimated that insufficient lighting creates a series of consequences, including [2]:
- visual fatigue;
- decreased work capacity;
- sensations of stinging or foreign bodies in the eyes;
- the appearance of vision disorders or even conditions such as myopia;
- increased waste;
- risk of trauma.

On the other hand, excessive lighting can produce a series of negative phenomena that refer to photophobia, tearing, pain in the eyeballs, headaches, etc. [2].

Hygienic requirements for room lighting refer to the following aspects [2]:
- to ensure a satisfactory level in the entire field of view;
- to ensure an optimal level for various activities;
- to be relatively uniform; to protect the eyes from radiation coming from the source or the reflection of surfaces;
- to ensure adequate radiation to avoid shadows;
- the light from artificial sources should have a spectrum as close as possible to that of natural light.

Even though the European Commission's SCENIHR (Scientific Committee on Emerging and Newly Identified Health Risks) committee states that it is very unlikely that artificial lighting is the cause of eye discomfort or even eye damage [3], there are

still sources that express some concerns and emphasize the importance of choosing the type of lighting, the quality of light sources, and changing lighting levels [4, 5]. However, in 2012, the same document [3] states that there is still a lack of relevant data regarding the effects of lighting on some medical conditions and that blue light and ultraviolet radiation are a potential risk factor for worsening symptoms in some patients with diseases such as chronic actinic dermatitis (a chronic papulopustular and eczematous facial dermatitis) and solar urticaria (Solar urticaria is a rare form of chronic inducible urticaria in which the skin swells within minutes of exposure to natural sunlight or an artificial light source that emits ultraviolet radiation.).

For this reason, it is very important that the choice of artificial light sources in healthcare buildings (hospitals, medical clinics, etc.) is well regulated. From the point of view of lighting installations for hospitals, in Romania, the regulatory framework is regulated by NP 015-2022 [6], which, however, does not address these aspects by referring to NP 061-2002 with the amendments and additions of 2023 [1], to the I7-2011 standard with subsequent amendments and additions [7] and to a series of standards, including SR EN 12464-1 [8], SR EN 12665:2024 [9], etc. On the other hand, various international institutions have established regulations for hospital lighting that take into account the safety and comfort of the patient, as well as of the hospital staff, namely: ANSI/IES RP-29-16 which recommends two different levels of lighting, one for the day and the other for the night correlated with the natural ability of the eye to adapt to the lighting conditions [10]. For example, the ANSI/IES RP-29-16 standard provides for a hospital lobby lighting of 800 lux during the day and 400 lux at night, taking into account the recommended lighting level for patients over 65 years old [10, 11], compared to the Romanian standard [1], which provides, according to Table 2, the values of 200 lux during the day and 50 lux at night. It can be seen that there is a difference in approach regarding the safety and comfort of patients and medicated staff, in favor of energy saving.

In general, in artificial lighting, certain types of lamps (including incandescent bulbs) can emit low-level UV radiation, which may increase the incidence of squamous cell carcinoma. The SCENIHR Committee [3] states that blue light from LED lamps and generally from improperly used lamps could theoretically induce retinal diseases, but other eye damage from chronic exposure to artificial light under normal lighting conditions is unlikely [3].

2. The main concepts addressed in lighting technology

Luminous flux represents the radiant flux emitted in the visible spectrum, evaluated by the intensity of the visual sensation. The radiation is emitted in the entire space around the light source. The unit of measurement is the Lumen (lm) and this measurement provides the best comparison between two sources that do not have directional light (>120°) (Figure 1). Between two lighting fixtures with directional light, the appropriate basis for comparison is the luminous flux emitted in an infinitely small solid angle. The unit of measurement is the Candela (cd) (Figure 1).

Unfortunately, the specifications only provide for the specification of the flux of the light sources, which in the case of light sources with a narrower angle distorts the comparison. The illumination of a surface is characterized by the density of the luminous flux on the surface whose unit of measurement is Lux (lx) [12] (Figure 1).

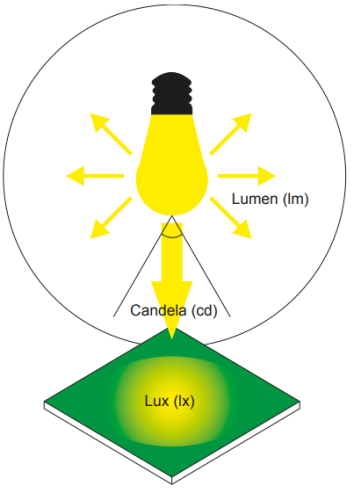

Fig. 1. Illumination of a surface [12]

Color rendering index

To express the color rendering index, worldwide, there are several expressions:
- general color rendering index (Ra) – used in Europe and Asia;
- special color rendering index (R9) – which measures the transmission of red tones;
- color rendering index CRI – used worldwide.

However, the CRI score is the most widely used measurement in North America and is internationally recognized as the standard measure of color rendering. The color rendering index (CRI) is a ratio that shows how accurately an object illuminated by artificial light reproduces its colors compared to natural light. The CRI ranges from 0 to 100, with a score of 100 representing perfect color rendering, meaning that the colors of objects illuminated by the light source appear exactly as they do in natural sunlight. Sunlight is considered to be 100, the minimum prescribed index for indoor lighting is 80, and for outdoor and industrial lighting it is a minimum of 70 [12,13]. The color rendering index is a critical factor in the design of lighting systems for applications where accurate color rendering is essential (laboratories, work areas for medical or care activities with high risk potential, etc.). The lower the index, the more inaccurately the colors are rendered, which can cause color distortion and affect the perception of the subject's appearance. An example of this is shown in Figure 2 [12,13].

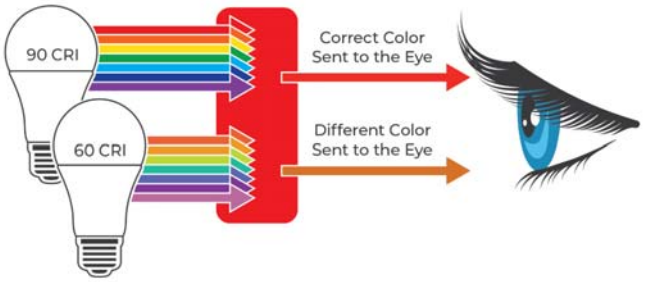

Fig. 2. Color perception by the human eye according to the CRI index [13]

Color rendering index has a significant impact on the ability to accurately assess organ anatomy during surgery. High CRI illumination ensures accurate color rendering of tissues and anatomical structures, helping to differentiate healthy from diseased tissues. Many anatomical structures present similar coloring and vastly complex anatomical particularities such as shape and positioning, as seen in Figure 3. Intra-operatory, the ability to accurately differentiate between anatomical structures is crucial. Thus the CRI standard is highly important in operating rooms.

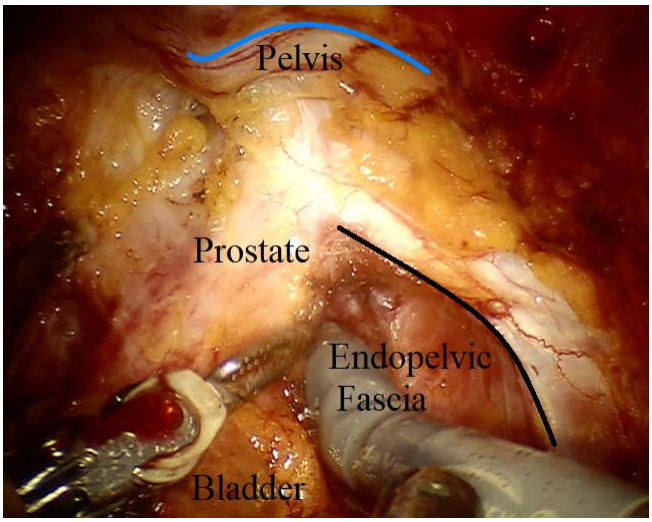

Fig. 3. Differentiating between various tissues[14]

The CRI index is calculated by comparing the color rendering of the light source to that of a reference light source for a set of eight color samples representing different hues, saturation levels, and skin tones, and assigned a value based on how accurately they are rendered by the tested light source. The results are then averaged to determine the color rendering index for the tested light source [13].

The CRI index is used to select suitable light sources for specific applications. LED lighting has become increasingly popular in recent years due to its energy efficiency and long lifespan. However, the CRI of LED lights can vary greatly, with some models scoring as high as 60 or 70. The general rule is: the higher the color rendering index, the better the color rendering ability. However, the CRI is not dependent on the color temperature. LED lights with lower CRIs can distort colors and

make it difficult to distinguish them accurately. In contrast, LED lights with higher CRIs, typically above 90, can provide excellent color rendering, making them ideal for applications where accuracy is important.

But, CRI index is not the only factor to consider when choosing a light source, as it does not take into account other aspects of light quality, such as temperature, brightness, and color consistency. However, it is an essential measure of color rendering and can provide valuable information when selecting a light source for specific applications.

In conclusion, CRI plays a vital role in lighting design, as it determines how well a light source can illuminate colors compared to natural sunlight.

Color temperature

Artificial lighting is correlated with the color temperature which is given in degrees Kelvin (K), essentially determining the ambient lighting. The higher color temperature is cooler, and the lower one designates the warmer light. Sunlight has an average value of 5500 K, which at sunset and sunrise warms up to around 4800 K. In general, in the range of 2700-3500 K of the color temperature we call it warm light (yellow-red range), in the range of 3500-5000 K neutral light and 5000 -6500 K cool light (green-blue range), aspects highlighted in Figure 3 [16, 17]. Geographically, warm light is more popular towards the north, while neutral and cool light are more popular further south [12].

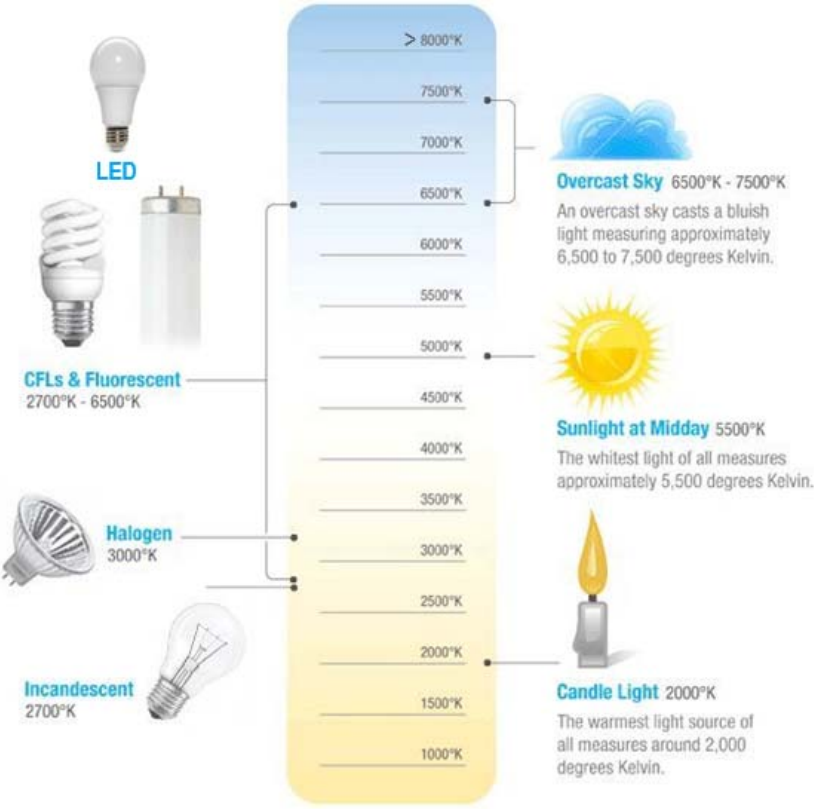

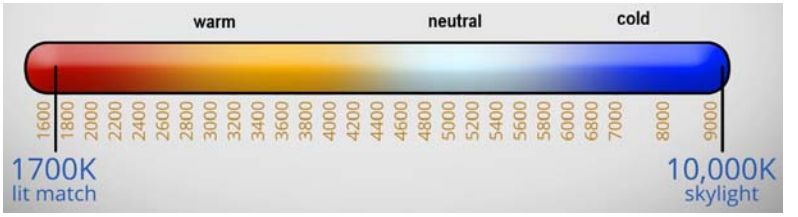

Fig. 3. Color temperature of light sources [16], [17]

LED sources are made up of several LEDs grouped in the same source to obtain higher luminous fluxes. In commercial LED sources, the color temperature can vary from 2800K to 12000K, with color rendering ranging from poor to excellent. Figure 4 shows the light spectrum obtained by 3 LED sources on the market. The difference in spectral shape is given by the execution technology of the LED source. To obtain cool and neutral color temperatures, single-chip LEDs are usually used, and for warm color temperatures, dual-chip LEDs are used.

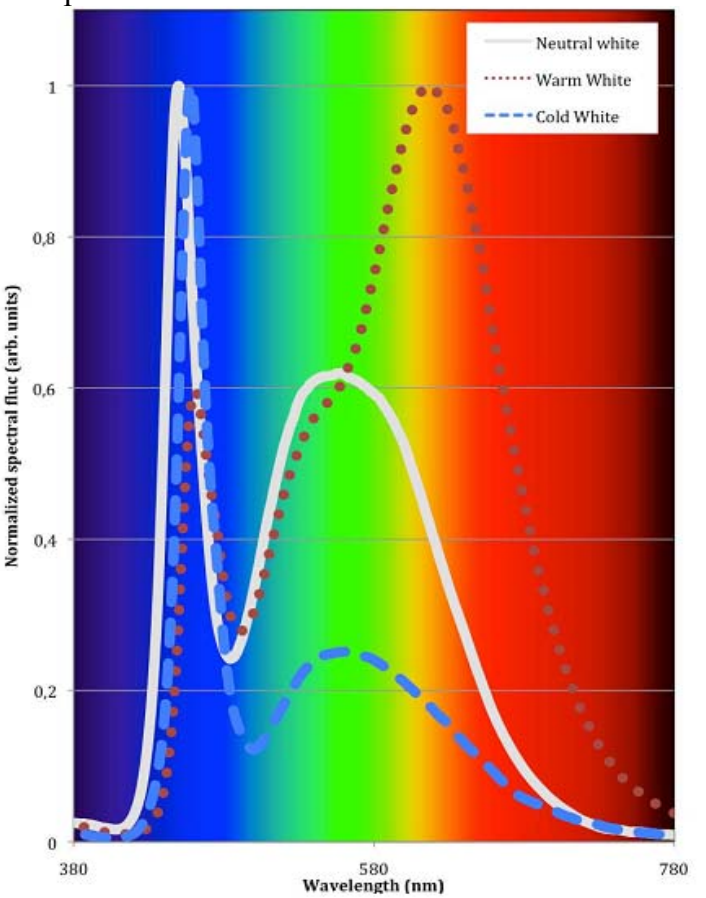

Fig. 4. The spectral flux of three different types of LEDs [3]

3. Light that affects health

With the pandemic, exposure to blue light from backlit screens and digital devices has increased. In fact, blue light, like any other visible color, is everywhere in

the environment. The sun, fluorescent light sources, incandescent light sources, and light-emitting diode (LED) technology all emit blue light, so people are exposed to a lot of blue light [18].

Some eye health experts have expressed concerns about exposure to blue light from backlit digital screens and devices. A 2020 study [19] found that so far, research in humans has not shown any concern about eye damage from blue light, but some animal studies have shown that blue light can damage cells in the retina [20]. It is known that the eye has structures that protect it from certain types of light (for example, the cornea and lens protect the light-sensitive retina at the back of the eye from harmful UV rays) (Figure 5 [21]).

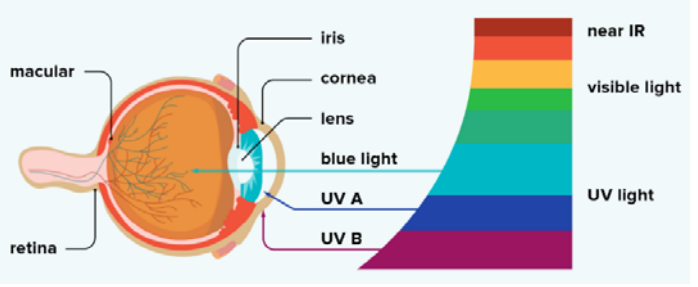

Fig. 5. The structure of the eye's protection from light [21]

Yet, there is a slow deterioration in eye health across all age groups and an awareness of eye fatigue, with degenerative changes in the structure of the retina (Figure 6) being observed due to artificial light [22].

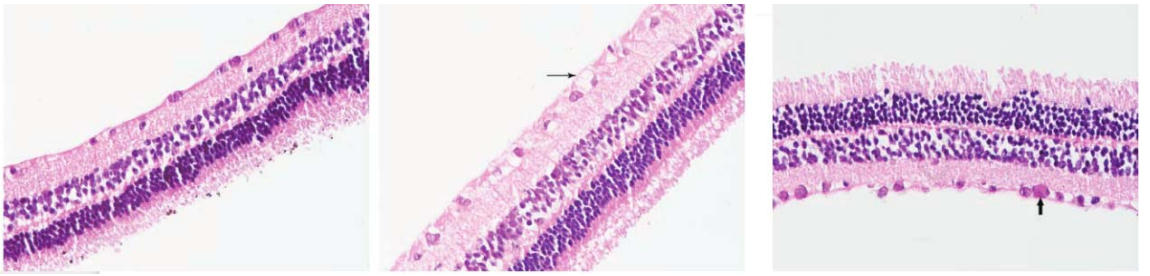

Fig. 6. Degenerative changes in the structure of the retina induced by artificial light [22]
a) natural light, b) LED lights, c) blue light

For this reason, relevant studies are needed that ultimately lead to the establishment of measures that minimize possible adverse effects. Therefore, it is difficult to conclude which of the light components (blue, red or infrared) have more pronounced negative effects on human health [19], but according to the opinion issued by SCENIHR [3] in 2008, blue and UV light represent a potential risk for the aggravation of certain diseases, such as: chronic actinic dermatitis and solar urticaria. This category includes compact fluorescent lamps (CFC), halogen lamps and even LED lamps, commonly found in educational and public health buildings due to their low electricity consumption.

Some researchers say that the information regarding LED devices is still uncertain due to the fact that they are relatively new and there are not enough long-term studies to certify the effects of blue light on health. On the other hand, papers claim that light with a strong blue component affects circadian cycles, the hormonal system and even the immune system [3].

For laparoscopy newer light sources were found that met the required CRI and safety standards. Liquid crystal and optic fiber cables most frequently used. While both are relatively safe options the lather one poses the risk of rupture. Both present burn risks especially liquid crystal cables [23]

6. Conclusions

In the context of promoting the widespread use of energy-saving lamps and the gradual elimination of incandescent lamps, the issue of verifying information according to which the symptoms of some diseases are or could be aggravated by energy-saving lamps arises.

The importance of ensuring a level of illumination, adopting lighting systems that are close to natural light, with a CRI index as close as possible to 100, is emphasized to ensure health, comfort and work efficiency. Greater attention must be paid to the design of lighting systems for healthcare spaces. Efficient lighting not only allows surgeons to perform procedures with precision but also plays a vital role in ensuring patient safety and optimal clinical outcomes.

Since the harmful effects of blue light are attributed to cardiovascular diseases, diabetes, osteoporosis and even breast cancer, it is necessary to continue research, to publish its results, putting human safety and health first. These results must also form the basis for updating lighting regulations, even at the expense of reducing electricity consumption.

References

[1] MDLPA, "Regulation for the design and execution of artificial lighting systems in buildings, with subsequent amendments and additions, indicative NP 061/2022", Official Gazette of Romania Part I no. 137 of February 17, 2023.

[2] C. Croitoru, „Cerinţele igienice faţă de iluminare”, available at: https://igienagenerala.usmf.md/wp-content/blogs.dir/151/files/sites/151/2016/09/Iluminarea.pdf, accessed: 12 April, 2025.

[3] European Commission – Committee Scientific Committee on Emerging and Newly Identified Health Risks (SCENIHR), „Health Effects of Artificial Light”, 2012, available at: https://ec.europa.eu/health/scientific_committees/emerging/docs/scenihr_o_035.pdf, accessed: April 12, 2025.

[4] A. Stockman, H. E. Smithson A.R. Webster, G. E. Holder N. A. Rana, C. Ripamonti, L. T. Sharpe, „The loss of the PDE6 deactivating enzyme, RGS9, results in precocious light adaptation at low light levels”, in Journal of Vision, vol. 8(1):10, 2008, pp. 1–10.

[5] D. S. Joyce, B. Feigl, A. J. Zele, „The Effects of Short-Term Light Adaptation on the Human Post-Illumination Pupil Response", in Investigative Ophthalmology & Visual Science, Vol.57, October 2016, pp. 5672-5680.
[6] MDLPA, Normativ pentru construcții spitalicești - Indicativ NP 015-2022, Monitorul Oficial, Partea I nr. 919 din 20 septembrie 2022.
[7] MDLPA, Normativ pentru proiectarea, executia si exploatarea instalatiilor electrice aferente cladirilor-Indicativ I7, Monitorul Oficial, nr. 512 din 12 iunie 2023.
[8] ASRO, SR EN 12464-1:2021 – Lumina si iluminat. Iluminatul locurilor de munca. Partea 1: Locuri de munca interioare, 2021.
[9] ASRO, SR EN 12665:2024 – Lumină și iluminat. Termeni de bază și criterii pentru specificarea cerințelor de iluminat, 2024.
[10] Ledyi, Aspecte legale și de reglementare ale iluminatului spitalelor, available at: https://www.ledyilighting.com/ro/hospital-lighting-why-choose-led-lights/#elementor-toc__heading-anchor-3, accessed: 12 April, 2025.
[11] P. Mustone, R. Kassouf, et all., „Lighting for Hospitals and Healthcare Facilities", in Illuminating Engineering Society, Illuminating Engineering Society of North America, 2016.
[12] Tracon Electric S.R.L., „Tehnica iluminatului", 2021, available at: https://electriccasabrasov.ro/fisiere/cataloage/tracon-tehnica-iluminatului-catalog.pdf, accessed: April 12, 2025.
[13] Partners Ltd, „Semnificația CRI – indice de redare a culorilor", available at: https://partners-ltd.com/ro/semnificatia-cri-indice-de-redare-a-culorilor/, accessed: 12 April 2025.
[14] A. M. Tokar, D. I. Nicoriuc, A. A. Pert, I. Moga, R. G. Rahota, "Presentation: Anatomical particularities for the preservation of potency after radical prostatectomy", available at: Conference of the Discipline of Anatomy-Embryology, 20-22 March, Oradea, Romania, 2025.
[15] Top LED, „Temperatura de culoare - Becuri LED", available at: https://www.top-led.ro/info/temperatura-de-culoare, accessed: 13.04.2025.
[16] ***, „Kelvin Color Temperature Scale Chart", in Printerest, available at: https://uk.pinterest.com/pin/448389706645554062/, accessed: 26.04.2025.
[17] J. Chaves, „White balance for film and video: A beginner's guide", available at: https://www.videomaker.com/article/c13/17840-let-there-be-white-white-balance-and-color-temperature-explained/, accessed: 26.04.2025.
[18] Healthline, What's Blue Light, and How Does It Affect Our Eyes?, Available at: https://www.healthline.com/health/what-is-blue-light#is-blue-light-bad-for-your-eyes, accessed: April 12, 2025.
[19] F. A. Bahkir, S.S. Grandee, „Impact of the COVID-19 lockdown on digital device-related ocular health", in Indian Jurnal of Ohthalmology Vol. 68(11), 26 Oct 2020, pp. 2378–2383.
[20] P. Chen, Z. Lai, Y. Wu, L. Xu, X. Cai, J. Qiu, P. Yang, M. Yang, P. Zhou, J. Zhuang, J. Ge, K. Yu, J. Zhuang, „Retinal Neuron Is More Sensitive to Blue Light-Induced Damage than Glia Cell Due to DNA Double-Strand Breaks", in Cells, Vol. 8(1), 18 January 2019, pp. 68.
[21] S. N. Frye, „What's Blue Light, and How Does It Affect Our Eyes? ", in Healthline, Available at: https://www.healthline.com/health/what-is-blue-light, accessed: April 26, 2025.
[22] X. Xu, J. Shi, C. Zhang, L. Shi, Y. Bai, W. Shi, Y. Wang, „Effects of artificial light with different spectral composition on eye axial growth in juvenile guinea pigs", in European Journal Histochemistry Vol. 67(1), 6 Feb 2023, ID article 3634.
[23] J. T. Hamdi, "Case Report Laparoscopic light source skin burn", Journal of Surgical Case Reports February 11, 2024, pp. 3.